



Article

Novel Artificial Tears Containing Cross-Linked Hyaluronic Acid: An In Vitro Re-Epithelialization Study

Arianna Fallacara ¹ , Silvia Vertuani ^{1,*}, Giacomo Panozzo ^{2, 3}, Alessandra Pecorelli ³, Giuseppe Valacchi ³ and Stefano Manfredini ¹ 

¹ Department of Life Sciences and Biotechnology, Master Course in Cosmetic Science and Technology (COSMAST), University of Ferrara, Via L. Borsari 46, 44121 Ferrara, Italy; arianna.fallacara@unife.it (A.F.); mv9@unife.it (S.M.)

² Ophthalmology Unit, Azienda ULSS n.22, 37012 Bussolengo, Italy; g.panozzo@iol.it

³ Department of Animal Sciences, Plants for Human Health Institute, North Carolina State University, NC Research Campus, 600 Laureate Way, Kannapolis, NC 28081, USA; apecore@ncsu.edu (A.P.); valacc@ncsu.edu (G.V.)

* Correspondence: vrs@unife.it; Tel.: +39-0532-455294; Fax: +39-0532-455378

Received: 1 November 2017; Accepted: 27 November 2017; Published: 30 November 2017

Abstract: Dry eye syndrome is a common disease which can damage the corneal epithelium. It is treated with eye drops to stimulate tear production and hydrate the corneal surface. The most prescribed artificial tear remedies contain hyaluronic acid (HA), which enhances epithelial wound healing, improving tissue health. To the best of our knowledge, only a few recent studies have investigated cross-linked HA (HA-CL) in eye drops for human applications. This work consists in an in vitro evaluation of the re-epithelialization ability of two different preparations containing a recently synthesized HA cross-linked with urea: 0.02% (*w/v*) HA-CL (solution 1, S1), and 0.4% (*w/v*) HA-CL (solution 2, S2). The study was conducted on both 2D human corneal cells (HCEpiC) and 3D reconstructed tissues of human corneal epithelium (HCE). Viability by 3(4,5-dimethylthiazol-2)2,5-diphenyltetrazolium bromide (MTT) test, pro-inflammatory cytokine release (interleukin-8, IL-8) by ELISA, and morphology by hematoxylin and eosin (HE) staining were evaluated. In addition, to understand the molecular basis of the re-epithelialization properties, cyclin D1 levels were assessed by western blot. The results showed no cellular toxicity, a slight decrease in IL-8 release, and restoration of epithelium integrity when the wounded 3D model was treated with S1 and S2. In parallel, cyclin D1 levels increased in cells treated with both S1 and S2.

Keywords: anti-inflammatory; artificial tears; corneal epithelium; cyclin D1; dry eye syndrome; HA; HA-CL; IL-8; re-epithelialization

1. Introduction

Dry eye syndrome or keratoconjunctivitis sicca (KCS) is a multifactorial disease of the tears and ocular surface, that results in symptoms of discomfort and visual disturbance, related to lacrimal film instability, with potential damage to the corneal epithelium [1]. It is accompanied by increased osmolarity of the tear film and inflammation of the ocular surface. When left untreated, this condition can provoke pain, ulcers, scars on the cornea, and even vision impairment [1]. Tear supplementation is the mainstay of the current therapy for the management of dry eye syndrome. This approach consists in the administration of artificial tears (which usually contain hydrophilic polymers) designed with a focus on physical properties relating to hydrating and lubricating of the ocular surface. Ideal tear replacement should recover and maintain a structurally and functionally normal ocular epithelium [1]

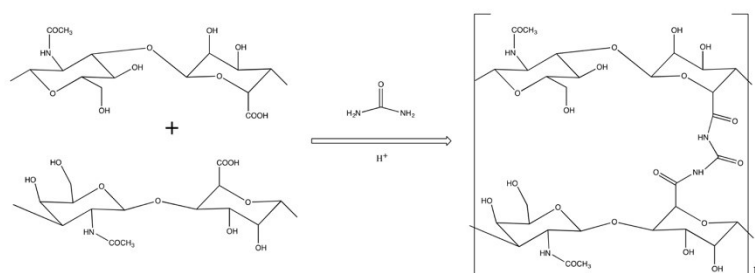
and consequently improve patient ocular comfort and quality of life by alleviating and eliminating both the signs (objective) and symptoms (subjective) of the disease.

Natural tears have a particular rheological profile; they are viscous under static conditions in the eye, while they are much less viscous during blinking. This behaviour could be well reproduced by hyaluronic acid (sodium salt) eye drops. HA is a biocompatible and biodegradable polymer. It is a vital component of human ocular physiology: it naturally occurs in the vitreous, lacrimal gland, corneal epithelium and conjunctiva [2–5], and it has also been found in tear fluid [6–8]. HA has a unique viscoelastic profile. During blinks, shear stress causes HA molecules to align with each other. As a result, the solution momentarily loses its viscosity and spreads easily over the cornea surface. Between blinks, HA chains form a tangled meshwork, and the solution becomes more viscous. This stabilizes the pre-corneal tear film, and maximizes the solution residence time on ocular surface, where HA is able to improve eye hydration and lubrication, due to its hygroscopic and mucus-adhesive properties [9]. Moreover, HA has been shown to stimulate corneal epithelial cell migration, and to possess anti-inflammatory and antioxidant properties: consequently, it might play a role in wound healing [10–14]. The complete set of all these properties makes HA well suited for use in artificial tears. Many studies have been conducted to evaluate the safety and efficacy of HA solutions as eye drops. They have all highlighted appreciable improvements of KCS symptoms and signs, associated with HA concentration and molecular weight (generally 0.1–0.4% solutions of 0.8–1.4 MDa HA) [4,15–20]. All this explains why actually there are several HA-containing eye drops commercially available. However, most of the HA-containing artificial tears available on the market are characterized by the linear form of this polymer; there are only few and recent examples of eye drops consisting of HA-CL. Cross-linking is a chemical strategy with the aims to increase the rigidity of the polymer network (i.e., the gel viscoelasticity), extend its permanence in the site of application and decrease its susceptibility to enzymatic degradation, thus reducing the daily number applications of a formulation [21]. To the best of our knowledge, only a few recent literature reports describe the effects of ophthalmic formulations –hydrogels, films, artificial tears-containing HA-CL for veterinary [22–26] and human uses [27–30]. These studies show promising results that open interesting perspectives to the ocular administration of cross-linked hyaluronans. Hence, the present work was devised with the aim to investigate the safety and the efficacy of eye drops based on a novel HA-CL to improve corneal re-epithelialization. More precisely, we examined the *in vitro* re-epithelialization capability of HA-CL preparations on both 2D and 3D human corneal epithelium model. In order to explore efficacy ranges, concentrations close to the ones of HA eye drops in the market, namely 0.02% and 0.4%, were assayed. The HA-CL used in this study is a recently patented polymer [31], provided with greater consistency as compared to naturally occurring hyaluronic acid [21,31]. This polymer consists of HA chains cross-linked by urea acting as a multifunctional agent [21,31]. Indeed, urea is not only a cross-linking agent –which increases native HA viscosity by linking its chains, thus possibly determining a longer retention on the corneal epithelium. Urea is also a non-toxic molecule with intrinsic healthy activity [21,31]. Therefore, urea-cross-linked hyaluronic acid is a promising polymer, because it has been developed not only to improve the mechanical properties of native HA, but also its biological activities [21,31]. In fact, urea is well known to be a moisturizing agent, thanks to its ability of water retention, which promotes cellular regeneration and reparation [21]. Charlton et al. [32] found that topical urea is able to encourage corneal re-epithelialization and to limit epithelial damage after injury to corneal epithelium. Therefore, all the beforehand mentioned studies about the ophthalmic use of HA and urea suggest that HA cross-linked with urea [31] could be an innovative promising ingredient for eye drops to induce corneal re-epithelialization. The herein described application of urea-crosslinked hyaluronan in the formulation of ophthalmic medicaments and medical devices is so far unprecedented.

2. Results and Discussion

2.1. Synthesis of HA-CL

Hyaluronic acid cross-linked with urea (Scheme 1) was prepared as reported by Citerinesi et al. [31].



Scheme 1. Synthesis of HA-CL with urea.

2.2. Physical-Chemical Characterization and Stability of HA-CL Solutions

In this study, two prototypes of eye drops were obtained by gently dissolving HA-CL into a saline-buffered aqueous solution. Immediately after their preparation, both the solutions displayed a transparent and homogenous appearance, and pH and viscosity (η) values were respectively 7.0 ± 0.0 and 1.6 ± 0.0 mPa·s for S1, and 7.1 ± 0.0 and 85.9 ± 0.0 mPa·s for S2; therefore suitable for ophthalmic formulations.

The stability study showed that the both S1 and S2 met the intended physical and chemical quality standards, as well as functionality and aesthetics, when stored under appropriate conditions. Indeed, both the formulations appeared homogeneous and perfectly transparent during the whole test, maintaining their initial appearance under all the conditions. The pH and viscosity values were pretty much constant during the whole study (Table 1). Conservation at high temperature condition (40 ± 2 °C) provoked only extremely limited modifications of pH and viscosity parameters, which were more than acceptable (Table 1).

Table 1. Stability of S1 and S2 during 6 months, at 23 ± 2 °C and at 40 ± 2 °C: pH and viscosity values.

Time	T (°C)	S1		S2	
		pH	η (mPa·s)	pH	η (mPa·s)
Day 7	23 ± 2	7.0 ± 0.0	1.6 ± 0.0	7.1 ± 0.0	85.9 ± 0.0
	40 ± 2	7.0 ± 0.0	1.6 ± 0.0	7.1 ± 0.0	85.8 ± 0.0
Month 1	23 ± 2	7.0 ± 0.1	1.6 ± 0.0	7.0 ± 0.0	85.9 ± 0.0
	40 ± 2	7.0 ± 0.0	1.6 ± 0.0	7.0 ± 0.0	85.8 ± 0.2
Month 2	23 ± 2	7.0 ± 0.0	1.6 ± 0.1	7.0 ± 0.1	85.9 ± 0.0
	40 ± 2	7.0 ± 0.0	1.6 ± 0.2	7.0 ± 0.2	85.8 ± 0.1
Month 3	23 ± 2	7.0 ± 0.0	1.6 ± 0.0	7.0 ± 0.0	85.9 ± 0.0
	40 ± 2	7.1 ± 0.1	1.5 ± 0.0	7.0 ± 0.0	85.6 ± 0.3
Month 6	23 ± 2	7.0 ± 0.1	1.6 ± 0.0	7.0 ± 0.0	86.0 ± 0.0
	40 ± 2	7.1 ± 0.0	1.5 ± 0.2	7.0 ± 0.0	85.7 ± 0.0

2.3. Cell Viability

Tear supplementation is the treatment of choice to control signs and symptoms of dry eye syndrome [1], and HA artificial tears eye drops are and among the most studied [4,10–12,15–20,29,30]. Corneal re-epithelialization, recovery and maintenance of ocular epithelium physiological conditions can be promoted also by urea therapy [32]. Hence, the novel hyaluronan derivative cross-linked with urea could be a valid therapy for KCS. Prior to specific markers screenings, the effect of HA-CL on human corneal cells viability was assayed. Table 2 reports cell viability results (MTT test) at 48 and 72 h, under the experimental conditions CTR−, CTR+ and treated with S1 and S2 solutions. As reported in Table 2, the wound caused a decrease of cell viability in damaged untreated tissues (CTR+); however, cell viability

increased during time (Table 2). The damaged and treated tissues showed a trend similar to the positive control at 48 h, while, after 72 h of exposure, the cell viability increased to reach values comparable to negative control (not damaged) (CTR−) (Table 2).

Table 2. Cell viability (MTT test) of CTR−, CTR+, S1 and S2 at 48 and 72 h.

Condition	Cell Viability		% Variation vs. CTR−		% Variation vs. CTR+	
	48 h	72 h	48 h	72 h	48 h	72 h
CTR−	100.0 ± 0.5	100.0 ± 8.4	-	-	-	-
CTR+	72.4 ± 2.2	81.8 ± 4.4	−27.6	−18.2	-	-
S1	76.4 ± 2.1	107.2 ± 0.5	−23.6	+7.2	+4.0	+25.4
S2	74.4 ± 0.7	102.3 ± 2.0	−25.6	+2.3	+1.9	+20.5

Statistical analysis showed that after 72 h there were significant differences in cell viability between damaged untreated tissue (CTR+) and treated tissues (S1 and S2), and no significant differences between undamaged untreated tissue (CTR−) and treated tissues (S1 and S2) (Table 3). The viability parameter is correlated to cell proliferation that it is an index of the degree of tissue repair. Based on the results obtained, it was possible to conclude that both HA-CL solutions completely restored cell viability, thus promoting the re-epithelialization of the studied cellular model after 72 h.

Table 3. ANOVA and Tukey-Kramer test statistical analysis of cell viability (MTT test) of the conditions CTR−, CTR+, S1 and S2 at 48 and 72 h (statistically significant values in bold, $p < 0.05$).

Condition	vs. CTR−		vs. CTR+		vs. S1		vs. S2	
	48 h	72 h	48 h	72 h	48 h	72 h	48 h	72 h
CTR−	-	-	0.00000	0.00983	0.00000	0.41310	0.00000	0.97145
CTR+	0.00000	0.00983	-	-	0.07789	0.00116	0.58301	0.00474
S1	0.00000	0.41310	0.07789	0.00116	-	-	0.52885	0.72684
S2	0.00000	0.97145	0.58301	0.00474	0.52885	0.72684	-	-

2.4. Effect of HA-CL on IL-8 Levels

To understand if HA-CL solutions were able to modulate inflammation due to wound induction, IL-8 levels were quantified in human corneal control and treated cells. The chemokine IL-8 was chosen as pro-inflammatory marker as it is released in epithelial tissues in a pro-inflammatory status. Table 4 reports the results of IL-8 levels (ELISA test) at 48 and 72 h, in the experimental conditions CTR−, CTR+ and treated with S1 and S2 solutions. The wound caused an increased release, over time, of IL-8 in wounded untreated tissues (CTR+) (Table 4). The treated tissues (conditions S1 and S2) showed a trend similar to the positive control (CTR+) throughout the exposure period, with an increase in IL-8 release compared to the negative control tissues (CTR−) (Table 4).

Table 4. IL-8 levels in CTR−, CTR+, S1 and S2 tissues assessed at 48 and 72 h by ELISA test.

Condition	IL-8 pg/mL		% Variation vs. CTR−		% Variation vs. CTR+	
	48 h	72 h	48 h	72 h	48 h	72 h
CTR−	616.5 ± 37.7	595.7 ± 35.9	-	-	-	-
CTR+	762.2 ± 40.3	720.7 ± 49.5	+23.6	+21.0	-	-
S1	699.5 ± 32.4	701.5 ± 36.4	+13.5	+13.8	−8.2	−2.7
S2	664.3 ± 52.3	714.5 ± 58.2	+7.8	+15.9	−12.8	−0.9

Statistical analysis showed that there was no significant difference in IL-8 levels between the positive control (CTR+) and the treated tissues (S1 and S2), and also between the two treated tissues at both 48 h (Table 5) and 72 h post-treatment (data not shown).

Although no sample was able to significantly modulate IL-8 release in this particular experimental system, it was anyway possible to observe a slight reduction of IL-8 level in treated tissues compared to the positive control, especially at 48 h (−8.2% S1 vs. CTR+, −12.8% S2 vs. CTR+, Table 4) suggesting a possible positive effect of S1 and S2.

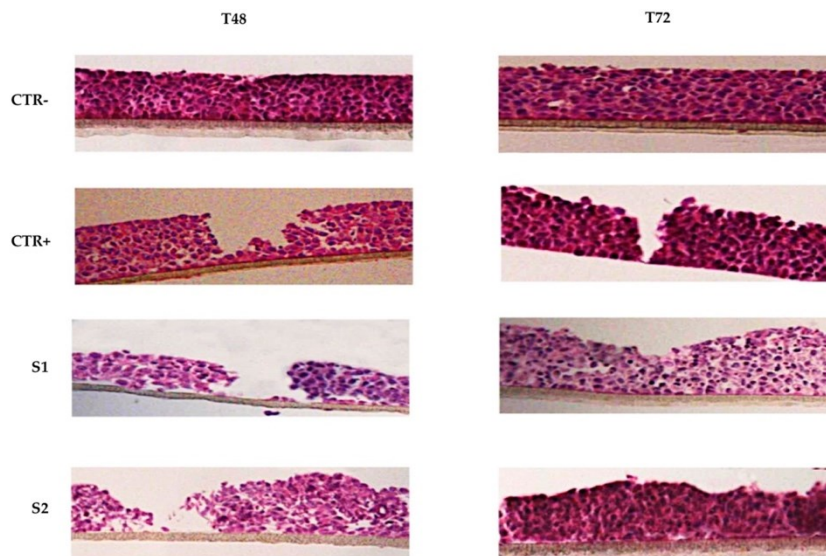
Table 5. ANOVA and Tukey-Kramer test statistical analysis of IL-8 levels in CTR−, CTR+, S1 and S2 tissues at 48 h (statistically significant values in bold, $p < 0.05$).

Condition	48 h			
	vs. CTR−	vs. CTR+	vs. S1	vs. S2
CTR−	-	0.00625	0.15548	0.61723
CTR+	0.00625	-	0.37554	0.07523
S1	0.15548	0.37554	-	0.82461
S2	0.61723	0.07523	0.82461	-

2.5. Epithelial Corneal Wound Closure

Histological analysis (HE staining) is a useful tool to study epithelial integrity and repair phenomena that follow the induction of mechanical damage. The histological images shown in Figure 1 present the overtime wound closure of the different samples. The negative control CTR− had an intact and correct structure for the entire period of exposure. After wound, it is possible to appreciate a recovery of the damage overtime in the positive control CTR+ samples at 48 h and 72 h. The epitheliums treated with the two solutions S1 and S2 exhibited a clear improvement in the wound closure respect to the positive control.

To confirm the wound healing properties of S1 and S2, we also tested the two HA-CL solutions in a scratch assay on a 2D monolayer model of HCEpiC cells. Consistent with the 3D results, at 36 h post-scratch, treated HCEpiC cells displayed a nearly (S1) or complete (S2) wound closure compared to untreated control cells (Figure 2). In particular, a significant difference in wound closure was observed between S2 treated HCEpiC and untreated control cells (Figure 3), showing that S2 importantly improved epithelial corneal wound closure.

**Figure 1.** Histological analysis (HE staining) of 3D reconstructed tissues of human corneal epithelium. After wounding, HCE cells were incubated in growth medium with or without S1 and S2 for 72 h. Representative images from each group were recorded at 48 and 72 h post-wounding.

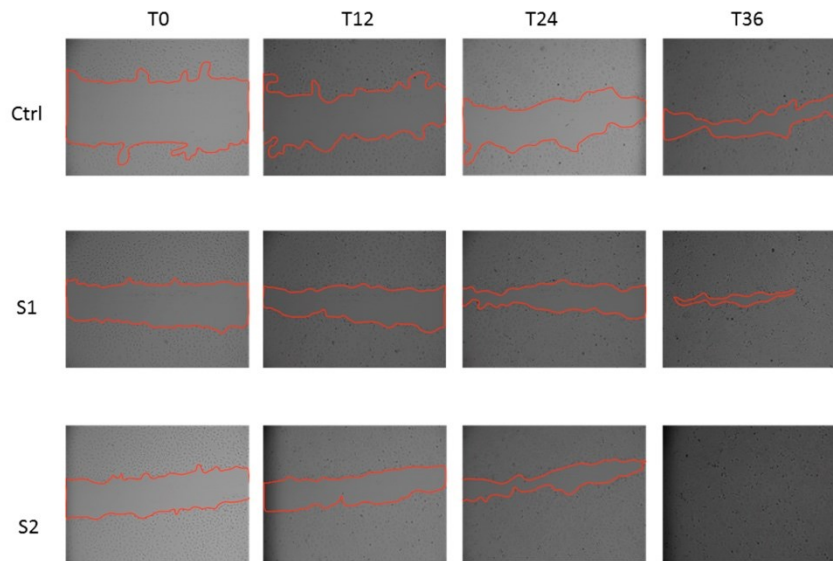


Figure 2. In vitro wound healing assay of human corneal epithelial cells. After the scratch, HCEpiC cells were incubated in fresh medium with or without S1 and S2 for 36 h. Representative images from each group were recorded at 0, 12, 24 and 36 h post-scratching. The red lines indicate the wound borders.

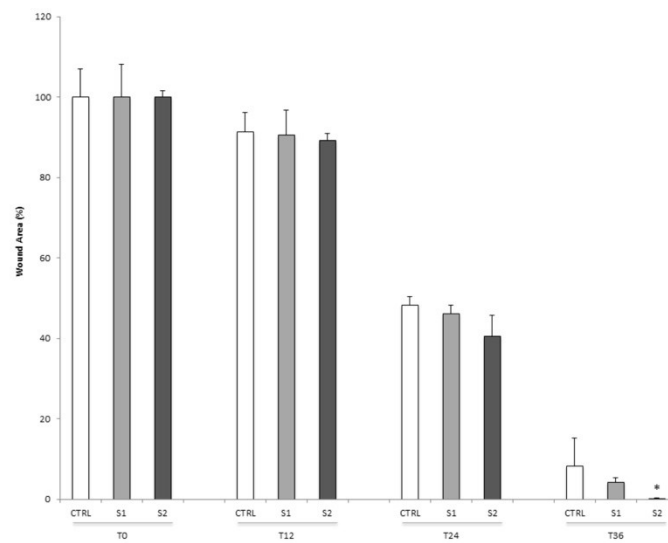


Figure 3. Quantification of wound healing in human corneal epithelial cells. The relative scratch gap was calculated as the percentage of the remaining wounded area at the given time point compared with the initially wounded area at 0 h. Data were expressed as mean \pm SD ($n = 3$). * $p < 0.05$ compared with control.

2.6. Cyclin D1 Protein Levels

To understand the molecular basis of the re-epithelialization properties of S1 and S2 in wound closure, the protein expression of cyclin D1, a cell-cycle regulator critical for G(1)-phase progression and S-phase entry, was also analyzed. As shown in Figure 4, both S1 and S2 treatments were able to induce a significant increase in cyclin D1 cellular levels after 12 h respect to the untreated control cells. This evidence suggested that S1 and S2 solutions might be able to accelerate epithelial wound closure by promoting a cyclin D1-induced cell proliferation.

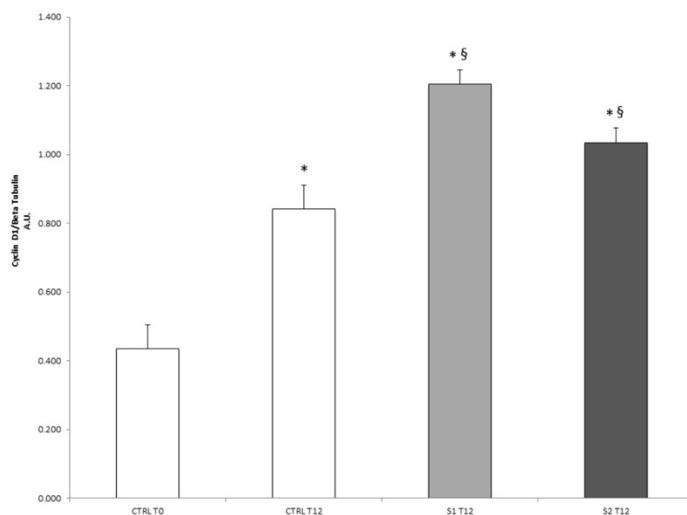


Figure 4. Effect of S1 and S2 on the proliferative marker cyclin D1 in HCEpiC cells. The graph shows the cyclin D1 protein levels in HCEpiC cells treated with S1 or S2 for 12 h. Data are means \pm SD of triplicate. * indicates statistically significant difference from untreated control at 0 h; § indicates statistically significant difference from untreated control at 12 h (one-way ANOVA, $p < 0.05$).

3. Experimental Section

3.1. Materials

HA-CL with urea (M_w 2.0–4.0 MDa) was a patented raw material [31] kindly provided by IRALab (Usmate Velate, Monza-Brianza, Italy). The solvent used for the preparation of HA-CL solutions was a saline-buffered solution consisting of Milli-Q water, NaCl, $\text{Na}_2\text{HPO}_4 \cdot 12\text{H}_2\text{O}$, and $\text{NaH}_2\text{PO}_4 \cdot \text{H}_2\text{O}$ (pH 7.0). All the salts were in compliance with European or USP Pharmacopoeia.

3.2. Formulation of HA-CL Solutions

Two different prototypes of solutions were formulated: 0.02% (w/v) HA-CL (solution 1, S1) and 0.4% (w/v) HA-CL (solution 2, S2). Each formulation was prepared by dissolving the polymer in the above described saline-buffered solution. The polymer was left to hydrate under gentle magnetic stirring, at room temperature, for about 1 h, until reaching a transparent and homogeneous appearance. The solutions were sterilized through 0.2 μm Stericup[®] vacuum driven sterile filters (Millipore, Canton-Schaffhausen, Switzerland), and then they were stored at room temperature (23 ± 2 °C) before being evaluated.

3.3. Physical-Chemical Characterization and Stability of HA-CL Solutions

Immediately after their preparation, the two prototypes of solutions were characterized by measuring in triplicate their pH and their viscosity (η , rotational viscometer VISCO-STAR equipped with TL5 spindle, Fungilab, Barcelona, Spain) at room temperature (23 ± 2 °C).

Moreover, pH, η and macroscopic appearance of HA-CL solutions were monitored during time to evaluate the physical-chemical stability of the eye drops prototypes. After the preparation, each formulation was divided into two aliquots, one stored for six months at ambient temperature (23 ± 2 °C, shelf life), and the other stored for six months in thermostatic oven (40 ± 2 °C, accelerate stability test). At selected time intervals (i.e., 1 week, 1, 2, 3, 6 months after the preparation), the samples were evaluated in triplicate for physical-chemical and organoleptic characteristics. Data were reported as mean values \pm standard deviations.

3.4. In Vitro Efficacy Study

3.4.1. Experimental Scheme

The adopted experimental scheme was:

- negative control condition: tissues not wounded and not treated (CTR-);
- positive control condition: tissues wounded but not treated (CTR+);
- treated condition: tissues wounded and treated with the samples (S1 and S2).

Four tissues for each experimental condition were used.

3.4.2. Cell Cultures

The in vitro evaluations of the safety and the re-epithelialization capability of HA-CL eye drops prototypes were performed on two different biological models: 3D reconstructed tissues of HCE and 2D HCEpiC.

The biological model consisting of 3D HCE, built from immortalized cells of human cornea (Model HCE-SkinEthic, Lyon, France) [33], was used for the viability study (MTT test), the determination of IL-8 release (ELISA test), and the morphological investigations (HE staining). The 3D HCE was a 0.5 cm² corneal epithelium reconstructed by airlifted culture of transformed human corneal keratinocytes, placed for 5 days in chemically defined medium, on inert polycarbonate filter, at the air/liquid interface. After 6 days of reconstruction, corneal tissues were wounded by scalpel (with the exception of the negative control) and placed into plates with growth medium for the different treatments. 30 μ L of test solutions (S1 and S2) were applied on the wounded tissues and incubated for 48 and 72 h at 36.5 °C/5% CO₂. No substance was applied to negative and positive control tissues. Tissues were thus subjected to MTT test, ELISA test and HE staining.

The 2D biological model consisting of commercial HCEpiC cells was employed to confirm the wound healing properties of S1 and S2 (scratch assay), and to understand the molecular basis of the re-epithelialization in wound closure induced by S1 and S2 (cyclin D1 quantification by Western blot). HCEpiC cells grown in the corneal epithelial cell medium (ScienCell Research Laboratories, Inc., Carlsbad, CA, USA). Cells were incubated at 37 °C for 24 h in 95% air/5% CO₂ until 80% confluence. The medium was changed every 4 days, and cells from passages 2–4 were used for experiments. Tissues were thus subjected to scratch assays and western blot tests.

3.4.3. Cell Viability

To evaluate the suitability, the safety and the effect on corneal cells viability of HA-CL eye drops prototypes, an in vitro MTT assay was conducted. After the treatment of 3D HCE cells as above described (Section 3.4.2), the tissues were rinsed three times with 1 mL of PBS, arranged in 300 μ L of 0.5 mg/mL MTT solution and then incubated for 3 h at 36.5 °C/5% CO₂. Each tissue was transferred into a well containing 1.5 mL of isopropanol and incubated for two h at room temperature. Hereafter,

the tissues were removed from the wells and homogenized to dissolve formazan salts. Two hundred μL of this solution were transferred in a 96 well-plate and absorbance reading was performed at 570 nm (isopropanol was used as blank for reading). For each test condition the ratio of the average optical density of the treated tissues on the average optical density of negative controls determined the viability rate. Data were reported as mean values \pm standard deviations (expressed in %), and as mean % variations compared to the controls.

3.4.4. IL-8 ELISA Test

The inflammatory state of control and treated (S1 and S2) tissues was evaluated using ELISA test to quantify the pro-inflammatory marker interleukin-8 (IL-8). Therefore, after 3D HCE cells preparation as above described (Section 3.4.2), controls and treated tissues were undergone to IL-8 dosage using IL-8 ELISA commercial kit (ThermoFisher Scientific, Milano, Italy), according to the manufacturer's instructions. For the quantitative determination, it was used a previously plotted calibration curve made-up of standard known and growing concentrations of IL-8. The results of IL-8 dosage in cell culture CTR-, CTR+ and treated with the two solutions at 48 and 72 h were reported as mean values \pm standard deviations (expressed in pg/mL), and as mean % variations compared to the controls.

3.4.5. Epithelial Corneal Wound Closure

Epithelial integrity and repair phenomena that followed wound induction were first of all studied on 3D HCE cells, and then confirmed on 2D HCEpiC.

Control and treated tissues of 3D HCE were cultured and prepared as previously described (Section 3.4.2), and after stained with hematoxylin-eosin (HE) [34]. Microscope examination permitted to investigate the histology of the tissues. Indeed, hematoxylin, being a basic dye, coloured in blue/violet the negatively-charged cellular components principally located in the nucleus -nucleic acids, membrane proteins, cellular membranes, elastin-, while eosin, being an acid dye, stained in pink the positively charged cellular components predominantly situated in the cytoplasm and in the extracellular area -proteins, mitochondrial proteins, collagen fibers. The staining permitted to examine tissue integrity.

To confirm the wound healing properties of S1 and S2, HCEpiC cells were subjected to wound healing assay performed as previously described [35]. Briefly, HCEpiC cells, grown to confluent monolayer on 48-well plates, were mechanically scratched with a 200- μL sterile pipette tip, washed and then allowed to re-epithelialize for 36 h in the presence of S1 and S2. Serial bright-field images of scratches were captured at different time points (i.e., 0, 12, 24 and 36 h post-scratch). Then, changes in wound area at various time points for each treatment group were measured using Image-J software (National Institutes of Health, Bethesda, MD, USA), and compared to the wound area at 0 h, which was arbitrarily set as 100.

3.4.6. Western Blot Analysis

To evaluate cell proliferation, HCEpiC cells were seeded on cell culture dishes and, at subconfluence (50%), treated with the two solutions S1 and S2. At 12 h, the cells were washed with ice-cold PBS and lysed in ice-cold lysis RIPA buffer. After centrifugation ($15,000 \times g$, 15 min at 4°C), the supernatants were collected. Protein concentrations were determined using the Bio-Rad protein assay kit (Bio-Rad Laboratories, Inc., Hercules, CA, USA). Total protein extracts (20 μg) were loaded onto 10% sodium dodecyl sulphate-polyacrylamide electrophoresis gels and separated by molecular size. Gels were electro-blotted onto nitrocellulose membranes and then blots were blocked for 1 h in Tris-buffered saline, pH 7.5, containing 0.5% Tween 20% and 3% milk. Membranes were incubated overnight at 4°C with Cyclin D1 antibody (Cell Signaling Technology, Inc., Danvers, MA, USA). The membranes were then incubated with horseradish peroxidase-conjugated secondary antibody for 1 h, and the bound antibodies were detected by chemiluminescence (Bio-Rad Laboratories, Inc.). β -actin (Cell Signaling Technology, Inc.) was used as loading control. Images of the bands

were recorded with a ChemiDoc imaging system (Bio-Rad Laboratories, Inc.) and the densitometry analysis was performed using Image-J software. Results are expressed in arbitrary units as relative to β -actin expression.

3.4.7. Statistical Analysis

Obtained data in the different experimental groups were subjected to statistical analysis and compared according to one-way ANOVA and Tukey-Kramer test. The variations were considered significant for $p < 0.05$.

4. Conclusions

Although the preliminary nature of this *in vitro* study, we have clearly shown, for the first time, promising results for the use of artificial tears containing HA-CL with urea for the treatment of dry eye disease and corneal injuries in human eyes. The two prototypes of eye drops developed were characterized by a good chemical-physical stability, and resulted safe for ophthalmic application. Despite both S1 and S2 were not able to significantly reduce IL-8 levels, they showed interesting wound healing properties. Indeed, according to the applied experimental protocol and to the data obtained, both the formulations showed a potential re-epithelialization efficacy on the cellular models analyzed: a clear recovery of the wound was observed in the 2D model and also in the 3D model. This was confirmed also by histological analysis, which showed the restoring of microscopic epithelial structure after treatment with S1 and S2. Our findings were in agreement with the results of previous *in vitro* and *in vivo* studies, which showed that corneal epithelial wound healing is promoted by native HA [10–12,36–38] and others type of HA-CL [22–30]. Moreover, western blot analysis evidenced that, after the treatment with S1 and S2 eye drops, the level of the proliferative marker cyclin D1 was increased compared to the control. Therefore, the two HA-CL solutions accelerated the tissue proliferative process related to post-wound re-epithelialization. This study opens encouraging perspectives, since HA-CL with urea may promptly alleviate both signs and symptoms of dry eye syndrome, even if used at concentration lower (0.02% *w/v*) than the usually employed for native HA artificial tears (generally 0.1–0.4%) [4,15–20,36]. Therefore, HA-CL with urea eye drops could allow a rapid improvement of patient ocular comfort and quality of life through a therapy with absolutely acceptable costs. All these evidences and considerations strongly support further investigations, both *in vitro* and *in vivo*, for a deeper characterization of the biological activity of artificial tears containing HA-CL with urea. Moreover, further researches will be necessary to understand the ocular surface residence time and thus the required dose-frequency of eye drops containing HA-CL with urea, as well as their potential delivery through the membrane.

Acknowledgments: This work was supported by the University of Ferrara FAR Grant 2014; Ambrosialab Srl, Ferrara; COC Farmaceutici Srl, Rovereto (Modena); IRALAB Srl, Usmate Velate (Milano). Authors wish to thank Farcoderm Srl (Milano) for HE staining.

Author Contributions: S.M., G.V. and G.P. conceived and designed the experiments, drafted the manuscript. S.V. coordinated the study, supervised the completion of the experiments and revised the manuscript. A.F. and A.P. performed and managed the study and wrote the final version of the paper. S.M. is the senior author responsible of the whole study.

Conflicts of Interest: The authors declare no conflict of interest. The founding sponsors had no role in the design of the study; in the collection, analyses, or interpretation of data; in the writing of the manuscript, and in the decision to publish the results.

Abbreviations

The following abbreviations are used in this manuscript:

CTR−	negative control condition
CTR+	positive control condition
ELISA	enzyme-linked immunosorbent assay
HA-CL	cross-linked hyaluronic acid
HA	hyaluronic acid
HCE	3D reconstructed tissues of human corneal epithelium
HCEpiC	2D human corneal epithelial cells
HE	hematoxylin and eosin
IL-8	interleukin-8
KCS	keratoconjunctivitis sicca
MTT	3(4,5-dimethylthiazol-2)2,5 difeniltetrazolium bromide
S1	solution 1, 0.02% (w/v) HA-CL
S2	solution 2, 0.4% (w/v) HA-CL

References

- Lemp, M.A.; Baudouin, C.; Bau, J.; Dogru, M.; Foulks, G.N.; Kinoshita, S.; Laibson, P.; Mc Culley, J.; Murube, J.; Pflugfelder, S.C.; et al. DEWS definition and classification subcommittee of the international dry eye workshop. The definition and classification of dry eye disease: Report of the definition and classification subcommittee of the international dry eye workshop. *Ocular Surf.* **2007**, *5*, 75–92.
- Berriaud, N.; Milas, M.; Rinaudo, M. Characterization and properties of hyaluronic acid (hyaluronan). In *Polysaccharides: Structural Diversity and Functional Versatility*, 2nd ed.; Dumitriu, S., Dekker, M., Eds.; CRC Press: New York, NY, USA, 2005; pp. 535–549.
- Lapcik, L., Jr.; Lapcik, L.; De Smedt, S.; Demeester, J.; Chabreček, P. Hyaluronan: Preparation, structure, properties, and applications. *Chem. Rev.* **1998**, *98*, 2663–2684. [[CrossRef](#)]
- Stuart, J.C.; Linn, J.G. Dilute sodium hyaluronate (Healon) in the treatment of ocular surface disorders. *Ann. Ophthalmol.* **1985**, *17*, 190–192. [[PubMed](#)]
- Yoshida, K.; Nitatori, Y.; Uchiyama, Y. Localization of glycosaminoglycans and CD44 in the human lacrimal gland. *Arch. Histol. Cytol.* **1996**, *59*, 505–513. [[CrossRef](#)] [[PubMed](#)]
- Berry, M.; Pastis, K.W.; Ellingham, R.B.; Frost, L.; Corfield, A.P.; Easty, D.L. Hyaluronan in dry eye and contact lens wearers. In *Lacrimal Gland, Tear Film, and Dry Eye Syndromes 2*; Sullivan, D.A., Dartt, D.A., Meneray, M.A., Eds.; Plenum Press: New York, NY, USA, 1998; pp. 785–790.
- Frescura, M.; Berry, M.; Corfield, A.; Carrington, S.; Easty, D.L. Evidence of hyaluronan in human tears and secretions of conjunctival cultures. *Biochem. Soc. Trans.* **1994**, *22*, 228s. [[CrossRef](#)]
- Fukuda, M.; Miyamoto, Y.; Miyara, Y.; Mishima, H.; Otori, T. Hyaluronic acid concentrations in human tear fluids. *Investig. Ophthalmol. Vis. Sci.* **1996**, *37*, 3916.
- Nakamura, M.; Hikida, M.; Nakano, T.; Ito, S.; Hamano, T.; Kinoshita, S. Characterization of water retentive properties of hyaluronan. *Cornea* **1993**, *12*, 433–436. [[CrossRef](#)] [[PubMed](#)]
- Gomes, J.A.P.; Amankwah, R.; Powell-Richards, A.; Dua, H.S. Sodium hyaluronate (hyaluronic acid) promotes migration of human corneal epithelial cells in vitro. *Br. J. Ophthalmol.* **2004**, *88*, 821–825. [[CrossRef](#)] [[PubMed](#)]
- Inoue, M.; Katakami, C. The effect of hyaluronic acid on corneal epithelial cell proliferation. *Investig. Ophthalmol. Vis. Sci.* **1993**, *34*, 2313–2315.
- Nishida, T.; Nakamura, M.; Mishima, H.; Otori, T. Hyaluronan stimulates corneal epithelial migration. *Exp. Eye Res.* **1991**, *53*, 753–758. [[CrossRef](#)]
- Presti, D.; Scott, J.E. Hyaluronan-mediated protective effect against cell damage caused by enzymatically produced hydroxyl (OH) radicals is dependent on hyaluronan molecular mass. *Cell Biochem. Funct.* **1994**, *12*, 281–288. [[CrossRef](#)] [[PubMed](#)]
- Scott, J.E. Extracellular matrix, supramolecular organization and shape. *J. Anat.* **1995**, *187*, 259–269. [[PubMed](#)]
- Aragona, P.; Papa, V.; Micali, A.; Santocono, M.; Milazzo, G. Long term treatment with sodium hyaluronate-containing artificial tears reduces ocular surface damage in patients with dry eye. *Br. J. Ophthalmol.* **2002**, *86*, 181–184. [[CrossRef](#)] [[PubMed](#)]

16. Dumbleton, K.; Woods, C.; Fonn, D. An investigation of the efficacy of a novel ocular lubricant. *Eye Contact Lens* **2009**, *35*, 149–155. [[CrossRef](#)] [[PubMed](#)]
17. Hamano, T.; Horimoto, K.; Lee, M.; Komemushi, S. Sodium hyaluronate eye drops enhance tear film stability. *Jpn. J. Ophthalmol.* **1996**, *40*, 62–65. [[PubMed](#)]
18. Johnson, M.E.; Murphy, P.J.; Boulton, M. Effectiveness of sodium hyaluronate eye drops in the treatment of dry eye. *Graefes Arch. Clin. Exp. Ophthalmol.* **2006**, *244*, 109–112. [[CrossRef](#)] [[PubMed](#)]
19. Prabhasawat, P.; Tesavibul, N.; Kasetsuwan, N. Performance profile of sodium hyaluronate in patients with lipid tear deficiency: Randomised, double-blind, controlled, exploratory study. *Br. J. Ophthalmol.* **2007**, *91*, 47–50. [[CrossRef](#)] [[PubMed](#)]
20. Sand, B.B.; Marner, K.; Norn, M.S. Sodium hyaluronate in the treatment of keratoconjunctivitis sicca. A double masked clinical trial. *Acta Ophthalmol.* **1989**, *67*, 181–183. [[CrossRef](#)]
21. Fallacara, A.; Manfredini, S.; Durini, E.; Vertuani, S. Hyaluronic acid fillers in soft tissue regeneration. *Facial Plast. Surg.* **2017**, *33*, 87–96. [[CrossRef](#)] [[PubMed](#)]
22. Williams, D.L.; Mann, B.K. Efficacy of a crosslinked hyaluronic acid-based hydrogel as a tear film supplement: A masked controlled study. *PLoS ONE* **2014**, *9*, e99766. [[CrossRef](#)] [[PubMed](#)]
23. Williams, D.L.; Mann, B.K. A crosslinked HA-based hydrogel ameliorates dry eye symptoms in dogs. *Int. J. Biomater.* **2013**, *2013*, 460437. [[CrossRef](#)] [[PubMed](#)]
24. Yang, G.; Espandar, L.; Mamalis, N.; Prestwich, G.D. A cross-linked hyaluronan gel accelerates healing of corneal epithelial abrasion and alkali burn injuries in rabbits. *Vet. Ophthalmol.* **2010**, *13*, 144–150. [[CrossRef](#)] [[PubMed](#)]
25. Wiroszko, B.; Mann, K.B.; Williams, D.L.; Prestwich, G.D. Ophthalmic uses of a thiol-modified hyaluronan-based hydrogel. *Adv. Wound Care (New Rochelle)* **2014**, *3*, 708–716. [[CrossRef](#)] [[PubMed](#)]
26. Williams, D.L.; Wiroszko, B.M.; Gum, G.; Mann, B.K. Topical cross-linked HA-based hydrogel accelerates closure of corneal epithelial defects and repair of stromal ulceration in companion animals. *Investig. Ophthalmol. Vis. Sci.* **2017**, *58*, 4616–4622. [[CrossRef](#)] [[PubMed](#)]
27. Calles, J.A.; Tàrtara, L.I.; Lopez-García, A.; Diebold, Y.; Palma, S.D.; Vallés, E.M. Novel bioadhesive hyaluronan-itaconic acid crosslinked films for ocular therapy. *Int. J. Pharm.* **2013**, *455*, 48–56. [[CrossRef](#)] [[PubMed](#)]
28. Calles, J.A.; Lopez-García, A.; Vallés, E.M.; Palma, S.D.; Diebold, Y. Preliminary characterization of dexamethasone-loaded cross-linked hyaluronic acid films for topical ocular therapy. *Int. J. Pharm.* **2016**, *509*, 237–243. [[CrossRef](#)] [[PubMed](#)]
29. Postorino, E.I.; Rania, L.; Aragona, E.; Mannucci, C.; Alibrandi, A.; Calapai, G.; Puzzolo, D.; Aragona, P. Efficacy of eye drops containing cross-linked hyaluronic acid and coenzyme Q10 in treating patients with mild to moderate dry eye. *Eur. J. Ophthalmol.* **2017**. [[CrossRef](#)]
30. Cagini, C.; Torroni, G.; Fiore, T.; Cerquaglia, A.; Lupidi, M.; Aragona, P.; Iaccheri, B. Tear film stability in Sjogren syndrome patients treated with hyaluronic acid versus crosslinked hyaluronic acid-based eye drops. *J. Ocul. Pharmacol. Ther.* **2017**, *33*, 539–542. [[CrossRef](#)] [[PubMed](#)]
31. Citernes, U.R.; Beretta, L.; Citernes, L. Cross-Linked Hyaluronic Acid, Process for the Preparation Thereof and Use Thereof. Patent WO/2015/007773 A1, 22 January 2015.
32. Charlton, J.F.; Schwab, I.R.; Stuchell, R. Topical urea as a treatment for non-infectious keratopathy. *Acta Ophthalmol. Scand.* **1996**, *74*, 391–394. [[CrossRef](#)] [[PubMed](#)]
33. Van Goethem, F.; Adriaens, E.; Alepee, N.; Straube, F.; De Wever, B.; Cappadoro, M.; Catoire, S.; Hansen, E.; Wolf, A.; Vanparys, P. Prevalidation of a new in vitro reconstituted human cornea model to assess the eye irritating potential of chemicals. *Toxicol. In Vitro* **2006**, *20*, 1–17. [[CrossRef](#)] [[PubMed](#)]
34. Fischer, A.H.; Jacobson, K.A.; Rose, J.; Zeller, R. Hematoxylin and eosin staining of tissue and cell sections. *CSH Protoc.* **2008**. [[CrossRef](#)] [[PubMed](#)]
35. Valacchi, G.; Pecorelli, A.; Mencarelli, M.; Carbotti, P.; Fortino, V.; Muscettola, M.; Maioli, E. Rottlerin: A multifaced regulator of keratinocyte cell cycle. *Exp. Dermatol.* **2009**, *18*, 516–521. [[CrossRef](#)] [[PubMed](#)]
36. Condon, P.I.; McEwen, C.G.; Wright, M.; Mackintosh, G.; Prescott, R.J.; McDonald, C. Double blind, randomized, placebo controlled, crossover, multicenter study to determine the efficacy of a 0.1% (w/v) sodium hyaluronate solution (Fermavisc) in the treatment of dry eye syndrome. *Br. J. Ophthalmol.* **1999**, *83*, 1121–1124. [[CrossRef](#)] [[PubMed](#)]

37. Papa, V.; Aragona, P.; Russo, S.; Di Bella, A.; Russo, P.; Milazzo, G. Comparison of hypotonic and isotonic solutions containing sodium hyaluronate on the symptomatic treatment of dry eye patients. *Ophthalmology* **2001**, *215*, 124–127. [[CrossRef](#)] [[PubMed](#)]
38. Williams, D.; Middleton, S.; Fattahian, H.; Moridpour, R. Comparison of hyaluronic acid-containing topical eye drops with carbomer-based topical ocular gel as a tear replacement in canine keratoconjunctivitis sicca: a prospective study in twenty-five dogs. *Vet. Res. Forum* **2012**, *3*, 229–232. [[PubMed](#)]

Sample Availability: Samples of the compound HA-CL with urea are not available from the authors.



© 2017 by the authors. Licensee MDPI, Basel, Switzerland. This article is an open access article distributed under the terms and conditions of the Creative Commons Attribution (CC BY) license (<http://creativecommons.org/licenses/by/4.0/>).

A.1.2. Other publications, patents and conference proceedings during candidacy

El Kechai, N., Geiger, S., Fallacara, A., Cañero Infante, I., Nicolas, V., Ferrary, E., Huang, N., Bochet, A., Agnely, F., 2017. Mixtures of hyaluronic acid and liposomes for drug delivery: Phase behavior, microstructure and mobility of liposomes. *Int. J. Pharm.* 523, 246-259.

Fallacara, A., Busato, L., Pozzoli, M., Ghadiri, M., Ong, H.X., Young, P.M., Manfredini, S., Traini, D., 2017. Conference abstract: Inhalable Hyaluronic Acid Derivate for Inflammatory Lung Diseases. Presented at the 2017 Drug Delivery Australia Conference, Wollongong, NSW, Australia.

Fallacara, A., Manfredini, S., Durini, E., Vertuani, S., 2017a. Hyaluronic acid fillers in soft tissue regeneration. *Facial Plast. Surg.* 33, 87-96.

Fallacara, A., Vertuani, S., Manfredini, S., Citernes, U.R., 2018. Patent Appl. Filed, n. 102018000008192.

Manfredini, S., Fallacara, A., De Caria, G., Vertuani, S., Anno Accademico 193: 2015-2016. L'acido ialuronico (AI) nei trattamenti estetici, una review critica. *Atti dell'Accademia delle Scienze di Ferrara.* 93, 115-139.

Manfredini, S., Radice, M., Ziosi, P., Dissette, V., Buso, P., Fallacara, A., Bino, A., Vertuani, S., 2017. Conference paper: Botanical photo-protection alternatives to synthetic UV filters. In *Proceedings of the 8th Annual Conference American Council for Medicinally Active Plants (ACMAP)*, Clemson University, Clemson, SC, USA.

Radice, M., Manfredini, S., Ziosi, P., Dissette, V., Buso, P., Fallacara, A., Vertuani, S., 2016. Herbal extracts, lichens and biomolecules as natural photo-protection alternatives to synthetic UV filters. A systematic review. *Fitoterapia.* 114, 144-162.



Contents lists available at ScienceDirect

International Journal of Pharmaceutics

journal homepage: www.elsevier.com/locate/ijpharm

Mixtures of hyaluronic acid and liposomes for drug delivery: Phase behavior, microstructure and mobility of liposomes



Naila El Kechai^a, Sandrine Geiger^a, Arianna Fallacara^{a,1}, Ingrid Cañero Infante^b, Valérie Nicolas^c, Evelyne Ferrary^d, Nicolas Huang^a, Amélie Bochot^{a,2}, Florence Agnely^{a,2,*}

^a Institut Galien Paris-Sud, CNRS UMR 8612, Univ. Paris-Sud, Université Paris-Saclay, 92290 Châtenay-Malabry, France

^b SPMS, Ecole Centrale Paris, UMR 8580 CNRS, Université Paris-Saclay, 92290 Châtenay-Malabry, France

^c UMS IPSIT, Plate-forme d'imagerie cellulaire, Univ. Paris-Sud, Université Paris-Saclay, 92290 Châtenay-Malabry, France

^d UMR-S 1159 Inserm/Université Pierre et Marie Curie – Sorbonne Universités "Minimally Invasive Robot-based Hearing Rehabilitation", 16 rue Henri Huchard, 75018 Paris, France

ARTICLE INFO

Article history:

Received 14 December 2016

Received in revised form 3 March 2017

Accepted 16 March 2017

Available online 18 March 2017

Chemical compounds studied in this article:

Cholesterol (PubChem CID: 5997)

1,2-distearoyl-sn-glycero-3-phosphoethanolamine-N-[methoxy-poly-(ethylene-glycol)-2000] (PubChem CID: 406952)

Phosphatidylcholine (PubChem CID: 52922911)

L- α -phosphatidylglycerol (PubChem CID: 24779550)

Rhodamine (PubChem CID: 6694)

Sodium hyaluronate (PubChem CID: 3084049)

Stearylamine (PubChem CID: 15793)

Keywords:

Atomic force microscopy

Depletion

Drug delivery

Hydrogel

Phase separation

Single particle tracking

ABSTRACT

Hyaluronic acid liposomal gels have previously demonstrated in vivo their great potential for drug delivery. Elucidating their phase behavior and structure would provide a better understanding of their use properties. This work evaluates the microstructure and the phase behavior of mixtures of hyaluronic acid (HA) and liposomes and their impact on the vesicle mobility. HA concentration and surface properties of liposomes (positively or negatively charged, neutral, with a polyethylene glycol corona) are varied while the liposome concentration remains constant. Below the entanglement concentration of HA (0.4%), the mixtures exhibit a depletion phase separation except for positively charged liposomes that interact with anionic HA through attractive electrostatic interactions. At high HA concentration, no macroscopic phase separation is observed, except a slight syneresis with cationic liposomes. The microstructure shows aggregates of liposomes homogeneously distributed into a HA network except for PEGylated liposomes, which seem to form bicontinuous interpenetrating networks. The diffusion of liposomes is controlled by HA concentration and their surface properties. Finally, PEGylated liposomes display the highest mobility at high HA concentration (2.28%) both macro- and microscopically. The microstructure of HA-liposomes mixtures and the diffusion of liposomes are key parameters that must be taken into account for drug delivery.

© 2017 Elsevier B.V. All rights reserved.

1. Introduction

In the field of drug delivery, nanomedicines are being developed based on colloidal carriers to deliver therapeutic agents to specific target tissues (Bozzuto and Molinari, 2015; Couvreur, 2013). Among colloidal particles, liposomes appear particularly attractive. Indeed, they are biodegradable and deformable, their surface can easily be tuned by lipid composition, their size can be controlled and they can also act as a reservoir for encapsulated molecules (Bozzuto and Molinari, 2015). Moreover, several liposomal

Abbreviations: AFM, atomic force microscopy; Chol, cholesterol; DSPE-PEG2000, 1,2-distearoyl-sn-glycero-3-phosphoethanolamine-N-[methoxy-poly-(ethylene-glycol)-2000]; EPC, egg phosphatidylcholine; Fl, fluoresceinamine; HA, hyaluronic acid; Lip, liposome; MSD, mean square displacement; Pdl, polydispersity index; PE, phosphatidylethanolamine; PEG, polyethylene glycol; PG, phosphatidylglycerol; Rh, rhodamine; SA, stearylamine.

* Corresponding author.

E-mail address: florence.agnely@u-psud.fr (F. Agnely).

¹ Present address: School of Pharmacy, Department of Life Sciences and Biotechnology, University of Ferrara, Via Luigi Borsari 46, 44121 Ferrara, Italy.

² Florence Agnely and Amélie Bochot contributed equally.

<http://dx.doi.org/10.1016/j.ijpharm.2017.03.029>

0378-5173/© 2017 Elsevier B.V. All rights reserved.

formulations are currently on the market (Bozzuto and Molinari, 2015; Allen and Cullis, 2013).

The incorporation of liposomes into concentrated polymer solutions or hydrogels is an efficient strategy to deliver drugs locally. The benefits of this combination are to prolong the residence time of drugs at the site of administration following local administration, to control the drug release for a longer period of time, to increase the stability of the liposomes and drugs and to avoid their rapid clearance (Lajavardi et al., 2009; El Kechai et al., 2016; Grijalvo et al., 2016; Ensign et al., 2014; O'Neill et al., 2017). Recently, Grijalvo et al. reviewed the biopolymers used to prepare liposome-encapsulated hydrogels for biomedical applications, the most studied being chitosan, alginate, gelatin and hyaluronic acid (HA) (Grijalvo et al., 2016). Among these polymers, HA is a very promising candidate. This linear polysaccharide composed of D-glucuronic acid and N-acetyl-D-glucosamine is mucoadhesive, biodegradable and biocompatible and is found in animals and human body. HA is soluble in water at neutral pH and behaves as a negatively charged semi-rigid polyelectrolyte (Gatej et al., 2005; Lapčik et al., 1998). High molecular weight HA chains start to overlap at a very low HA concentration to form a transient network (Krause et al., 2001; De Smedt et al., 1993) with viscoelastic properties (Lapčik et al., 1998; Masuda et al., 2001; Scott and Heatley, 1999). Due to these properties and its strong hydrophilic character, HA has important structural and functional roles in the body, especially in the eye, the joint and the skin (Volpi et al., 2009).

Our group has designed and evaluated *in vivo* mixtures of PEGylated liposomes and HA (1.5MDa). For these studies, a polymer concentration of 2.28% was selected to obtain comparable viscoelastic properties to that of a commercial HA gel used in ophthalmic surgery (Provisc[®]) (Lajavardi et al., 2009). A high lipid concentration (50 or 80 mM) was chosen to maximize drug loading in the final formulation and was easily obtained by the direct rehydration of the HA powder with the liposomal suspension. This system demonstrated its efficacy in rats in the treatment of endotoxin-induced uveitis using vasoactive intestinal peptide as an immunosuppressive agent. Indeed, an intravitreal injection of the HA liposomal formulation reduced significantly the clinical score and the number of inflammatory cells infiltrating the eye (Lajavardi et al., 2009). Recently, we also showed that after an injection in the middle ear of guinea pigs, such mixture sustained the delivery of a corticoid at therapeutic dose until 30 days in perilymph, the liquid of the inner ear (El Kechai et al., 2016).

Interestingly, PEGylated liposomes were able to diffuse through the HA network and to accumulate within the round window, the biological membrane separating the middle and the inner ear (El Kechai et al., 2016). To better understand these promising results and to design a new formulation platform, we performed a physicochemical study of mixtures of HA and liposomes with various surface properties (neutral, cationic, anionic or PEGylated) (El Kechai et al., 2015). Whatever the characteristics of the liposomes added, the viscosity and the elasticity of HA aqueous solutions at 2.28% (the concentration used *in vivo*) increased in a lipid concentration-dependent manner. Indeed, liposomes strengthened the HA network. This effect depended on liposome composition and concentration. The highest viscosity and elasticity were observed with PEGylated liposomes and the lowest with neutral liposomes (El Kechai et al., 2015).

Elucidating the phase behavior, the structure and the interactions in these composite formulations would provide a better understanding and control of their use properties. The first goal of the present study was to evaluate the microstructure and the compatibility of HA liposomal mixtures at different HA concentrations using highly concentrated liposomes characterized by different surface properties. Thus, different types of interactions could occur between the polymer and the vesicles. The second goal was to study the influence of HA concentration and liposome composition on their mobility into HA solutions. Indeed, the diffusion of liposomes is a key parameter for drug delivery. These migration properties were correlated to the interactions between HA and liposomes and to the microstructure of the mixtures.

2. Materials and methods

2.1. Materials

Egg phosphatidylcholine (EPC, purity 96%) was provided by Lipoid GmbH (Ludwigshafen, Germany). Cholesterol (Chol), egg L- α -phosphatidylglycerol (PG), stearylamine (SA) and fluorescein-amine (purities >98%) and triton X-100, were purchased from Sigma-Aldrich Co. (St. Louis, USA). 1,2-distearoyl-sn-glycero-3-phosphoethanolamine-N-[methoxy-poly-(ethyleneglycol)-2000] (DSPE-PEG2000) and phosphatidylethanolamine-N-(lissamine rhodamine B sulfonyl) (PE-Rh) (purities >99%) were obtained from Avanti Polar Lipids, inc. (Alabaster, USA). Sodium hyaluronate (HA, Mw 1.5 MDA, purity 95%) was provided by Acros Organics (New Jersey, USA). All other chemicals were of analytical grade.

Table 1
Composition and physicochemical properties of liposomes.

Liposome Denomination ^a	Composition Lipid ratios (mole%) ^a	Hydrodynamic Diameter, d_h (nm)	<i>Pdl</i>	ζ -Potential (mV)
Lip	EPC:Chol 65:35	167 ± 49	0.09	-1 ± 6
Lip-Rh	EPC:Chol:PE-Rh 64:35:1	163 ± 52	0.10	-9 ± 7
Lip SA	EPC:Chol:SA 55:35:10	153 ± 50	0.07	64 ± 12
Lip SA-Rh	EPC:Chol:SA:PE-Rh 54:35:10:1	164 ± 59	0.08	30 ± 7
Lip PG	EPC:Chol:PG 55:35:10	147 ± 62	0.11	-57 ± 10
Lip PG-Rh	EPC:Chol:PG:PE-Rh 54:35:10:1	158 ± 60	0.13	-41 ± 8
Lip PEG	EPC:Chol:DSPE-PEG ₂₀₀₀ 60:35:5	132 ± 50	0.11	-25 ± 10
Lip PEG-Rh	EPC:Chol:DSPE-PEG ₂₀₀₀ :PE-Rh 59:35:5:1	134 ± 44	0.06	-22 ± 11

^a Abbreviations are defined in the material Section (2.1).

2.2. Preparation and characterization of liposomes

Liposomes labeled with rhodamine (PE-Rh) and unlabeled liposomes were prepared by the thin film hydration method. The composition and denomination of all the formulations used in this study are presented in Table 1. Briefly, lipids dissolved in chloroform were introduced in a round bottom flask. After evaporation of the organic phase, the resulting lipid film was hydrated with HEPES/NaCl buffer (10/145 mM, pH 7.4) to achieve a theoretical final lipid concentration of 20 mM and 100 mM for labeled and unlabeled liposomes respectively. The liposome suspensions were subsequently extruded 10 times through 0.2 μm polycarbonate filters fitted in LIPEX extruder (Whitley, Vancouver, Canada).

The hydrodynamic diameter and the zeta potential of the liposomes were determined in triplicate by dynamic light scattering (DLS) at 25 °C using a Zetasizer Nano ZS (Malvern, Worcestershire, UK following a 1/50 (v/v) dilution in milliQ water.

The concentration of EPC in unlabeled liposomes was evaluated after extrusion through an enzymatic phospholipid assay (Biolabo SA, Maizy, France) (El Kechai et al., 2015). The total amount of lipids in liposome suspensions was then calculated from EPC concentration assuming that lipid composition remained unchanged during the different steps of liposome preparation. The final lipid concentration varied between 90 and 95 mM corresponding to a percent of lipid loss after extrusion between 5 and 10%. Then, the liposome suspensions were diluted into HEPES/NaCl buffer to obtain the desired final lipid concentration. Since rhodamine interferes with absorbance measurements, the lipid concentration of rhodamine-conjugated liposomes was estimated by taking into account the average percentage of lipid loss after extrusion.

2.3. Preparation of HA liposomal formulations

2.3.1. Formulations for rheological study and macroscopic observation

HA solutions (from 0.05 to 2.28% (w/v)) were prepared by dissolving HA powder in HEPES/NaCl buffer (10/145 mM, pH 7.4). HA liposomal mixtures (HA-Lip, HA-Lip SA or HA-Lip PEG) were prepared by dissolving HA (from 0.05 to 2.28% w/v) in unlabeled liposome suspensions, each at 80 mM final lipid concentration. HA solutions and HA-liposomes mixtures were then homogenized by vortexing for 5 min, maintained at room temperature for 1 h and then stored at 4 °C for at least 12 h prior to rheological measurements. Their homogeneity was assessed in storage conditions (4 °C) by macroscopic observation 36 h after preparation.

2.3.2. Formulations for confocal microscopy and atomic force microscopy (AFM)

The microstructure of HA liposomal mixtures was studied on the same formulations both by confocal and atomic force microscopies. To localize HA and liposomes by confocal microscopy, liposomes were labeled with rhodamine (see Section 2.2) and HA with fluoresceinamine (FI-HA) as described previously (Lajavardi et al., 2009). Briefly, 25 mg of HA was dissolved in 20 mL milliQ water and mixed with 20 mL dimethylsulfoxide. Then, fluoresceinamine (12.5 mg) dissolved in dimethylsulfoxide (0.25 mL) containing acetaldehyde (12.5 μL) and cyclohexyl isocyanide (12.5 μL) was added to the mixture and the pH was adjusted to 4.5. The solution was maintained for one night at room temperature under magnetic stirring and protected from light. FI-HA was then precipitated in cold absolute ethanol by adding a saturated NaCl solution, centrifuged and resuspended in water. Centrifugation was repeated three times and the final pellet was resuspended in 12.5 mL milliQ water and then purified by dialysis (cellulose dialysis membranes, Mw cut off 50 kDa) against 2 L

milliQ water for 48 h with repeated changes of water and protected from light. FI-HA purified solution was finally freeze-dried and stored at 4 °C before use.

Fluorescent HA liposomal mixtures were prepared at a 2.28% (w/v) final HA concentration and a 80 mM final lipid concentration. To avoid a saturation of the fluorescence signals, FI-HA was combined with unlabeled HA and Rh-liposomes with unlabeled liposomes as follows. Freeze-dried FI-HA (8.2 mg corresponding to 4.6 mg HA) was mixed with HA powder (41 mg) before rehydration with 2 mL of Lip/Lip-Rh, Lip SA/Lip SA-Rh, Lip PG/Lip PG-Rh or Lip PEG/Lip PEG-Rh respectively (at a molar lipid ratio of 72 unlabeled/8 labeled).

2.3.3. Formulations for videomicroscopy

The aim of the videomicroscopy study was to assess the mobility of liposomes within HA below and above its entanglement concentration as a function of their surface properties. The final lipid concentration in the mixtures was 80 mM and HA concentration was 0.25% or 2.28% (w/v). To obtain a suitable number of fluorescent particles for single particle tracking, 0.01% (v/v) of rhodamine-conjugated liposomes were introduced in unlabeled liposome suspensions. HA-liposomes mixtures were prepared as described previously by dissolving HA powder in liposome suspension blends (see Section 2.3.1).

2.4. Rheological measurements

Flow measurements were carried out using a rotational rheometer ARG2 (TA instruments, New Castle, USA) using an aluminum cone/plate geometry (diameter 4 cm, angle 1° and cone truncation 28 μm). Flow measurements were performed at 37 °C by a shear rate sweep. After a 2-min equilibration time, the shear rate was increased gradually from 0.01 to 1000 s^{-1} . Measurements were at least triplicated and performed under steady state conditions. The viscosity curves were fitted according to the Cross equation (Cross, 1968) to determine the zero-shear rate viscosity (El Kechai et al., 2015). For HA solutions from 0.05 to 2.28% (w/v), the specific viscosity (η_{sp}) was calculated according to Eq. (1):

$$\eta_{sp} = \frac{\eta_0 - \eta_{solv}}{\eta_{solv}} \quad (1)$$

where η_0 is the zero-shear rate viscosity of the HA solution and η_{solv} is the viscosity of the solvent (HEPES/NaCl buffer 10/145 mM, pH 7.4, $\eta_{solv} = 0.83 \text{ mPa s}$ measured at 37 °C).

2.5. Confocal microscopy

Fluorescent HA liposomal mixtures (HA-Lip, HA-Lip SA, HA-Lip PG, HA-Lip PEG) and fluorescent HA, placed between glass slide and slip cover, were observed with an inverted confocal laser scanning microscope Leica TCS SP8 (Leica, Germany) using a HC PL APO CS2 63 \times /1.40 oil immersion objective lens. The excitation sources were provided by a white light laser (WLL) (495 nm and 552 nm selected excitation wavelength). The corresponding fluorescence emission was collected in sequential mode using 504–542 nm (fluorescein) and 565–700 nm (rhodamine B) wide slits respectively. The pinhole was set at 1.0 Airy unit. 12-bit numerical images were obtained with Leica SP8 LAS AF software (Version 3.6; Leica, Germany). For each HA liposomal mixture, three different samples were observed at different locations and with various magnifications. The microscopic aspect for each HA, HA-Lip, HA-Lip SA, HA-Lip PG and HA-Lip PEG samples analyzed was equivalent over the entire surface of the sample.

2.6. Atomic force microscopy (AFM)

AFM images were collected in air at room temperature (22 °C) using a commercial Multimode-8 equipped with a NanoScope V controller and an “E” scanner (10 μm) from Bruker manufacturer (Bruker, AXS, France). Topographical and mechanical properties (dissipation and Young modulus) were imaged using the QNM (Quantitative NanoMechanical Property) mode with a nano-indentation frequency of 2 kHz. SCANASYST-AIR cantilevers of a nominal spring constant of 0.4 N m⁻¹ were used (tip radius of about 8 nm). The scan rate was adjusted in the range of 1 Hz over selected areas in dimension of 1.0 μm × 1.0 μm and 10.0 μm × 10.0 μm. The samples (HA, HA-Lip, HA-Lip SA, HA-Lip PG, HA-Lip PEG) were deposited on clean mica surfaces fixed on a magnetic disk directly mounted on top of the AFM scanner. The samples were dried at room temperature for at least 1 h before imaging. Data processing was performed with the WSxM and Bruker softwares.

2.7. Turbiscan® optical analysis

A Turbiscan MA 2000 (Formulacion, L'Union, France) was used to optically assess the migration of Lip, Lip SA, Lip PG and Lip PEG prepared as described previously into HA solution at 2.28%. HA samples (4 mL) were prepared in the cylindrical glass cells supplied by the manufacturer and analyzed prior to liposome addition. Each liposome suspension (1 mL at 80 mM) was subsequently placed in the cell in contact with HA solution and the sample was analyzed instantly (t_0). All the samples were then incubated at 37 °C for 10 days and acquisitions were performed at 1, 3, 7 and 10 days of incubation (t_1 , t_3 , t_7 , t_{10} respectively). The detection head of Turbiscan MA 2000 was composed of a pulsed near-infrared light source ($\lambda = 850$ nm) and two synchronous transmission and back scattering detectors. The transmission detector received the light which crosses the sample (at 180° from the incident beam), while the back scattering detector received the light scattered backward by the sample (at 45° from the incident beam). The detection head scanned the entire height of the sample, acquiring the transmitted and back scattered intensities every 40 μm for each time point (t_0 , t_1 , t_3 , t_7 , t_{10}).

2.8. Videomicroscopy and single particle tracking

The mobility of Lip, Lip SA, Lip PG, Lip PEG into HA (0.25 or 2.28% w/v) was measured using videomicroscopy and single particle tracking by analyzing the trajectories of the rhodamine-labeled liposomes. HA-liposomes samples (100 μL) were deposited in 8-well glass chambers (Labtek, Campbell, CA) and incubated for 20 min in an XL incubator at 37 °C before microscopic observation. 30 s movies with a 100 ms temporal resolution were acquired thanks to a charge-coupled device (CCD) H5m camera (9.9 μm pixel size) mounted on an inverted epifluorescence AxioObserver Z1-Colibri videomicroscope (Carl Zeiss, Germany). Time-lapse images were acquired with a 63x/1.4-numerical-aperture (NA) oil-immersion objective lens, a 555 nm light-emitting diode (LED) for excitation, and a band-pass 605/70 nm filter to collect the emission of fluorescence. Movies were analyzed using the 3D Tracking module of Image J and Matlab software. 3 independent experiments were performed and a total of 100 <math>n < 300</math> trajectories were analyzed for each condition. The coordinates of particle centroids were transformed into time-averaged mean square displacement (MSD) as described before by Suh et al. (2005).

3. Results

3.1. Characterization of liposomes

Different liposome formulations – fluorescently labeled or not – were prepared. Their denomination, composition and properties are gathered in Table 1. All unlabeled liposomes (Lip, Lip SA, Lip PG, Lip PEG) and their equivalent rhodamine-conjugated liposomes (Lip-Rh, Lip SA-Rh, Lip PG-Rh, Lip PEG-Rh) showed narrow size distributions characterized by mean hydrodynamic diameters around 150 nm and a $PDI \leq 0.2$ (Table 1). Zeta potential values were almost neutral for Lip and Lip-Rh, positive for Lip SA and Lip SA-Rh, negative for Lip PG, Lip PG-Rh, Lip PEG and Lip PEG-Rh (Table 1). The presence of rhodamine did not alter the surface properties of liposomes except for the positively charged ones in which rhodamine slightly decreased the zeta potential value (Table 1).

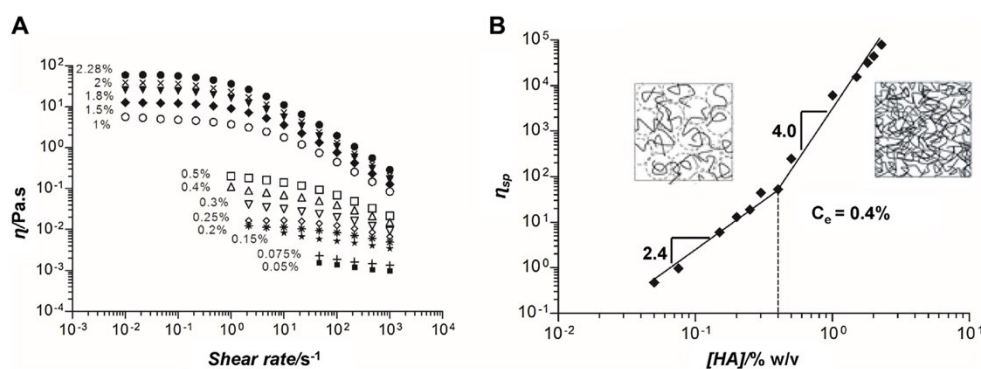


Fig. 1. Determination of the entanglement concentration (C_e) of HA in HEPES/NaCl buffer (10/145 mM, pH 7.4) at 37 °C. A: apparent viscosity as function of shear rate for HA solutions in the range 0.05–2.28% (w/v). B: variations of specific viscosities (η_{sp}) versus concentrations of HA. 2.4 and 4.0 represent the scaling exponents in semi-dilute unentangled and entangled regimes respectively.

3.2. Entanglement concentration of HA (C_e)

Variations of the apparent viscosity of HA in HEPES/NaCl buffer as function of shear rate at 37 °C are given in Fig. 1A. The rheograms show a shear-thinning behavior of HA solutions all over the concentration range studied (0.05 to 2.28% w/v). The specific viscosity (η_{sp}) was calculated as described in the experimental section (Section 2.4) for each HA solution and the concentration dependence of η_{sp} was plotted in Fig. 1B. The entanglement concentration (C_e) characterizes the transition between the semi-dilute unentangled and the entangled regimes. It is represented by a change in the slope of the logarithmic η_{sp} versus concentration curve and was determined to be $C_e=0.4\%$ (w/v) for HA at 37 °C (Fig. 1B). The scaling laws obtained for the variation of specific viscosity were $\eta_{sp} \sim C^{2.4}$ ($C < C_e$) and $\eta_{sp} \sim C^{4.0}$ ($C > C_e$).

3.3. Phase behavior of HA liposomal mixtures

Liposome suspensions without HA remained homogeneous for at least 15 days except for Lip suspension that showed a reversible

aggregation and sedimentation due to the zeta potential value close to zero. HA solutions between 0.05 and 2.28% containing 80 mM unlabeled liposomes (Lip, Lip SA, Lip PEG) were macroscopically homogeneous 30 min after their preparation indicating that HA liposomal mixtures did not undergo instantaneous phase separation. At 36 h, for HA concentrations above C_e , all samples appeared homogeneous except Lip SA into HA at 2.28%, which exhibited a slight syneresis (Fig. 2). At 37 °C, the viscosity of the HA liposome samples at a 2.28% polymer concentration strongly depended on liposome composition (Table 2) in the following order: Lip PEG > Lip PG > Lip SA > Lip. At 36 h, below C_e , HA-Lip SA mixtures remained homogeneous while a macroscopic phase separation was observed between 0.05 to 0.25% for Lip and between 0.075 and 0.4% for Lip PEG (Fig. 2). HA-Lip PG (not presented in Fig. 2) was studied at two HA concentrations and showed a macroscopic phase separation at 0.25% and none at 2.28%. Phase separation was characterized by a higher opacity at the bottom of the sample whereas its surface became more transparent suggesting sedimentation of liposomes.

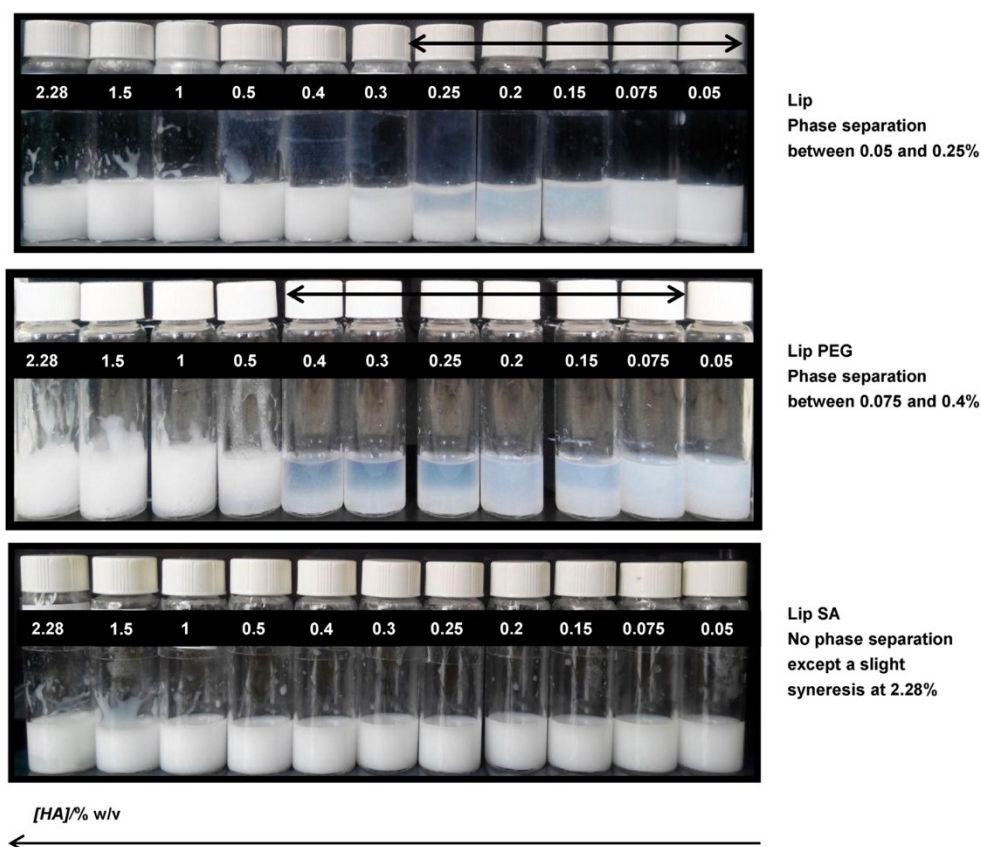


Fig. 2. Phase behavior of HA liposomal formulations (Lip, Lip PEG and Lip SA). Images were taken 36 h after preparation of HA solutions (0.05 to 2.28% (w/v)) containing liposomes (80 mM). Samples were stored at 4 °C.

Table 2
Rheological and diffusion properties of HA liposomal formulations.

[HA] % (w/v)	Liposomes	[Lipids] mM	η_0^a (Pa s)	α^b	D_w/D_{HA}^c	Median $\text{Log}_{10}(\text{MSD}_{t=1s})^d$
0.25	Lip	80	nd ^e	0.03	106	-2.12
	Lip SA	80	0.05 ± 0.01	0.01	444	-2.22
	Lip PG	80	nd	0.42	30	-0.33
	Lip PEG	80	nd	0.31	67	-0.68
2.28	Lip	80	245 ± 38	8.5×10^{-4}	7126	-3.23
	Lip SA	80	319 ± 33	9.8×10^{-5}	6613	-3.07
	Lip PG	80	436 ± 22	1.1×10^{-3}	1226	-2.75
	Lip PEG	80	786 ± 67	5.0×10^{-3}	946	-2.75

^a η_0 is the zero-shear rate viscosity representing the viscosity at rest of the HA liposomal formulations at 37 °C.

^b α is the slope of the average MSD versus time curve on a logarithmic scale. Brownian diffusion is represented by $\alpha = 1$, whereas a decrease in α indicates an increased hindrance to diffusion. A particle is completely immobile when $\alpha = 0$.

^c D_w is the theoretical diffusivity of liposomes in water calculated from the Stokes-Einstein equation $D_w = \frac{k_B T}{3\pi\eta_w d_h}$, where k_B is the Boltzmann constant, T is the absolute temperature, η_w is the viscosity of water at this temperature (0.692 mPa.s), and d_h is the hydrodynamic diameter of the liposomes. D_{HA} is the effective diffusivity of liposomes in HA determined from single particle tracking experiments at a time scale of 1 s. The ratio D_w/D_{HA} indicates by which factor the movements of liposomes in HA are slower than in water.

^d MSD is the mean square displacement of the liposomes expressed in μm^2 .

^e nd: non determined because of the phase separation of the sample.

3.4. Microscopic structure of HA liposomal mixtures

Both confocal microscopy and AFM revealed a micro-phase separation between HA and liposomes.

3.4.1. Confocal microscopy

For confocal microscopy experiments, HA was labeled with fluoresceinamine (green) and liposomes with rhodamine (red). Confocal image of HA solution (2.28%) without liposomes (Fig. 3A), shows a homogeneous green fluorescence. In presence of neutral,

negatively charged or PEGylated liposomes (HA-Lip, HA-Lip PG and HA-Lip PEG, Fig. 3B, D, E respectively), distinguishable and non-overlapping red and green fluorescences are observed indicating segregation between HA and liposomes. In Fig. 3C (Lip SA), beside the red and the green fluorescence, non-fluorescent zones were also visualized.

3.4.2. Atomic force microscopy (AFM)

AFM images were acquired both in topographic (Fig. 4A) and dissipation (Fig. 4B) modes. Both types of images showed

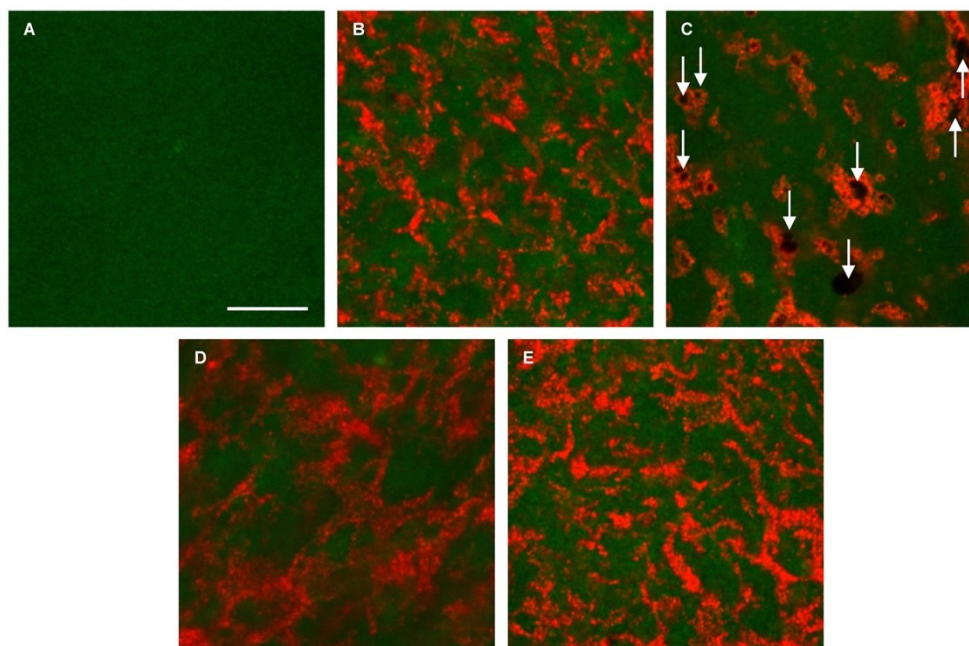


Fig. 3. Confocal images of HA liposomal formulations: HA without liposomes (A), HA-Lip (B), HA-Lip SA with white arrows pointing at non-fluorescent zones (C), HA-Lip PG (D) and HA-Lip PEG (E). HA was labeled with fluoresceinamine (green) and liposomes were labeled with rhodamine (red). The final concentrations were 2.28% (w/v) for HA (10% HA-fl and 90% unlabeled HA) and 80 mM for liposomes (10% liposomes-Rh and 90% unlabeled liposomes). Scale bar = 10 μm . (For interpretation of the references to colour in this figure legend, the reader is referred to the web version of this article.)

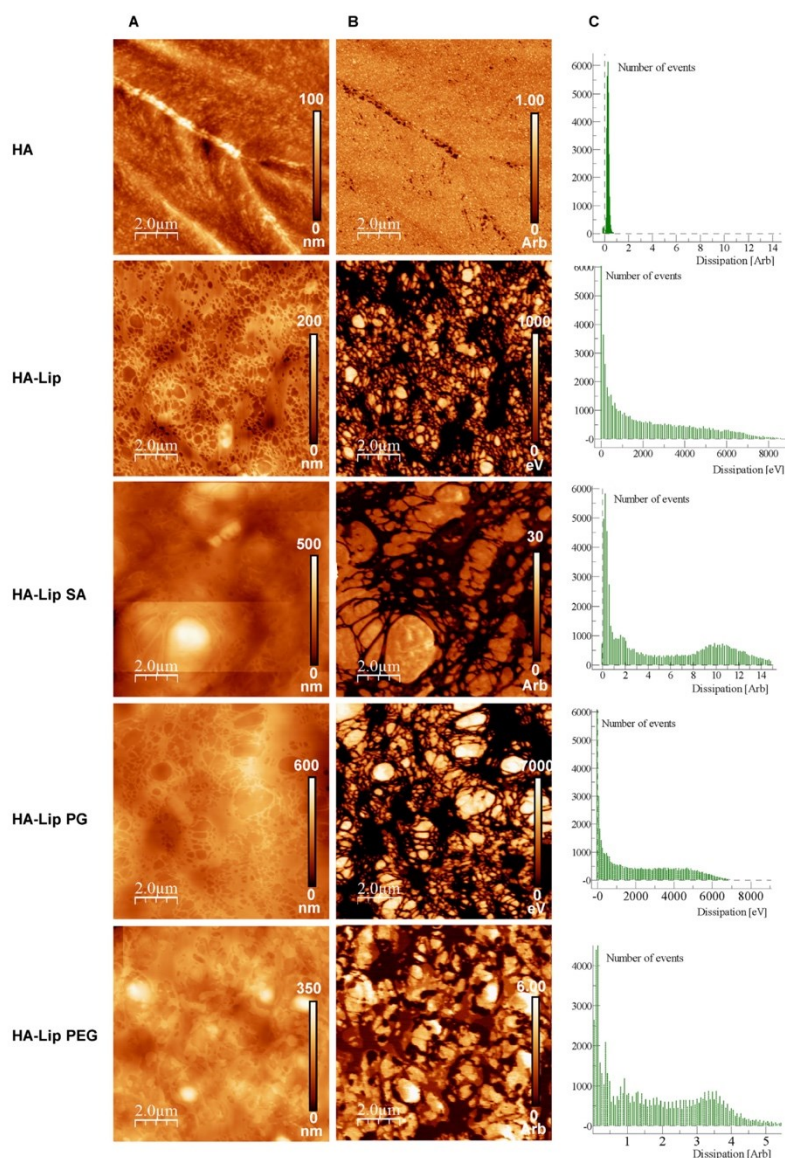


Fig. 4. AFM characterization of HA without liposomes and HA liposomal mixtures (HA-Lip, HA-Lip SA, HA-Lip PG, HA-Lip PEG). The concentration was 2.28% (w/v) for HA and 80 mM for liposomes. AFM images at a $10\ \mu\text{m}$ scan range in topographic mode (A) and dissipation mode (B). Dissipation profiles (C). Scale bar = $2\ \mu\text{m}$.

qualitatively the same features. However, the dissipation mode exhibited a more pronounced contrast. $1 \times 1\ \mu\text{m}$ AFM images showed vesicle-like shapes only in HA liposomal mixtures (data not shown). These objects were identified as liposomes as their size was comparable to that of the liposomes prepared (between 100 and 200 nm). From these data, the high dissipation property that appears as clear zones on AFM images in dissipation mode was attributed to liposomes, whereas the dark zones, corresponding to

low dissipation areas, were attributed to HA. In order to observe the segregation between HA and liposomes, the samples were imaged under a larger scale (Fig. 4). HA displayed uniform mechanical properties (Fig. 4B) represented by a unimodal dissipation peak (Fig. 4C). Conversely, all HA liposomal mixtures presented two zones with distinguishable mechanical properties: a liposome-rich area represented by clear zones dispersed within a dark network corresponding to HA (Fig. 4B). The segregation

between HA and liposomes led to a bimodal distribution of the dissipation as shown in Fig. 4C. A dissipation profile was determined for each formulation by taking a diagonal line in dissipation images (Fig. 4B). This allows measuring approximately the range of size of the liposome aggregates. HA-Lip seems to exhibit more and smaller liposome-rich areas (between 0.14 and 0.57 μm), whereas HA-Lip SA presents larger ones (between 0.21 and 2.12 μm). Aggregate sizes of HA-Lip PG (between 0.14 and 0.68 μm) were close to that of HA-Lip. For Lip PEG, the contrast between the two kinds of areas is less pronounced than for the others and aggregate sizes were between 0.17 and 1.08 μm .

The Young modulus measured from AFM experiments based on the DMT model (Derjaguin et al., 1975) was found to be 25–35 MPa for the liposome-rich phase and around 130–150 MPa for the HA-

rich phase. This values were obtained by taking a Poisson's ratio $\nu = 0.4$.

3.5. Mobility of liposomes into HA

The diffusion of liposomes with different surface characteristics was assessed both macroscopically using optical analysis and microscopically using single particle tracking.

3.5.1. Turbiscan[®] optical analysis of the migration of liposomes into HA

The principle of the experiment was based on the migration of the liposomes deposited at the surface of a HA solution (2.28%) (Fig. 5A), resulting in a variation of transmission and back scattered

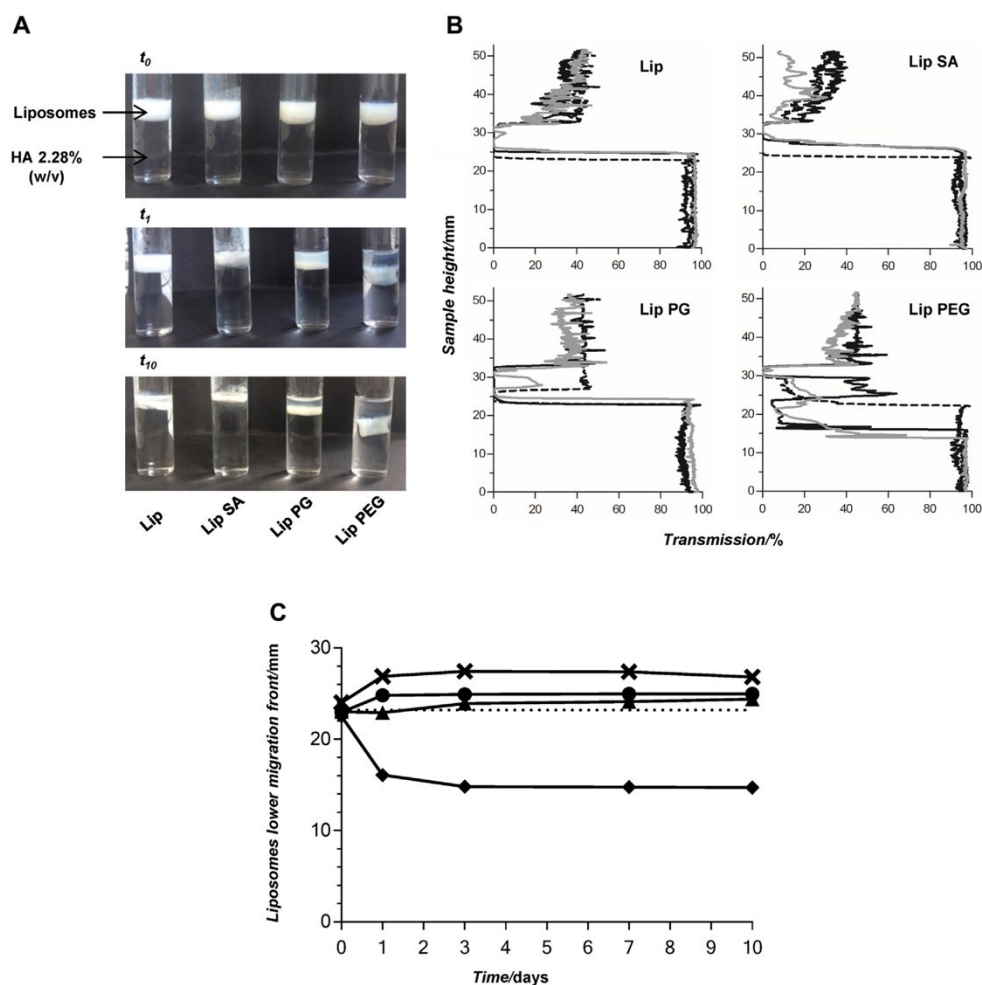


Fig. 5. Migration of the different liposome formulations at 80 mM into HA solution (2.28% (w/v)). A: Macroscopic observation. B: Turbiscan[®] optical analysis showing the % of light transmitted across the samples at different days: t_0 (discontinuous, black), t_1 (continuous, black) and t_{10} (grey). C: Liposome lower migration fronts for the various liposomes as function of time obtained from optical analysis: Lip (●), Lip SA (×), Lip PG (▲), Lip PEG (◆). The dotted line represents the position of liposomes at t_0 (~23 mm). (n = 1). The maximal uncertainty of the measurements is estimated to be 10%.

signals. Fig. 5B gives the variations of the percent of light transmitted across the sample when scanning its whole height. At t_0 , the 4-mL transparent HA sample (height around 25 mm) resulted in almost 100% of light transmission (Fig. 5B). The addition of the white opaque liposome suspensions led to a sharp decrease in light transmission at the surface of the sample (height between 23 and 35 mm). This allows to detect the location of the liposomes and their migration front as a function of time (Fig. 5C). Only Lip PEG were able to migrate into HA. Indeed, a migration front was observed macroscopically (Fig. 5A) and by optical analysis (Fig. 5B) starting from t_i . The migration of Lip PEG into HA was rapid within the first 24 h (t_i) and slowed down between t_i and t_{10} . No migration towards the bottom of the tube was noticed for the other formulations. However, a displacement of the liposome front upwards (towards the surface of the sample) occurred up to t_i , with no further evolution. This can be explained by the swelling of HA with the aqueous phase of the liposome suspension deposited on its surface at t_0 (Fig. 5C).

3.5.2. Microscopic mobility of liposomes in HA

Single particle tracking was used to quantitatively assess the diffusion of liposomes as a function of their surface properties (neutral, positive, negative or PEGylated) into HA solution at two concentrations. The lowest HA concentration (0.25%) was below the entanglement concentration ($C_e=0.4\%$) whereas the highest one (2.28%) was well above. Examples of videos are given in Supplementary data.

Whatever their composition, liposome movements in HA 2.28% were strongly hindered compared to their movements in HA 0.25%. This was demonstrated by significantly lower MSD and α values in

HA 2.28% compared to 0.25% (Table 2, Fig. 6C compared to Fig. 6A) and highly constrained trajectories in HA 2.28% (Fig. 6D compared to Fig. 6B). The liposomes with different surface characteristics displayed different diffusion profiles but followed the same trend in both HA 0.25% and 2.28% (Lip PEG = Lip PG > Lip > Lip SA, Fig. 6 and Table 2).

At 0.25% of HA, Lip PEG and Lip PG, which are both negatively charged, displayed the best diffusion properties, evidenced by their extended trajectories (Fig. 6B) and relatively high MSD (Fig. 6A). In addition, α values for Lip PEG and Lip PG were 0.31 and 0.42 respectively and their diffusion in HA 0.25% was only 30- and 67-fold lower than their theoretical diffusion in water (Table 2). Conversely, neutral (Lip) and positively charged liposome (Lip SA) movements were hindered in HA 0.25% with the lowest mobility for Lip SA. This was demonstrated by constrained trajectories (Fig. 6B), reduced MSD (Fig. 6A) and α values close to 0 (0.03 for Lip SA and 0.01 for Lip). Overall, the MSD plot for individual liposomes showed quite narrow distributions except for Lip and Lip SA in 0.25% HA where a wider distribution was obtained (Fig. 7).

4. Discussion

The aim of this work was to perform a thorough physicochemical characterization of a drug delivery system based on a mixture of HA and liposomes that has demonstrated its efficiency in vivo for the local administration of both hydrophilic small molecules (corticoid) (El Kechai et al., 2016) and macromolecules (peptide) (Lajavardi et al., 2009). We have already shown that liposome composition, size as well as lipid concentration are key parameters governing the rheological properties of concentrated HA solution

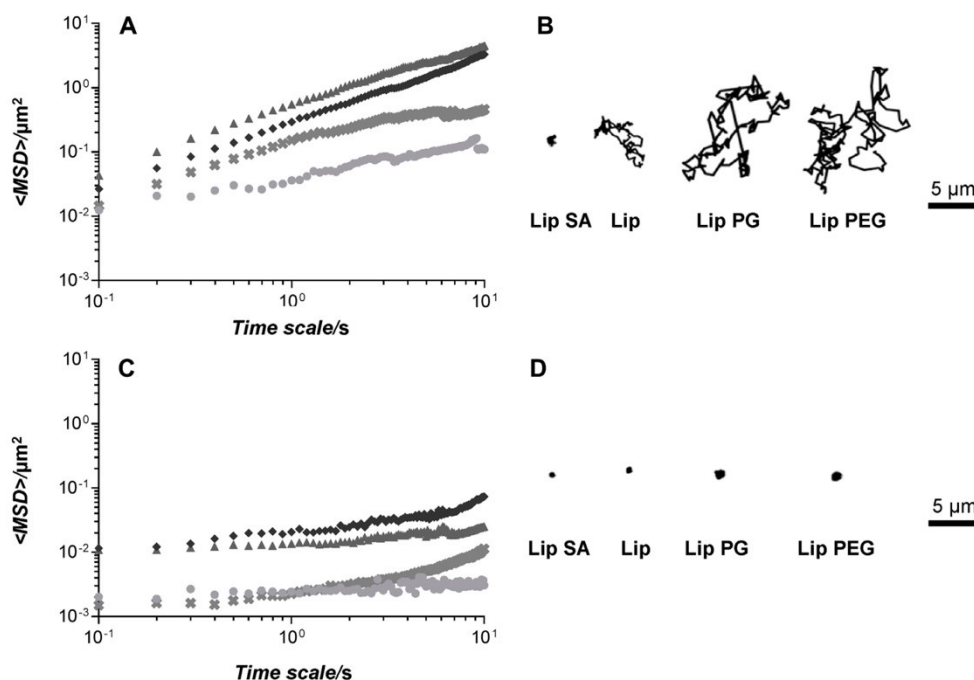


Fig. 6. Mobility of liposomes in HA solutions. A and C: average MSD as function of time scale for 80 mM Lip (●), Lip SA (×), Lip PG (▲), Lip PEG (◆) in HA solutions at 0.25% (w/v) (A) or 2.28% (w/v) (C). B and D: representative trajectories of the different liposomes in HA at 0.25% (w/v) (B) or 2.28% (w/v) (D).

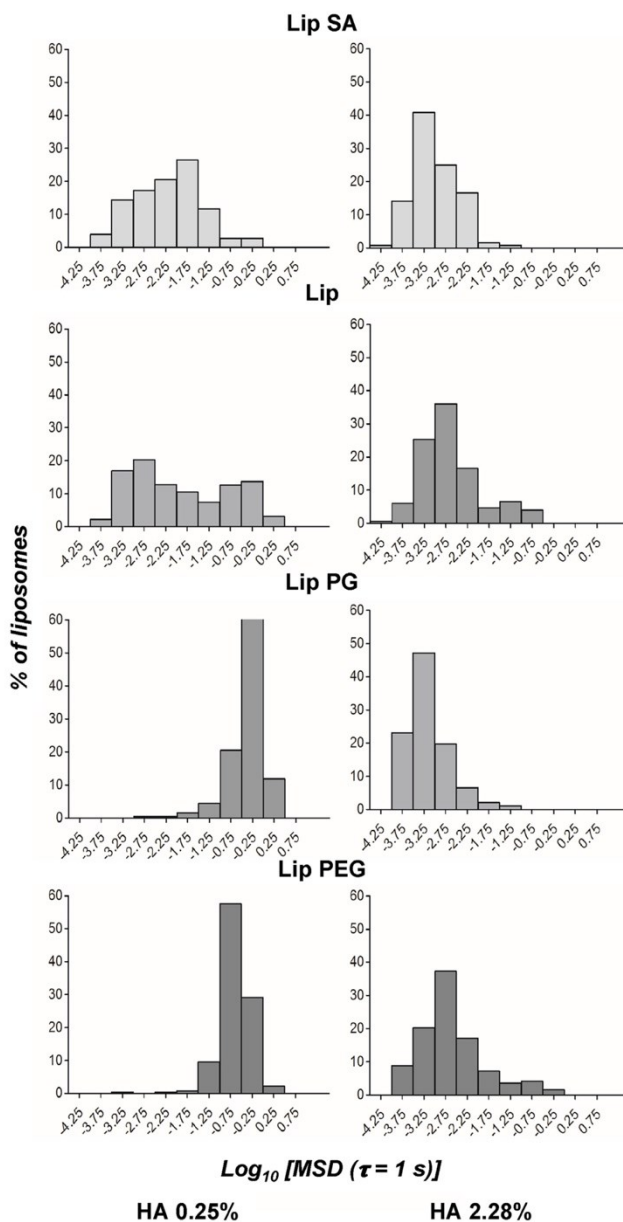


Fig. 7. Distributions of the individual logarithms of MSD at a time scale of 1 s for the different liposome formulations at 80 mM into HA at 0.25% (w/v) (left graphs) or 2.28% (w/v) (right graphs).

at 2.28% (w/v). Indeed, above a lipid concentration of 30 mM, liposomes strengthened the network formed by HA chains resulting in a viscosity increase. This effect was less pronounced when the size of the vesicle was increased (1 μm compared to 150 nm) (El Kechai et al., 2015). Thus, the knowledge of the phase

behavior and structure of such systems would provide a better understanding of their rheological and diffusion properties.

As reported in the introduction, other groups previously studied the combination of polymer solutions or hydrogels and liposomes for medical and pharmaceutical applications. In these studies, the

final lipid concentration in the formulations generally varied between 1 and 20 mM, the size of the vesicle between 80 nm and 5 μm and a chemical or physical crosslinking of the polymer was used or not (Ruel-Gariépy et al., 2002; Hurler et al., 2013; Billard et al., 2015; Alinaghi et al., 2014; Ciobanu et al., 2014; Dong et al., 2013; Widjaja et al., 2014). Only few of these works were devoted to a systematic investigation of the effect of the nature of the liposome surface and charge (Hurler et al., 2013; Billard et al., 2015; Alinaghi et al., 2014; Martens et al., 2013). Some authors characterized the association of polyelectrolytes and oppositely charged lipid vesicles or hydrophobically modified polymers (associative polymers) and vesicles (Huh et al., 2007, 2011; Antunes et al., 2009). However, most of these works were conducted in the dilute concentration regime of the polymer. In our study, liposome size was fixed (around 150 nm) for all formulations to specifically assess the liposome composition effect. This size was a good compromise between the capacity to encapsulate a sufficient amount of hydrophilic drugs within the aqueous compartment of the liposomes and the ability of the vesicles to be internalized by cells. Compared to the other systems mentioned above, the lipid concentration was significantly higher (80 mM). The originality of our approach was also to investigate a range of HA concentrations below and above its entanglement concentration.

In a first step, it was important to characterize the behavior of HA alone in aqueous solution. The HA solutions studied in the present work are in the “high salt limit” since HA was dissolved in a HEPES/NaCl buffer (10/145 mM, pH 7.4) mimicking biological fluids. De Gennes theory (de Gennes, 1979) gives scaling laws for the specific viscosity of polyelectrolytes in the high salt limit and describes three concentration regions: dilute, semi-dilute and concentrated regions. The overlap concentration C^* characterizes the transition between the dilute and unentangled semi-dilute regimes whereas the entanglement concentration C_e corresponds to the limit between the unentangled and the entangled semi-dilute domains. In the semi-dilute unentangled regime ($C^* < C < C_e$), the exponent of the scaling laws for the variations of the specific viscosity with concentration determined in this study (2.4) is higher than the predicted one (1.25). In the concentrated regime ($C > C_e$), the exponent (4.0) is slightly higher but in the same order of magnitude than the theoretical one (3.75). Overall, our exponents at 37 °C are in good agreement with those previously reported in the literature for HA with M_w around 1.5 MDa in the high salt limit at temperatures ranging between 20 and 60 °C (Krause et al., 2001; Oelschlaeger et al., 2013). The higher concentration dependence of η_{sp} compared to the theoretical predictions can be explained by the possible formation of aggregates at high HA concentration presumably due to the formation of hydrogen bonds or hydrophobic interactions between HA chains leading to an increase in the apparent molecular weight of HA (Oelschlaeger et al., 2013; Esquenet and Buhler, 2002; Scott et al., 1991). Krause et al., (Krause et al., 2001) reported that $C^* = 0.059\%$ (w/v) and $C_e = 0.24\%$ (w/v) for HA in phosphate buffered saline at 25 °C (concentration range between 0.009 and 0.87% w/v) whereas Oelschlaeger et al., (Oelschlaeger et al., 2013) obtained $C_e = 0.7\%$ (w/v) at 20 °C in 0.1 M NaCl. In this study, $C_e = 0.4\%$ (w/v) but the overlap concentration C^* was not determined since our rheometer did not allow to accurately measure low viscosities. However, with the assumption that $\eta_{sp}(C) = 2$ (Krause et al., 2001), we determined graphically that the dilute region of HA appeared for HA concentrations below 0.1% approximately.

De Gennes assumed that the transient network formed in a semi-dilute polymer solution can be considered as a collection of “blobs” which can be each characterized by a correlation length (ξ) (de Gennes, 1979). This parameter describes the average distance

between the entanglement points of HA chains and can be considered as a measure of the mesh size of the transient network. This theory is supported by Eqs. (2) and (3):

$$C^* \cong \frac{M}{3\pi R_g^3 N_A} \quad (2)$$

$$\xi \cong R_g \left(\frac{C^*}{C}\right)^{3/4} \quad (3)$$

where M is the molecular weight of the polymer, R_g is the radius of gyration of the polymer, N_A is the number of Avogadro.

The radius of gyration of HA in our experimental conditions was calculated from Eq. (2) by estimating $C^* = 0.1\%$ (w/v) and was found to be $R_g = 84$ nm. By taking a $3/4$ exponent, which characterizes polymers in good solvent, the mesh size at a 2.28% HA concentration, calculated from Eq. (3) is $\xi = 8$ nm. Using the exponent (0.58) reported by De Smedt et al., (De Smedt et al., 1994) for HA in phosphate buffered saline, we calculated a correlation length of 14 nm. Another work estimated HA mesh size $\xi = 9$ nm (at 1.4% w/v, HEPES/NaCl buffer 50/100 mM, pH 7). Studies performed with HA of different molecular weights and different concentrations in the high salt limit determined mesh sizes between 10 and 20 nm using FRAP technique (Masuda et al., 2001; De Smedt et al., 1994) and around 11 nm using electron spin resonance technique (Shenoy et al., 1995). The mesh size is thus much smaller than that of the liposomes.

In a second step, the phase behavior of mixtures of HA and liposomes was assessed in the semi-dilute unentangled regime of HA ($C^* < C < C_e$) and in the entangled one ($C > C_e$) with a constant and high lipid concentration (80 mM). In the absence of HA, the density of liposomes is very close to that of the suspending media (i.e. 1 g mL^{-1} for HEPES/NaCl buffer) (Bucher et al., 1980) allowing a good stability of the suspension if no spontaneous aggregation of liposomes occurs (Torchilin and Weissig, 2016). Thus, the phase separation observed in Fig. 2 for low HA concentrations with Lip. Lip PEG and Lip PG is due to the addition of HA.

Phase separation was widely described for different colloid-polymer mixtures such as nanocomposites or polymeric particles, lipid vesicles dispersed within polymer solutions as well as nanoemulsions (Huh et al., 2007, 2011; Tuinier et al., 2003; Poon, 1998; Pelissetto and Hansen, 2006; Hooper and Schweizer, 2006). It is well known that mixtures of polymer and colloids exhibit complex structural and phase behaviors. A hard-sphere colloidal suspension in the presence of a non adsorbing polymer can exist as homogeneous fluid, can macroscopically phase separate, crystallize or form non equilibrium gels depending on the size and the concentration of the polymer (Hooper and Schweizer, 2005). The mechanism involved in this behavior is polymer depletion. As polymer segments cannot penetrate the solid colloidal particles, the number of chain conformations and the entropy are reduced. This effect can induce a segregative phase separation into a colloid-rich phase and a colloid-poor one. More complexity arises when the chains are even weakly attracted to the particle surface. Indeed, both enthalpy and entropic effects are then involved. A steric stabilization of the colloidal suspension can be observed due to the adsorbed polymer layer. However, bridging attraction or depletion can also occur leading either to associative or segregative phase separation or physical gelation (Hooper and Schweizer, 2005). A crucial parameter characterizing the mixture of colloids and polymers is the size ratio $\lambda = R_c/R_g$ between the colloid (R_c) and the polymer coil (R_g). The case $\lambda \gg 1$ is referred to the colloid limit and can be described through the Asakura and Osawa and Vrij models for a non adsorbing polymer (Asakura and Oosawa, 1954; Vrij, 1976). The polymer is excluded from a layer Δ around the particles

with $\Delta \approx R_g$ (Bolhuis et al., 2002). Theoretical simulations provide a good description of the phase diagrams obtained with nanoparticles (Tuinier et al., 2003; Bolhuis et al., 2002) but also with emulsions (Meller and Stavans, 1996; Meller et al., 1999; Tuinier and De Kruif, 1999). The case $\lambda < 1$ is less understood. The polymer can wrap around the smaller particles and phase separation can also be observed with such systems. The case $\lambda \ll 1$, called the protein limit, is also theoretically described (Odijk, 2009). A simulation was developed to semi-quantitatively predict the phase diagrams both in the colloid and the protein regimes (Pelissetto and Hansen, 2006). Yet, most of experimental and theoretical studies on the mixtures of non adsorbing polymer and colloids were performed in dilute or in unentangled regimes. In the entangled semi-dilute regime, it is most likely that the correlation length ξ should come into play instead of R_g .

In the present study, the mixture of liposomes ($R_c = 75$ nm) and HA ($R_g = 84$ nm) is in the case $\lambda < 1$ ($\lambda = 0.9$). The phase separation can be explained by a depletion mechanism in which interparticle attractions can be induced via the polymer excluded from the space between particles that pushes them together by osmotic pressure (Asakura and Oosawa, 1954; Vrij, 1976). In our study, depletion effect is likely to cause segregative phase separation for HA-Lip, HA-Lip PG and HA-Lip PEG mixtures. However, in addition to the entropically driven depletion effect, there are attractive electrostatic interactions between the positively charged liposomes (Lip SA) and the negatively charged HA. For these systems, no segregative macroscopic phase separation was observed over the entire HA concentration range studied (HA-Lip SA, Fig. 2), except a slight syneresis detected for 2.28% HA concentration. For the other liposomal formulations, the high viscosity of the systems (Table 2) and their viscoelasticity (El Kechai et al., 2015) dramatically slow down the dynamic of the system thereby allowing kinetic stability above the entanglement concentration. Therefore, no phase separation was noticed macroscopically for those HA liposomal mixtures.

The structure of HA at 2.28% containing different liposome formulations was also studied microscopically by confocal microscopy and atomic force microscopy (AFM). From both techniques, the microstructure of HA-Lip, HA-Lip SA and HA-Lip PG exhibits aggregates of liposomes homogeneously dispersed within a HA network. Contri et al. also observed similar microstructures when an excessive amount of nanocapsules were dispersed into chitosan hydrogels (Contri et al., 2014). The formation of this microstructure is probably driven by the depletion effect mentioned before that triggers the aggregation of liposomes upon addition of HA (Huh et al., 2011). The non-fluorescent zones in Fig. 3C with HA-Lip SA can be attributed to areas containing the buffer only and are consistent with the syneresis phenomenon observed macroscopically for HA-Lip SA (Section 3.3). Due to the attractive electrostatic interactions between negatively charged HA and positively charged liposomes, densely packed mixed aggregates are probably formed leading to water expulsion. Moreover, the attractive interactions between HA and liposomes could also increase the permeability of the lipid bilayer resulting in the release of a part of the aqueous content of the liposomes. The microstructure of HA-Lip PEG is slightly different on AFM images and could be assimilated to bicontinuous interpenetrating networks of HA and PEGylated liposomes. A similar organization was already described for cationic vesicles of 256 nm diameter dispersed within a cationic polymer ($R_g = 11.2$ nm, $C < C_c$) using confocal microscopy (Huh et al., 2011). This organization could explain the higher viscosity and elasticity displayed with the systems containing Lip PEG (El Kechai et al., 2015). The Young modulus values obtained in the liposome-rich areas (25–35 MPa) are consistent with the values previously determined on liposomes by AFM (Liang et al., 2004) and the

micropipette-aspiration technique (Rodowicz et al., 2010). The Young modulus values of the HA-rich regions are much higher than the one obtained with a 3% chemically crosslinked HA gel (130–150 MPa instead of 20.2 kPa) (Suriano et al., 2014). However, the fact that these authors performed their experiment directly on the swollen hydrogel whereas our samples were let to dry for one hour before the AFM measurements could explain this difference. Indeed, in our conditions, HA-rich zones were probably dehydrated more rapidly and to a larger extent than the aqueous core of liposomes that was protected by the lipophilic bilayer. Consequently, HA zones were concentrated and Young modulus values for these areas were increased compared to the hydrated state. On the contrary, Young modulus values of liposomes remained unchanged.

The mobility of the different liposomes into HA was studied at two polymer concentrations (0.25% and 2.28%, respectively below and above C_c). Basically, two factors can influence the migration of molecules or particles in a polymeric network. First, the diffusion depends on physicochemical interactions between the diffusing molecule or particle and the polymer chains in the network. Second, it is also influenced by the steric hindrance which depends both on size and shape of the diffusing molecule or particle (Phillies and Clomenil, 1993) and on the network structure of the polymer solutions (De Smedt et al., 1994). Particles smaller than the mesh size formed by the entangled polymer chains are supposed to diffuse rapidly through the polymer network, whereas particles larger than the pores are sterically trapped within the network (Xu et al., 2013; Braeckmans et al., 2010). HA chains in solution form a transient network and are in permanent movement (Masuda et al., 2001; De Smedt et al., 1994). The mesh size and the shape of the HA network change continuously within its lifetime and thus, may adapt depending on the interactions with molecules or colloids dispersed within the network. Due to this dynamical effect, the effective pore size for the diffusion of liposomes may be significantly larger than the theoretical one (8–14 nm for HA 2.28%). Thus, depending on the nature of the interactions between HA and liposomes, this dynamic structure may allow a better diffusion of liposomes at longer time scales compared to what might be expected from diffusion experiments at short time scales.

At 0.25% HA concentration, liposomes exhibited a more or less rapid diffusion, depending on the formulations (Fig. 6), as their movements are slightly hindered by the unentangled polymer chains that can be seen as obstacles. At 2.28% (above the entanglement concentration), the movements of liposomes were strongly hindered by the HA network (Fig. 6). Regarding the microstructure described here for the mixture of liposomes and HA at 2.28%, and due to the depletion phenomenon, the liposomes form aggregates that are trapped into a highly viscoelastic HA network (El Kechai et al., 2015).

Positively charged liposomes (Lip-SA) should interact with HA by electrostatic attractions and complexation that led to an important immobilization of those liposomes even at low HA concentration. The hydrophobic surface of neutral liposomes (Lip) can potentially interact with HA by binding the hydrophobic regions along the HA chain (Scott et al., 1991; Heatley and Scott, 1988), which also led to slow down the diffusion of those liposomes compared to Lip PEG and Lip PG that are both negatively charged. The negative charge at the surface of Lip PG, providing electrostatic repulsions with the negatively charged carboxylate groups of HA, resulted in a diffusion profile close to that of the PEGylated liposomes microscopically at short time scales. However, this was not confirmed macroscopically at long time scale (Fig. 5). Even in 2.28% HA, the PEGylated liposomes were the most mobile both macro- and microscopically. In addition to the repulsive electrostatic interaction, steric repulsions between the

PEG chains at the surface of liposomes and HA chains (Sanders et al., 2007) as well as steric repulsions between PEGylated liposomes in the liposome rich-phase allow liposome movements at short and long time scales. The bicontinuous microstructure observed for HA-Lip PEG (Fig. 4) favors the long-distance migration of the vesicles into the liposome network (Fig. 5) whereas Lip PG are trapped within delimited liposome aggregates. The results obtained with Lip PEG are in good agreement with those of Martens et al. (2013) and Xu et al. (2013) who both demonstrated ex vivo that PEG-coated or negatively charged nanoparticles freely diffused in the vitreous, which contains HA at concentrations ranging from 0.05 to 0.57% (Käsärdorf et al., 2015) while positively charged nanoparticles with similar size were completely immobilized. Lajavardi et al. observed the mobility of PEGylated liposomes into the vitreous in vivo (Lajavardi et al., 2007). Following a transtympanic injection of a HA liposomal mixture, PEGylated liposomes were also able to diffuse through HA (2.28%) to reach the physiological membrane separating the middle and the inner ear (El Kechai et al., 2016). PEGylation is a well-known strategy to improve the colloidal stability of nanoparticles and to reduce interactions with biopolymers (Sanders et al., 2007). Furthermore, PEGylated nanoparticles for drug and gene delivery are also known as “mucus penetrating particles” due to their ability to overcome the mucus barrier which is mainly composed of mucin, a high molecular weight glycoprotein with a high negative charge (Lai et al., 2009). The HA-liposomal mixtures appear as a flexible formulation platform exhibiting different vesicle mobility properties depending on the nature of the surface of the liposomes. This is likely to modulate the location of the release of an encapsulated drug and thus its release kinetics. However, it is difficult to predict the drug release from such mixtures. Indeed, the release of a drug from liposomes depends on the physicochemical properties of the drug, of those of the liposomes (composition, pH, osmotic gradient) and of the surrounding environment (Dos Santos Giuberti et al., 2011).

5. Conclusion

The aim of this work was to characterize the physicochemical properties of HA-liposomal mixtures in aqueous media regarding phase behavior, microstructure and mobility of liposomes. The entanglement concentration of HA was determined to be 0.4% (w/v). Liposomes dispersed within HA exhibited a macroscopic phase separation at low HA concentration except for the positively charged ones. At high HA concentration, the microstructure probably induced by a depletion mechanism seems to be either aggregates of liposomes into HA network (HA-Lip, HA-Lip SA, HA-Lip PG) or bicontinuous interpenetrating networks of HA and liposome aggregates (HA-Lip PEG). The diffusion of liposomes was controlled by their surface characteristics and the concentration of HA. PEGylated liposomes displayed the highest mobility into HA at high concentration both macro- and microscopically. The microstructure of the HA-liposomes mixtures and the diffusion of liposomes are key parameters that must be taken into account for drug delivery. The ability of the vesicles to migrate or not into HA, considered as a formulation or a biological media, allows them either to act as a reservoir of drug at the injection site or to reach the target cells or tissues to deliver an encapsulated drug.

Conflict of interest

The authors have non conflict of interest to declare.

Funding sources

This work was supported by a PhD grant (Naila El Kechai) from the French Ministry of National Education. The authors are very grateful to the ANR (The French National Research Agency) for its financial support (No. ANR-15-CE19-0014-01).

Author contributions

The manuscript was written through contributions of all authors. All authors have given approval to the final version of the manuscript.

Acknowledgments

The authors would like to thank “la région Ile-de-France” for the purchase of the confocal microscope and Claire Albert and Thaïs Nascimento for their technical assistance in the Turbican® and single particle tracking experiments, respectively.

Appendix A. Supplementary data

Supplementary data associated with this article can be found, in the online version, at <http://dx.doi.org/10.1016/j.ijpharm.2017.03.029>.

References

- Alinaghi, A., Rouini, M.R., Johari Daha, F., Moghimi, H.R., 2014. *Int. J. Pharm.* 459, 30–39.
- Allen, T.M., Cullis, P.R., 2013. *Adv. Drug Delivery Rev.* 65, 36–48.
- Antunes, F.E., Marques, E.F., Miguel, M.G., Lindman, B., 2009. *Adv. Colloid Interface Sci.* 147, 18–35.
- Asakura, S., Oosawa, F., 1954. *Chem. Phys.* 1255–1256.
- Billard, A., Pourchet, L., Malaise, S., Alcouffe, P., Montembault, A., Ladavière, C., 2015. *Carbohydr. Polym.* 115, 651–657.
- Bolhuis, P., Louis, A., Hansen, J., 2002. *Phys. Rev. Lett.* 89, 128–302.
- Bozzuto, G., Molinari, A., 2015. *Int. J. Nanomed.* 10, 975–999.
- Braeckmans, K., Buyens, K., Bouquet, W., Vervaeck, C., Joye, P., Vos, F.D., Plawinski, L., Dœuvre, L., Angles-Cano, E., Sanders, N.N., Demeester, J., Smedt, S.C.D., 2010. *Nano Lett.* 10, 4435–4442.
- Bucher, D.J., Kharitonov, I.G., Zakomirdin, J.A., Grigoriev, V.B., Klimenko, S.M., Davis, J.F., 1980. *J. Virol.* 36, 586–590.
- Ciobanu, B.C., Cadinou, A.N., Popa, M., Desbrières, J., Peptu, C.A., 2014. *Mater. Sci. Eng. C Mater. Biol. Appl.* 43, 383–391.
- Contri, R.V., Soares, R.M., Pohlmann, A.R., Guterres, S.S., 2014. *Mater. Sci. Eng. C Mater. Biol. Appl.* 42, 234–242.
- Couvreux, P., 2013. *Adv. Drug Delivery Rev.* 65, 21–23.
- Cross, M.M., 1968. *Polymer Systems: Deformation and Flow*. MacMillan, London, UK.
- de Gennes, P.-G., 1979. *Scaling Concepts in Polymer Physics*. Cornell University Press, London, UK.
- De Smedt, S.C., Dekeyser, P., Ribitsch, V., Lauwers, A., Demeester, J., 1993. *Anglais* 30, 31–41.
- De Smedt, S.C., Lauwers, A., Demeester, J., Engelborghs, Y., De Mey, G., Du, M., 1994. *Macromolecules* 27, 141–146.
- Derjaguin, B.V., Muller, V.M., Toporov, Y.P.J., 1975. *Colloid Interface Sci.* 53, 314–326.
- Dong, J., Jiang, D., Wang, Z., Wu, G., Miao, L., Huang, L., 2013. *Int. J. Pharm.* 441, 285–290.
- Dos Santos Giuberti, C., de Oliveira Reis, E.C., Ribeiro Rocha, T.G., Leite, E.A., Lacerda, R.G., Ramaldes, G.A., de Oliveira, M.C., 2011. *J. Liposome Res.* 21, 60–69.
- El Kechai, N., Bochet, A., Huang, N., Nguyen, Y., Ferrary, E., Agnely, F., 2015. *Int. J. Pharm.* 487, 187–196.
- El Kechai, N., Mamelle, E., Nguyen, Y., Huang, N., Nicolas, V., Chaminade, P., Yen-Nicolay, S., Gueutin, C., Granger, B., Ferrary, E., Agnely, F., Bochet, A., 2016. *J. Controlled Release* 226, 248–257.
- Ensign, L.M., Cone, R., Hanes, J., 2014. *J. Control. Release* 190, 500–514.
- Esquet, C., Buhler, E., 2002. *Macromolecules* 35, 3708–3716.
- Gatej, I., Popa, M., Rinaudo, M., 2005. *Biomacromolecules* 6, 61–67.
- Grijalvo, S., Mayr, J., Eritja, R., Diaz, D.D., 2016. *Biomater. Sci.* 4, 555–574.
- Heatley, F., Scott, J.E., 1988. *Biochem. J.* 254, 489–493.
- Hooper, J.B., Schweizer, K.S., 2005. *Macromolecules* 38, 8858–8869.
- Hooper, J.B., Schweizer, K.S., 2006. *Macromolecules* 39, 5133–5142.
- Huh, J.Y., Lynch, M.L., Furst, E.M., 2007. *Phys. Rev. E* 76, 051409.
- Huh, J.Y., Lynch, M.L., Furst, E.M., 2011. *Ind. Eng. Chem. Res.* 50, 78–84.
- Hurler, J., Žakelj, S., Mravljak, J., Pajk, S., Kristl, A., Schubert, R., Škalko-Basnet, N., 2013. *Int. J. Pharm.* 456, 49–57.
- Käsärdorf, B.T., Arends, F., Lieleg, O., 2015. *Biophys. J.* 109, 2171–2181.

- Krause, W.E., Bellomo, E.G., Colby, R.H., 2001. *Biomacromolecules* 2, 65–69.
- Lai, S.K., Wang, Y.-Y., Hanes, J., 2009. *Adv. Drug Delivery Rev.* 61, 158–171.
- Lajavardi, L., Bochof, A., Camelo, S., Goldenberg, B., Naud, M.-C., Behar-Cohen, F., Fattal, E., de Kozak, Y., 2007. *Invest. Ophthalmol. Visual Sci.* 48, 3230–3238.
- Lajavardi, L., Camelo, S., Agnely, F., Luo, W., Goldenberg, B., Naud, M.-C., Behar-Cohen, F., de Kozak, Y., Bochof, A., 2009. *J. Controlled Release* 139, 22–30.
- Lapčič, L., Lapčič, L., De Smedt, S., Demeester, J., Chabreček, P., 1998. *Chem. Rev.* 98, 2663–2684.
- Liang, X., Mao, G., Ng, K.S., 2004. *J. Colloid Interface Sci.* 278, 53–62.
- Martens, T.F., Vercauteren, D., Forier, K., Deschout, H., Remaut, K., Paesen, R., Ameloot, M., Engbersen, J.F.J., Demeester, J., De Smedt, S.C., Braeckmans, K., 2013. *Nanomedicine* 8, 1955–1968.
- Masuda, A., Ushida, K., Koshino, H., Yamashita, K., Kluge, T., 2001. *J. Am. Chem. Soc.* 123, 11468–11471.
- Meller, A., Stavans, J., 1996. *Langmuir* 12, 301–304.
- Meller, A., Gisler, T., Weitz, D.A., Stavans, J., 1999. *Langmuir* 15, 1918–1922.
- O'Neill, H.S., Herron, C.C., Hastings, C.L., Deckers, R., Lopez Noriega, A., Kelly, H.M., Hennink, W.E., McDonnell, C.O., O'Brien, F.J., Ruiz-Hernández, E., Duffy, G.P., 2017. *Acta Biomater.* 48, 110–119.
- Odijk, T., 2009. *J. Phys. Chem. B* 113, 3941–3946.
- Oelschlaeger, C., Cota Pinto Coelho, M., Willenbacher, N., 2013. *Biomacromolecules* 14, 3689–3696.
- Pelissetto, A., Hansen, J.-P., 2006. *Macromolecules* 39, 9571–9580.
- Phillies, G.D.J., Clomenil, D., 1993. *Macromolecules* 26, 167–170.
- Poon, W.C.K., 1998. *Curr. Opin. Colloid Interface Sci.* 3, 593–599.
- Rodowicz, K.A., Francisco, H., Layton, B., 2010. *Chem. Phys. Lipids* 163, 787–793.
- Ruel-Gariépy, E., Leclair, G., Hildgen, P., Gupta, A., Leroux, J.C., 2002. *J. Control. Release* 82, 373–383.
- Sanders, N.N., Peeters, L., Lentacker, I., Demeester, J., De Smedt, S.C., 2007. *J. Controlled Release* 122, 226–235.
- Scott, J.E., Heatley, F., 1999. *Proc. Georgian Natl. Acad. Sci.* 96, 4850–4855.
- Scott, J.E., Cummings, C., Brass, A., Chen, Y., 1991. *Biochem. J.* 274, 699–705.
- Shenoy, V., Rosenblatt, J., Vincent, J., Gaigalas, A., 1995. *Macromolecules* 28, 525–530.
- Suh, J., Dawson, M., Hanes, J., 2005. *Adv. Drug Delivery Rev.* 57, 63–78.
- Suriano, R., Credi, C., Levi, M., Turri, S., 2014. *Appl. Surf. Sci.* 311, 558–566.
- Torchilin, V., Weissig, V., 2016. *Liposomes: a Practical Approach*. Oxford University Press, pp. 2003.
- Tuinier, R., De Kruif, C., 1999. *J. Colloid Interface Sci.* 218, 201–210.
- Tuinier, R., Rieger, J., de Kruif, C.G., 2003. *Adv. Colloid Interface Sci.* 103, 1–31.
- Volpi, N., Schiller, J., Stern, R., Soltes, L., 2009. *Curr. Med. Chem.* 16, 1718–1745.
- Vrij, A., 1976. *Pure Appl. Chem.* 48, 471–483.
- Widjaja, L.K., Bora, M., Chan, P.N., Lipik, V., Wong, T.T., Venkatraman, S.S., 2014. *J. Biomed. Mater. Res. A* 102, 3056–3065.
- Xu, Q., Boylan, N.J., Suk, J.S., Wang, Y.-Y., Nance, E.A., Yang, J.-C., McDonnell, P.J., Cone, R.A., Duh, E.J., Hanes, J., 2013. *J. Controlled Release* 167, 76–84.

Inhalable Hyaluronic Acid Derivate for Inflammatory Lung Diseases

Authors in alphabetic order:

L. Busato^{1,2}, A. Fallacara^{1,2}, M. Pozzoli¹, M. Ghadiri¹, HX. Ong¹, P. Young¹, S. Manfredini² and D. Traini¹

¹ Woolcock Institute of Medical Research, Glebe, Australia;

² Department of Life Science and Biotechnology, Università degli Studi di Ferrara, Ferrara, Italy
Michele.pozzoli@sydney.edu.au

Introduction: Sodium hyaluronate (NaHY) has gained attention for inhalation due to its therapeutic potential in inflammatory lung disorders, in particular for asthma, emphysema and chronic obstructive pulmonary diseases and its activity as biocompatible and biodegradable drug carrier [1].

Purpose: The aim of this study was to develop an inhaled formulation using a novel derivate of NaHY, in combination with an antioxidant drug (Sodium Ascorbyl Phosphate, NaP) as potential synergic anti-inflammatory and anti-oxidant therapy. The formulation was evaluated for its in vitro efficacy to reduce inflammation on Calu-3 epithelial lung cells.

Material & Methods: Microspheres were produced by spray-drying using a mini spray-dryer B-290. Briefly, NaHY derivate and NaP were dissolved in water with a concentration of 0.15 (w/w %) and 0.45 (w/w %), respectively, and the solution was spray-dried at the following process parameters: inlet temperature 150 °C, solution feed rate of 3.0 mL/min and nozzle diameter of 1.4 mm. Under these conditions an outlet temperature ranging from 78 to 82 °C was observed. A dehumidifier B-296 was used to control the air humidity of the system. Particle size of the obtained microspheres was measured using laser diffraction (Mastersizer, Malvern Instruments).

The biological effect of the formulation was tested on Calu-3 cells. Inflammation was induced with 10 ng/mL Lipopolysaccharides (LPS) 24 h after cell seeding. Subsequently, cells were treated with the combination of NaHY and NAP therapy and compared to NaHY alone and NaP alone as controls. Supernatants were collected and IL-6 cytokine was quantified as inflammatory marker using commercially available ELISA kit (BD OptEia, BD Biosciences).

Results and Discussion: The microspheres obtained showed suitable aerodynamic sizes for delivery to the lung with a Dv10, 50 and 90 of $1.2 \pm 0.1 \mu\text{m}$, $3.4 \pm 0.3 \mu\text{m}$ and $17.9 \pm 7.6 \mu\text{m}$, respectively (Figure 1). It was found that LPS-induced Calu-3 cells produced $1165.7 \pm 202.0 \text{ pg/mL}$ of IL-6, compared to a basal level (no stimuli) of $270.7 \pm 18.7 \text{ pg/mL}$. All treatments showed the ability to reduce IL-6 level, compared to untreated LPS induced cells. More specifically, NaHY decreased IL-6 levels to $655.3 \pm 135.0 \text{ pg/mL}$, and NaP to $868.1 \pm 262.1 \text{ pg/mL}$, respectively. Furthermore, a significant improvement of the anti-inflammatory activity was obtained with the combination of NaP and NaHY (IL-6 concentration $431.3 \pm 61.7 \text{ pg/mL}$) (Figure 2)

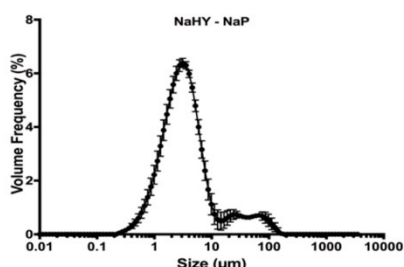


Figure 1. Particle Size distribution of the spray-dried formulation NaHY-NAP

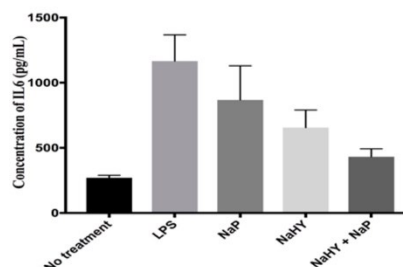


Figure 2. IL-6 production of Calu-3 cells after stimuli with LPS and treatment with NaHY, NaP and combination NaHY-NAP

Conclusions: The innovative co-spray dried NaHY and NAP formulation appears to be a promising inhalable dry powder formulation for the treatment of inflammatory lung diseases.

References:

1. Martinelli F, Balducci AG, Kumar A, Sonvico F, Forbes B, Bettini R, et al. Int J Pharm. 2017;517:286–95.

Hyaluronic Acid Fillers in Soft Tissue Regeneration

Arianna Fallacara¹ Stefano Manfredini¹ Elisa Durini, PhD¹ Silvia Vertuani, PhD¹

¹ Department of Life Science and Biotechnology, Università degli Studi di Ferrara Dipartimento di Scienze della Vita e Biotecnologie, Ferrara, Emilia-Romagna, Italy

Facial Plast Surg 2017;33:87–96.

Address for correspondence Stefano Manfredini, Department of Life Science and Biotechnology, Università degli Studi di Ferrara Dipartimento di Scienze della Vita e Biotecnologie, Via L. Borsari 46 Ferrara 44100, Emilia-Romagna, Italy (e-mail: smanfred@unife.it; vrs@unife.it).

Abstract

Over the last years, hyaluronic acid (HA) injectable dermal fillers (DFs) have become the most popular agents for soft tissue contouring and volumizing. HA fillers are characterized by most of the properties that an ideal DF should have, due to HA unique chemical-physical properties, biocompatibility, biodegradability, and versatility. Therefore, HA DFs have revolutionized the filler market with a high number of products, which differ in terms of HA source, cross-linkage (agent and degree), HA concentration, hardness, cohesivity, consistency, inclusion or lack of anesthetic, indication, and longevity of correction. The article first provides a general introduction to DF world, and an overview of the different materials is available for fillers. Second, it describes the characteristics and the peculiarities of HA fillers, their differences from the other available materials, and therefore the reasons at the base of their success. Moreover, an update regarding the main Food and Drug Administration (FDA) approved fillers is presented.

Keywords

- ▶ dermal filler
- ▶ hyaluronic acid
- ▶ soft tissue volumization
- ▶ aesthetic medicine
- ▶ nonsurgical procedures.

Ferrara. Copyrighted material.

[Production note: this paper is not included in this digital copy due to copyright restrictions.]

Fallacara, A., Manfredini, S., Durini, E., Vertuani, S., 2017a. Hyaluronic acid fillers in soft tissue regeneration. *Facial Plast. Surg.* 33, 87-96.

DOI: 10.1055/s-0036-1597685

View/Download from publisher's site:

<https://www.thieme-connect.com/DOI/DOI?10.1055/s-0036-1597685>

LETTERA D'INCARICO

(Art. 201 D. Lgs. 10 febbraio 2005, n. 30)

La sottoscritta



con la presente conferisce incarico all'Avv. **Secondo Andrea Feltrinelli, Ing. Riccardo Fuochi (iscr. Albo n. 823B)** domiciliati presso APTA S.r.l. in Via Ca' di Cozzi, 41 - 37124 VERONA - ITALIA (qui di seguito "Ufficio"), di rappresentare e difendere, con poteri di nomina di altri rappresentanti abilitati e di revoca di ogni precedente mandatario, il/la sottoscritto/a e di operare per il/la sottoscritto/a di fronte all'E.P.O., all'O.M.P.I. e all'U.I.B.M., ed ai Servizi Provinciali agenti per l'U.I.B.M. e per l'O.M.P.I., alla S.I.A.E. in tutte le procedure ed operazioni (ivi compresi: deposito e ritiro di domande, pagamento di tasse, richieste di rimborsi e loro riscossione, repliche ad obiezioni, opposizioni, ricorsi, ecc.), previste dalle leggi, dai regolamenti e dalle convenzioni internazionali vigenti sulla Proprietà intellettuale.

Il presente mandato è relativo a:

Deposito domanda di brevetto italiano per invenzione industriale avente titolo



ed è risolutivamente condizionato all'esistenza di un valido ed efficace rapporto di collaborazione fra il suddetto "Ufficio" e i sopraindicati mandatarî, o alla loro qualità di titolari, procuratori, o soci dell'"Ufficio", rapporto o qualità individualmente considerata e risolutiva. Il/La sottoscritto/a elegge agli effetti di ogni comunicazione, notifica e/o consegna amministrativa ad opera dell'E.P.O., dell'O.M.P.I., dell'U.I.B.M. e/o dei Servizi Provinciali agenti per detto U.I.B.M. e O.M.P.I., della S.I.A.E. domicilio presso APTA S.r.l., Via Ca' di Cozzi, 41 - 37124 VERONA.

Firma



POWER OF ATTORNEY

(Art. 201, L.D. February, 10, 2005. n. 30)

I/we the undersigned

Confers the power to **Mr. Secondo Andrea Feltrinelli, Mr. Riccardo Fuochi (under 823B)** having place of business at APTA S.r.l., Via Ca' di Cozzi, 41 - 37124 VERONA - ITALY (hereinafter referred to as the "Patent Attorneys Office"), to represent and defend the said undersigned and with the authorisation to appoint substitutes and revoke any prior power and to act on behalf of the said undersigned before the E.P.O., the W.I.P.O., the I.P.T.O., and the Provincial Services acting for the said I.P.T.O., and for the W.I.P.O., the S.I.A.E. as far as all proceedings and operations are concerned (including: filing and withdrawing of applications, payment of official fees, requests and cashing of refunds, replies to official objections, oppositions and appeals, etc.), which are provided for by the Italian and International Laws and Conventions on Intellectual Property.

The present power refers to:

and is subject to the condition of termination concurred with the termination of an employment, proxy, association or partnership agreement now in force between said "Patent Attorneys Office" and the above mentioned Patent Attorney(s), each individually considered as far as the termination condition is concerned. The undersigned elects as to any communication, notifying or delivery of administration papers from the E.P.O., the W.I.P.O., the I.P.T.O. and/or the Provincial Services acting for the said I.P.T.O. and the W.I.P.O., and from the S.I.A.E. domicile c/o APTA S.r.l., Via Ca' di Cozzi, 41 - 37124 VERONA.

Applicant's signature



[Production note: this patent application is not included in its digital copy due to agreement with third parties and copyright restrictions.]

Fallacara, A., Vertuani, S., Manfredini, S., Citernesi, U.R., 2018. Patent Appl. Filed, n. 102018000008192.

ATTI
DELL'ACCADEMIA
DELLE SCIENZE
DI FERRARA



Estratto

Volume 93
Anno Accademico 193
2015-2016

Volume 93
Anno Accademico 193
2015-2016

Proprietario e copyright

Accademia delle Scienze di Ferrara
Palazzo Manfredini - via L.A. Muratori, 9 - 44121 Ferrara
tel. - fax (0532) 205209
e-mail: info@accademiascienze.ferrara.it
sito web: <http://www.accademiascienze.ferrara.it>

Direttore responsabile

Prof. Roberto Tomatis

Redattori

Prof.ssa Giovanna Cavallaro
Prof. Paolo Zanardi Prospero
Dott.ssa Giuliana Avanzi Magagna

Periodicità annuale

Autorizzazione n. 178 Reg. Stampa
in data 6 maggio 1972 del Tribunale di Ferrara

Composto per la stampa

Sara Storari
Studio editoriale Fuoriregistro
via Zucchini, 79 - 44122 Ferrara
e-mail: studiofuoriregistro@gmail.com

ISSN 0365-0464

INDICE GENERALE

Consiglio Direttivo	pag.	5
Note storiche	»	7
I Presidenti dalla fondazione ad oggi	»	13
Elenco dei Soci	»	15
<i>Comunicazioni scientifiche</i>	»	23
INAUGURAZIONE DEL CXCIII ANNO ACCADEMICO	»	25
GIORGIO ZAULI, PAOLA SECCHIERO, ELISA BARBAROTTO, MARIO TIRIBELLI, CARLOTTA ZERBINATI, MARIA GRAZIA DI IASIO, ARIANNA GONELLI, FRANCESCO CAVAZZINI, DIANA CAMPIONI, RENATO FANIN, ANTONIO CUNEO Functional integrity of the p53-mediated apoptotic pathway induced by the nongenotoxic agent nutlin-3 in B-cell chronic lymphocytic leukemia (B-CLL)	»	29
STELLA PATITUCCI UGGERI “La Romanizzazione dell’antico delta padano” aggiornamento archeologico	»	53

GIOVANNI UGGERI “La Romanizzazione dell’antico delta padano” 40 anni dopo: una revisione	» 79
FABIO FABBIAN Prevenzione non farmacologica della calcolosi renale	» 105
STEFANO MANFREDINI, ARIANNA FALLACARA, GIORGIA DE CARIE, SILVIA VERTUANI L’Acido Ialuronico (AI) nei trattamenti estetici, una <i>review</i> critica	» 115
LUIGI PEPE Ariosto e Copernico	» 141
PAOLO STURLA AVOGADRI Ferrara: la cultura, l’Università, le Accademie	» 159
RICCARDO CAPUTO, GABRIELE TARABUSI Il complesso sistema di sorgenti sismogeniche nell’area ferrarese e i loro effetti nella storia	» 161
ALESSANDRA FIOCCA “A cose nuove, uomini nuovi”: filosofi, matematici e tecnici tra bonifiche e trasmissione della scienza antica nella Ferrara del XVI secolo	» 179

Stefano Manfredini*, Arianna Fallacara,
Giorgia De Carie, Silvia Vertuani

L'ACIDO IALURONICO (AI) NEI TRATTAMENTI ESTETICI, UNA REVIEW CRITICA

Relazione svolta
nella seduta accademica
del 2 febbraio 2016

1. L'ACIDO IALURONICO

L'acido ialuronico (AI) (DEREK H. *et al*, 2009) è una molecola con proprietà chimico-fisiche uniche ed incomparabili, ed ha numerosissime funzioni biologiche (LAURENT TC *et al*, 1995). L'AI è estremamente versatile ed è biocompatibile, biodegradabile (LIAO YH *et al*, 2005) e muco-adesivo (MAYOL L. *et al*, 2008). Queste caratteristiche del biopolimero, in aggiunta alla sua unica natura visco-elastica, hanno condotto al suo utilizzo in differenti applicazioni mediche, farmaceutiche e cosmetiche (LIAO YH *et al*, 2005).

1.1 Proprietà chimico-fisiche dell'AI e delle soluzioni acquose di AI

L'AI (così come il suo sale sodico) è un polimero lineare, con carica netta negativa, appartenente alla classe dei glicosaminoglicani. La catena polisaccaridica dell'AI è formata da migliaia di unità disaccaridiche uguali, costituite da residui di acido D-glucuronico e N-acetil-D-glucosamina, legati tra loro da legami glicosidici β -1,4. I vari disaccaridi, invece, sono legati tra loro da legami glicosidici β -1,3.

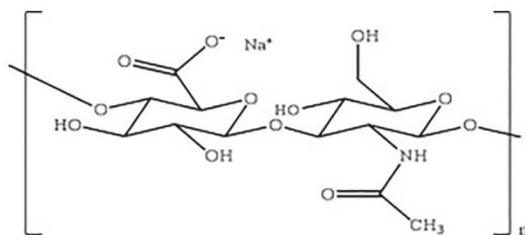


Figura 1: Struttura chimica del sodio ialuronato.

(*) Scuola di Farmacia e dei Prodotti della Salute, Dipartimento di Scienze della vita e biotecnologie, Master in Scienza e Tecnologia Cosmetiche, Università di Ferrara, Via L. Borsari 46, 44121 Ferrara, Italia.

L'AI è un polisaccaride che può avere differenti pesi molecolari, i quali ne determinano le proprietà chimico-fisiche, biologiche e, quindi, le differenti applicazioni terapeutiche.

Tipo di composto	Usi terapeutici e potenziali
Basso PM AI (<0,5 MDa)	regolazione dell'angiogenesi inibizione della loro funzione come segnali di pericolo inibizione dell'immuno-stimolazione e dell'effetto proinfiammatorio stimolazione della frequenza di sbattimento ciliare in malattie polmonari
Medio PM AI (0,5-1 MDa)	viscosupplementazione
Alto PM AI (>1 MDa)	anti-angiogenesi antiinfiammatorio protezione della cartilagine differenziazione cellulare migrazione cellulare protezione dello strato epiteliale delle cellule immunosoppressivo rigenerazione riempimento stimolazione di sintesi dell'AI viscosupplementazione riparazione delle ferite

Tabella 1: Usi terapeutici e potenziali dell'AI e dei suoi derivati (MENDOZA G, 2009).

È stato precedentemente dimostrato che, quando l'AI è disciolto in soluzione acquosa, si forma un'estesa rete di legami a idrogeno, tanto più compatta quanto maggiore è il peso molecolare del biopolimero (SCOTT JE *et al*, 1999). L'elevato numero di gruppi polari e carichi delle molecole di AI è responsabile di interazioni dipolo-dipolo che connettono, intramolecolarmente, residui zuccherinici vicini. Inoltre, si formano anche legami a idrogeno intermolecolari tra l'idrogeno acetamidico di una catena polimerica e il gruppo carbossilico dell'acido D-glucuronico di un'altra catena. L'AI si caratterizza anche per associazioni idrofobiche derivanti dai gruppi CH contigui di ogni anello zuccherinico (SCOTT JE, 1989). Le parti idrofobiche della molecola portano alla formazione di associazioni idrofobiche

intra- e inter-molecolari. A causa sia dei legami a idrogeno, che delle interazioni idrofobiche, l'AI forma degli aggregati e, più precisamente, quando la sua concentrazione è sufficientemente elevata (ovvero superiore alla *critical concentration of entanglement*) un vero e proprio reticolo generato da interazioni fisiche (*physical cross-linked system*, ovvero *physical cross-linked network*). Essendo deboli, tali interazioni generano un reticolo temporaneo, ovvero un gel reversibile (SCOTT JE, 1989), con proprietà dipendenti dalla concentrazione del biopolimero e dal suo peso molecolare (FAKHARI A. *et al*, 2013). Pertanto, la formazione di idrogeli di AI è basata su un meccanismo di cross-linking di tipo fisico (SCOTT JE, 1989), che è alla base del loro comportamento reofluidificante, non-tissotropico e viscoelastico. Infatti, le interazioni di tipo fisico (e non covalenti) tra le catene polimeriche di AI consentono ai gel, quando sottoposti ad uno stress, di subire una destrutturazione puramente reversibile e transiente. La *physical cross-linked network* si riforma, infatti, nel momento in cui la sollecitazione termina, ed i gel riacquisiscono così le loro strutture iniziali e, conseguentemente, le loro viscosità iniziali (LAPČIK LUBOMIR JR *et al*, 1998). Le proprietà reologiche delle soluzioni di AI le rendono ideali per utilizzi in campo medico, farmaceutico, e cosmetico, poiché consentono una semplice applicazione del prodotto, ed una rapida immobilizzazione della formulazione a livello del sito bersaglio.

1.2 AI in natura: caratteristiche e funzioni biologiche

Nel 1934 il biochimico Karl Meyer e il suo assistente John W. Palmer isolarono, per la prima volta, AI (DEREK H. *et al*, 2009) dall'umor vitreo di bovino (FAKHARI A. *et al*, 2013). L'AI, infatti, è uno dei componenti fondamentali dei tessuti connettivi dei mammiferi - incluso l'uomo - (GOLD MICHAEL *et al*, 2009), nei quali si trova principalmente come sodio ialuronato (che è anche la forma più comune di AI disponibile in commercio) (KABLIK J. *et al*, 2009). Nell'uomo, l'AI è sintetizzato dalle ialuronano-sintasi a livello di cellule che poi lo secernono quali, ad esempio, i fibroblasti, i cheratinociti, i condrociti e conferisce idratazione, turgidità, plasticità e viscosità ai numerosi tessuti in cui si trova (FAKHARI A. *et al*, 2013). In effetti, nel corpo umano, l'AI è praticamente ubiquitario: esso è presente nella pelle, nelle cartilagini (D. RICHARD *et al*, 2007), nei tendini, nelle articolazioni (KABLIK J. *et al*, 2009), nel cordone ombelicale (FAKHARI A. *et al*, 2013), nell'umor vitreo (FAKHARI A. *et al*, 2013) e nelle pareti dell'aorta (D. RICHARD *et al*, 2007), ove svolge numerose funzioni fisiologiche. A livello della pelle, l'AI conferisce proprietà di resistenza e mantenimento della forma; una sua carenza determina, infatti, un indebolimento della

pelle con la conseguente formazione di rughe (SANTORO S. *et al*, 2011). L'AI non ha soltanto importanti funzioni fisiologiche, ma è anche coinvolto nella regolazione di stati patologici. Infatti, l'AI è coinvolto nella risposta iniziale ad un danno tissutale, che prevede la formazione di una matrice temporanea estremamente ricca di AI e fibrina, la quale supporta la migrazione di fibroblasti e cellule endoteliali nell'area della lesione (D. RICHARD *et al*, 2007). L'AI, quindi, è in grado di contribuire alla modulazione della reazione infiammatoria (viene prodotto in risposta alle citochine infiammatorie), e non solo regolando la migrazione cellulare (FAKHARI A. *et al*, 2013), ma anche esercitando un'azione di scavenger dei radicali liberi, proteggendo così i tessuti dai danni ossidativi (FAKHARI A. *et al*, 2013).

Fisiologicamente, la concentrazione di AI nei tessuti tende a diminuire con l'avanzare dell'età, a causa della naturale presenza di enzimi che catalizzano la degradazione delle catene polimeriche: ialuronidasi, BD-glucuronidasi e β -N-acetil-esosaminidasi (FAKHARI A. *et al*, 2013). La degradazione enzimatica rompe la macromolecola di AI in polimeri più piccoli: oligosaccaridi e acido ialuronico a basso peso molecolare, che perdono le funzioni dell'AI da cui sono originati (D. RICHARD *et al*, 2007).

1.3 Metodi di produzione e gradi di purezza dell'AI

1.3.a Metodi di produzione dell'AI

Inizialmente l'AI veniva estratto dai tessuti tra i quali il cordone ombelicale, la pelle e la cresta del gallo. Tuttavia, alcuni studi hanno dimostrato che queste tre fonti contengono impurità come, ad esempio, acidi nucleici e proteine (YAMADA T. *et al*, 2005); infatti, in questi tessuti l'AI si trova complessato con proteoglicani. Pertanto, l'isolamento dell'AI da queste fonti comportava difficoltà non indifferenti e conseguentemente costi abbastanza importanti. Inoltre, in seguito all'iniezione di AI ottenuto da queste fonti, sono stati anche riscontrati casi di allergie e reazioni infiammatorie in soggetti predisposti a reazioni allergiche da prodotti aviari (YAMADA T. *et al*, 2005). Per tutti questi motivi, nel corso degli anni, con il progresso della tecnologia, si sono cercate fonti di AI alternative a quella animale.

È risultata promettente la produzione di AI per via microbiologica fermentativa. In questo caso, l'AI viene sintetizzato da alcuni gruppi patogeni di *Streptococcus Lancefield A e C*, *Streptococcus equi* e *zoepidemicus* attraverso processi di fermentazione su scala industriale (O'REGAN M. *et al*, 1994). L'AI è sintetizzato in tali batteri come una capsula extracellulare che, oltre ad avere un ruolo nei confronti del sistema immunitario umano, ha anche la funzione di fornire al batterio una protezione nei

confronti di ossidi reattivi rilasciati dai leucociti umani e, quindi, una protezione nei confronti della fagocitosi. Poiché i batteri possono usare l'AI per migrare attraverso gli strati epiteliali dei tessuti, è evidente che la capsula di AI contribuisce in larga parte alla patogenicità di tale batterio (CHONG BF *et al*, 2005).

A causa dell'elevata viscosità dell'AI raggiungibile durante il processo fermentativo, la concentrazione massima per questioni pratiche è fissata a 5-10 g/l, raggiunta dopo un periodo di coltivazione di 6-16 ore (CHONG BF *et al*, 2005). Le capsule di AI sono inizialmente legate al batterio. Successivamente, queste vengono rimosse dalle cellule e sono libere di essere sospese in soluzione; infatti, in seguito alla coltivazione, il terreno di crescita altamente viscoso viene diluito con acqua e i batteri vengono rimossi mediante filtrazione o centrifugazione. La rimanente soluzione contenente AI viene sottoposta a successiva purificazione e concentrazione eliminando, così, le proteine attraverso trattamenti con proteasi. In seguito, l'AI è normalmente precipitato dalla soluzione acquosa con solventi miscibili con acqua quali l'etanolo, l'acetone o l'isopropanolo (VOLPI N. *et al*, 2009).

1.3.b Gradi di purezza dell'AI

L'AI può avere diversi gradi di purezza a seconda dei materiali grezzi utilizzati per produrlo e della relativa metodologia di lavorazione.

Sodio ialuronato Standard

Questa formulazione è caratterizzata da una concentrazione di endotossine compresa tra 500 UE/g e 0,5 UI/mg, un peso molecolare tra 40-3000 kDa e una viscosità intrinseca tra 0,2-3,2 m³/kg. Si tratta, pertanto, di una formulazione per uso parenterale come alimento funzionale, per uso topico e per applicazioni intravescicali.

Sodio ialuronato Plus

Questa formulazione è caratterizzata da una concentrazione di endotossine compresa tra 40 UE/g e 0,4 UI/mg, un peso molecolare tra 40-3000 kDa e una viscosità intrinseca tra 0,2-3,2 m³/kg. Si tratta, pertanto, di una formulazione per uso parenterale, come gocce oftalmiche, e per applicazioni intravescicali e per aerosol.

Sodio ialuronato Ultrapuro

Questa formulazione è caratterizzata da una concentrazione di endotossine compresa tra 5 UE/g e 0,005 UI/mg, un peso molecolare tra 40-3000 kDa e una viscosità intrinseca tra 0,2-3,2 m³/kg. Si tratta, pertanto, di una formulazione per uso

intrarticolare, intraoculare, ideale per produrre *cross-linking systems* e sistemi di viscosupplementazione.

1.4 Applicazioni biomediche dell'AI e dei suoi derivati

Affinché l'AI possa essere impiegato in maniera ottimale e sicura in campo umano nelle diverse aree applicative, è importante controllare oltre che la purezza, in termini di assenza di contaminanti, anche i processi produttivi che devono portare all'ottenimento delle frazioni di AI a differente peso molecolare in maniera riproducibile e costante. Ciò garantisce che i prodotti finali contengano un AI perfettamente caratterizzato dal punto di vista del peso molecolare e dunque ottimizzato per l'uso specifico.

Le aree di applicazioni cliniche dell'AI e dei suoi derivati sono state classificate come segue:

1. *visco-chirurgiche*: per proteggere i tessuti delicati durante le manipolazioni chirurgiche, come nella chirurgia oftalmica;
2. *visco-aumento*: per riempire e potenziare spazi tessutali, come nella pelle e nei tessuti vocali e della faringe;
3. *visco-separazione*: per separare la superficie del tessuto connettivo traumatizzata da interventi chirurgici o lesioni, al fine di prevenire aderenze e formazione di cicatrici eccessive;
4. *visco-supplementazione*: per sostituire o integrare fluidi dei tessuti, come la sostituzione di liquido sinoviale;
5. *visco-protezione*: per proteggere superfici tessutali sane, ferite o danneggiate dalla disidratazione o dagli agenti ambientali nocivi, e promuoverne poi la guarigione.

1.5 Applicazioni mediche ed estetiche dell'AI

La biocompatibilità, la biodegradabilità (LIAO YH *et al*, 2005), la muco-adesività (MAYOL L. *et al*, 2008) e la viscoelasticità dell'AI (LIAO YH *et al*, 2005) sono solo alcune delle proprietà che rendono tale polimero particolarmente utile sia in campo medico-farmaceutico, sia in campo cosmetico-estetico. Infatti, diversi prodotti contenenti AI sono stati approvati per l'utilizzo in chirurgia oftalmica, dermatologica e nella riparazione tissutale (D. RICHARD *et al*, 2007). Vantaggio non indifferente è che quasi tutte le persone che lo necessitano possono sottoporsi ad una terapia con un prodotto a base di AI, poiché quest'ultimo, essendo prodotto per via biotecnologica, è chimicamente identico all'AI prodotto naturalmente dal corpo umano, per cui non presenta rilevanti effetti collaterali. Solamente in casi molto rari, l'AI può creare allergia che si manifesta con eritema transitorio o lieve gonfiore. In questi

casi, tuttavia, il problema può essere facilmente evitato effettuando un semplice test di allergia cutanea prima di iniziare la terapia (D. RICHARD *et al*, 2007).

1.5.a AI come sistema di drug delivery: idrogel di AI

L'AI presenta notevoli vantaggi rispetto ad altri sistemi usati per la veicolazione dei farmaci (*drug delivery*), soprattutto per la sua biodegradabilità e per la sua non-immunogenicità - è "invisibile" al sistema immunitario, essendo un componente naturale dei fluidi corporei, ed è metabolizzato dai lisosomi delle cellule (JAROSLAV D, 1991). Il ruolo principale del *carrier* consiste nel ritardare i processi di eliminazione del farmaco dall'organismo, permettendo al principio attivo di avere un'efficacia più prolungata (JAROSLAV D, 1991). L'AI, essendo mucoadesivo e, formando, quando disciolto in acqua, soluzioni/gel di viscosità via via crescente man mano che aumenta la sua concentrazione, permette al principio attivo di rimanere *in situ* per un tempo sufficiente a dare un effetto curativo prolungato (JAROSLAV D, 1991). L'AI, quindi, si può comportare da *drug delivery system* per applicazione locale, intramuscolare, intrasinoviale, subcutanea (JAROSLAV DROBNIK, 1991) e intratimpanica (BORDEN RC *et al*, 2010). Gli effetti benefici dell'AI nel *dermal delivery* del diclofenac, per esempio, sono stati a lungo studiati sia *in vitro* che *in vivo* ed è emerso che l'AI è in grado di migliorare significativamente sia la diffusione del diclofenac nella pelle che il suo mantenimento e la sua localizzazione nell'epidermide. Da questi studi è emerso anche che l'AI produce effetti simili anche in combinazione con l'ibuprofene (LIAO YH *et al*, 2005). L'AI è stato, inoltre, utilizzato come *carrier* per farmaci oftalmici, per via della sua viscoelasticità e della sua mucoadesività. È stato dimostrato, ad esempio, che l'AI è in grado di prolungare la permanenza della pilocarpina nell'area precorneale, aumentandone, così, la biodisponibilità (LIAO YH *et al*, 2005).

Gli idrogel di AI possono essere costituiti da AI lineare, AI cross-linkato e da prodotti dall'associazione di AI a *nanocarriers*.

Generalmente, l'AI allo stato puro utilizzato dalle industrie farmaceutiche è sotto forma di polvere; mischiando questa polvere all'acqua si crea una formulazione a base AI libero, non modificato, non cross-linkato. Essa viene eliminata dalla zona in cui è applicata in maniera relativamente rapida, poiché le ialuronidasi degradano prontamente le catene del polimero (TEZEL A. *et al*, 2008). Tuttavia, si osserva, comunque, un rilascio prolungato del principio attivo quando questo è associato al gel di AI, rispetto a quando il principio attivo è somministrato da solo. Borden *et al*, per esempio, hanno utilizzato un modello di maialino della Guinea per determinare se un idrogel di AI legato al desametasone sia un efficiente *delivery system* nel trattamento

intratimpanico. Dal loro studio è emerso che dopo 24 ore dall'iniezione, la concentrazione di desametasone nell'orecchio trattato con il farmaco legato all'idrogel di AI era notevolmente maggiore rispetto a quello trattato con il solo desametasone (BORDEN RC *et al*, 2010).

Per aumentare il tempo di permanenza *in situ* dell'AI, le industrie farmaceutiche ricorrono al *cross-linking*. Tramite un agente cross-linkante, Butandiolo Diglicil Etere (BDDE) o Divinil Sulfone (DVS), si legano covalentemente più catene di AI, creando una vera e propria rete polimerica (TEZEL A. *et al*, 2008). Il gel risultante dal *cross-linking* è molto più resistente alla degradazione enzimatica sia dal punto di vista chimico che fisico. Infatti, le ialuronidasi hanno più difficoltà a penetrare nel gel e lo degradano più lentamente, permettendo, così, alla formulazione di permanere più a lungo nelle aree di applicazione, e al farmaco da essa veicolato di avere un'azione più prolungata (TEZEL A. *et al*, 2008).

Esistono anche idrogel di AI associato a nanosistemi di *drug delivery*. Molti studi hanno dimostrato che offre risultati interessanti nel trattamento di diverse zone (LAJAVARDI L. *et al*, 2009) (MORGEN M. *et al*, 2013) con nuove proprietà che permettono di prolungare il rilascio di sostanze attive e migliorare l'efficacia dei trattamenti.



Figura 2: AI lineare.

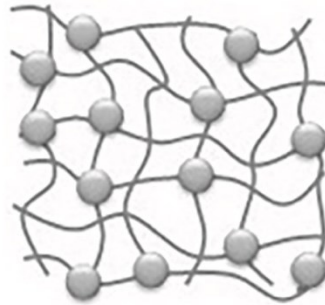


Figura 3: AI cross-linkato.

1.5.b AI per le rughe

L'utilizzo dell'AI si è enormemente diffuso negli ultimi anni in quanto risulta essere molto efficace nel prevenire la comparsa delle rughe e nella cura di quelle già esistenti. L'AI, infatti, stimola la creazione di nuovo collagene ed elastina, ridonando elasticità e tonicità alla pelle ed attenuando, così, la formazione delle rughe (KONTIS TC *et al*, 2012). I prodotti a base di AI attualmente disponibili e più comunemente

utilizzati sono i fillers iniettabili e le creme idratanti e antirughe. In merito a queste ultime, il mercato offre una vasta scelta in base anche alla diversa composizione, tuttavia la percentuale di AI al loro interno è sempre molto limitata. Per questo motivo gli effetti di queste creme sono decisamente più blandi rispetto alle iniezioni a base di AI. Da alcuni studi, tuttavia, l'utilizzo di alcune creme antirughe con una percentuale pari allo 0.1% di AI hanno dato risultati positivi nel ridonare idratazione ed elasticità a particolari aree del viso come, per esempio, l'area periorbitale (PAVICIC T. *et al*, 2011). È inoltre emerso che l'AI a basso peso molecolare è più efficace nel ridurre la profondità delle rughe rispetto a quello ad alto peso molecolare grazie alla sua migliore capacità di penetrare nella pelle e idratarla (PAVICIC T. *et al*, 2011).

2. DERMAL FILLERS DI AI

Il ricorso ai trattamenti estetici a base di DF per l'aumento dei tessuti molli è in continua crescita negli ultimi anni grazie alle nuove tecnologie e al perfezionamento dei prodotti disponibili sul mercato. I DF a base di AI sono attualmente i più popolari grazie alle loro caratteristiche di resistenza e durabilità nel tempo, di bassa immunogenicità, di un'elevata convenienza a livello economico e del successo che riscuote nei pazienti (BORREL M. *et al*, 2011).

2.1 Fillers di AI cross-linkati e grado di cross-linking

Il limite principale dell'AI, quando utilizzato tal quale (catene "libere"), è la sua scarsa durata nel tempo - circa 1-2 giorni - a causa della rapida degradazione enzimatica. Per questo motivo, le industrie farmaceutiche ricorrono a strategie di *cross-linking* per rendere l'AI più resistente, in modo da prolungarne la durata dell'effetto (BORREL M. *et al*, 2011).

Le due principali variabili nei fillers di AI cross-linkati sono rappresentate dalla quantità di catene di AI cross-linkate e dal grado di *cross-linking* (percentuale di agente cross-linkante). Per una data concentrazione di AI, infatti, minore è l'AI libero, maggiore è la coesività del gel. Parametri quali la viscosità lineare (modulo elastico G'), il grado di *cross-linking* e la coesività influenzano le caratteristiche di estrusione poiché il gel è soggetto a forze di iniezione attraverso un ago sottile. In generale, quando G' aumenta (all'aumentare della quantità di catene di AI cross-linkate e del grado di *cross-linking*), diventa più difficile iniettare il gel; di conseguenza è necessario incorporare nel filler una piccola quantità di AI libero allo scopo di lubrificare

e rendere più fluido il gel (diminuisce, infatti, la coesività del prodotto) (BORREL M. *et al*, 2011).



Figura 4: AI allo stato libero (KABLIK J. *et al*, 2009).

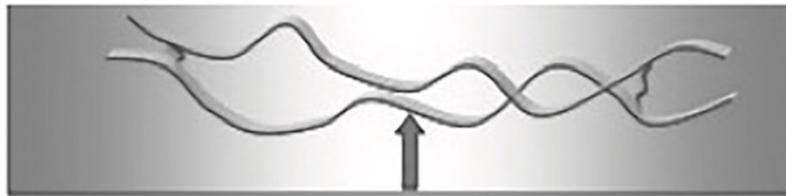


Figura 5: AI a basso grado di *cross-linking* (morbido) (KABLIK J. *et al*, 2009).

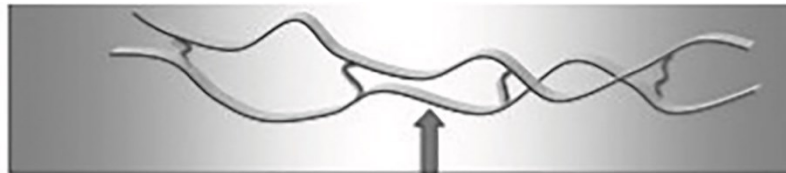


Figura 6: AI ad alto grado di *cross-linking* (rigido) (KABLIK J. *et al*, 2009).

2.2 Proprietà reologiche dei fillers di AI

2.2.a Consistenza dei fillers di AI

Tra i fattori che influenzano le proprietà dei DF a base di AI vi è la consistenza, intesa come la dimensione delle molecole che compongono il gel. In seguito al processo di *cross-linking*, infatti, il gel deve essere ridimensionato per renderlo idoneo all'iniezione nella pelle. Il ridimensionamento viene generalmente eseguito facendo

scorrere il gel attraverso una serie di setacci che ne assottigliano la struttura. Un metodo alternativo per ridimensionare il gel e renderlo idoneo all'iniezione è quello di frammentarlo attraverso un processo di omogenizzazione. Il risultato di questo processo è un gel caratterizzato da una consistenza liscia che assomiglia al tuorlo d'uovo, dovuta presumibilmente ad una più ampia distribuzione delle molecole del gel rispetto a quella ottenuta utilizzando i setacci. I prodotti elaborati con questo processo sono formulazioni gel più morbide, con un valore di G' più basso, risultando più fluide al momento dell'iniezione (TEZEL A. *et al*, 2008).

La dimensione delle molecole è, inoltre, strettamente legata al grado di degradazione dell'AI nel corpo in seguito all'iniezione del filler. Le molecole di AI più grandi, infatti, offrono agli enzimi una superficie limitata di azione, rendendone così più complicata la penetrazione nel gel e, quindi, la degradazione. Le molecole di AI più piccole, invece, offrono agli enzimi una superficie più vasta, facilitandone la penetrazione nel gel e la conseguente degradazione (TEZEL A. *et al*, 2008).

2.2.b Viscoelasticità e forza di estrusione dei fillers di AI

La viscosità di un DF e la forza necessaria per farlo transitare attraverso un ago sono legate innanzitutto al suo grado di *cross-linking* (TEZEL A. *et al*, 2008); a parità di condizioni, infatti, aumentando il grado di *cross-linking* dell'AI, il gel risulta più compatto ed aumentano conseguentemente anche la sua viscoelasticità e forza di estrusione.

Inoltre, la viscosità di un DF e la forza necessaria per farlo transitare attraverso un ago dipendono anche dal suo metodo di ridimensionamento e dal suo processo di produzione (TEZEL A. *et al*, 2008). I DF di AI ridimensionati attraverso l'uso dei setacci tendono ad avere una maggiore viscoelasticità e richiedono, quindi, una maggiore forza di estrusione rispetto a quelli prodotti con la tecnica di omogenizzazione.

Anche la presenza di AI libero influisce sulla forza di estrusione in quanto facilita la transizione del gel attraverso l'ago; maggiore è la quantità di AI libero all'interno di un gel, minore è la forza di estrusione necessaria al momento dell'iniezione nella pelle (TEZEL A. *et al*, 2008). Nei DF a base di AI attualmente sul mercato, il valore di G' varia (anche in base al processo di produzione) tra 10 e 1000 Pa; essi possono essere, quindi, considerati fillers leggeri, visto che il loro modulo elastico non supera il valore di 1000 Pa (PIERRE S. *et al*, 2015). I fillers di AI caratterizzati da un elevato modulo elastico sono più indicati per iniezioni profonde nello strato sub-cutaneo della pelle, mentre quelli caratterizzati da un modulo elastico più basso sono preferibili per l'impianto negli strati più superficiali della pelle, per la correzione di rughe o solchi

leggeri (PIERRE S. *et al*, 2015). L'utilizzo di un filler ad alta o bassa viscoelasticità modifica notevolmente il risultato estetico finale a livello del tessuto in cui viene iniettato. Per esempio, un filler a bassa viscoelasticità, applicato a livello delle labbra tende ad espandersi conferendo ad esse una consistenza più naturale e morbida al tatto. Al contrario, un filler ad alta viscoelasticità applicato a livello delle labbra, tende a rimanere *in situ*: ne risultano labbra più plastiche e rigide al tatto (SUNDARAM H. *et al*, 2010).

2.2.c Coesività e compressione dei fillers di AI

La coesività definisce come un filler si comporta, in quanto gel, una volta iniettato nel viso ed è strettamente correlata al grado di interazioni attrattive tra le unità di AI cross-linkate che compongono il gel stesso. Queste forze di attrazione dipendono dalla concentrazione di AI e dalla tecnologia utilizzata nel processo di *cross-linking* (PIERRE S. *et al*, 2015). Una volta iniettati nel viso e soggetti alle forze di compressione (contatto con superfici esterne come, ad esempio, appoggiarsi ad un cuscino), i fillers di AI con una bassa coesività tendono a perdere la loro forma più facilmente rispetto a quelli ad alta coesività, e a disperdersi nel derma fino a diventare uno strato piatto. Il grado di dispersione dipende dalla zona in cui viene iniettato il prodotto. Se la zona è ristretta, la dispersione è minima grazie all'integrazione nella matrice dermica; se, invece, la zona è più vasta, la dispersione è più elevata. Pertanto si evince che la mancanza di coesività tra le molecole formanti il gel aumenta la possibilità delle stesse di separarsi, facilitando, potenzialmente, la migrazione del filler (PIERRE S. *et al*, 2015).

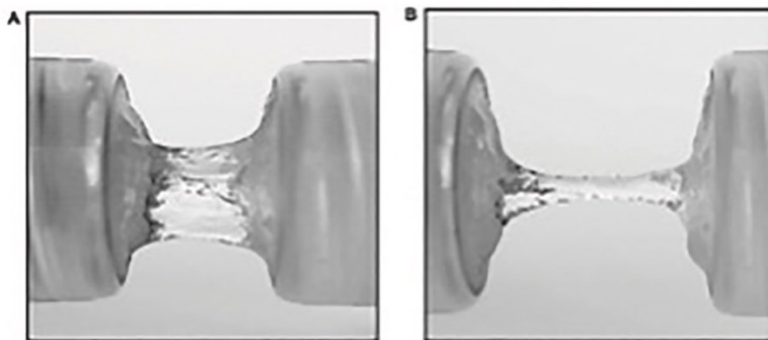


Figura 7: Confronto tra AI ad alta coesività (A) e AI a bassa coesività (B). (BORRELL M. *et al*, 2011).

3. VANTAGGI DEI FILLERS A BASE DI AI

Vi sono molteplici benefici nell'utilizzo dei DF a base di AI per il ringiovanimento del viso. Gli effetti, infatti, sono visibili immediatamente dopo il trattamento e includono un aspetto più idratato e lucente della pelle nella zona trattata. I pazienti, inoltre, possono tornare alla loro quotidiana routine già lo stesso giorno in cui viene effettuato il trattamento, in quanto gli effetti collaterali dell'AI sono rari e di lieve entità. Il grande vantaggio derivante dall'utilizzo dei filler di AI rispetto agli altri fillers è che sono completamente reversibili, grazie alle ialuronidasi, e non provocano danni tissutali (CARRUTHERS J. *et al*, 2010).

4. LE IALURONIDASIS

Le ialuronidasi sono enzimi ampiamente utilizzati in medicina estetica per prevenire le complicazioni dovute ad un uso improprio o eccessivo dell'AI. Esse appartengono alla categoria delle endoglicosidasi e depolimerizzano l'AI riducendone l'alta viscosità e, quindi, conseguentemente, la sua azione lubrificante. Le ialuronidasi utilizzate in ambito medico derivavano inizialmente da estratti grezzi del tessuto testicolare ovino o bovino e sono disponibili in forma di polvere e soluzione (SMALL R, 2014). Gli enzimi ottenuti da queste fonti, tuttavia, provocavano problemi per via della loro impurità e della loro immunogenicità: infatti, contenevano proteasi, immunoglobuline e fattori vasoattivi (CAVALLINI M. *et al*, 2013). Successivamente, fu introdotta la tecnica di produzione di ialuronato-liasi dallo *Streptococcus agalactiae*; questi enzimi risultavano più puri, e maggiormente specifici (CAVALLINI M. *et al*, 2013). Attualmente è disponibile una nuova formulazione chiamata Hylenex®: si tratta di una combinazione di ialuronidasi di origine umana, ed è considerata meno immunogena e più sicura. Infatti, tale formulazione facilita l'eliminazione dell'AI attraverso i reni e il suo effetto dura approssimativamente 48 ore. Nel caso in cui le ialuronidasi siano utilizzate per la correzione di un'eccessiva quantità di AI iniettata, la dose da somministrare dipende principalmente dalla zona di iniezione (CAVALLINI M. *et al*, 2013).

5. EFFETTI COLLATERALI DEI FILLERS DI AI

Gli effetti secondari alla somministrazione di AI sono considerati minimi e trascurabili rispetto a quelli di tutti gli altri fillers. Tra gli effetti avversi non immuno-mediati, i più comuni sono senza dubbio quelli legati alle reazioni in sede di inoculo, quali lividi, eritema, edema, prurito e gonfiore; questi, tuttavia, tendono a regredire spontaneamente nell'arco di poche ore o, al massimo, di pochi giorni. Alternativamente può verificarsi la formazione di ecchimosi superficiali come conseguenza della rottura traumatica dermica e dell'azione anticoagulante dell'AI. Questi effetti collaterali possono anche essere causati da errori nella metodica di esecuzione del trattamento stesso, così come dal posizionamento troppo superficiale del filler o da una distribuzione inadeguata che possono determinare la formazione di noduli o cicatrici ipertrofiche. Inoltre, nonostante l'AI sia non immunogenico, sono stati riscontrati dei rari casi di reazioni immunomediate conseguenti all'utilizzo di fillers a base di AI. Tra queste la più comune è senza dubbio l'insorgenza, a qualche settimana dall'applicazione, di granulomi da corpo estraneo. Secondo alcuni studi, questo tipo di reazioni non sembrerebbero legate alla molecola di AI in sé, ma piuttosto alla presenza di impurità derivanti dai processi di produzione, quali tracce di proteine o DNA batterico. Sembra, infatti, che alcuni preparati di AI, forse a causa della presenza di contaminanti (in particolare di acidi nucleici) stimolino i monociti a secernere interleuchina 12 e tumor necrosis factor alfa, con conseguente risposta infiammatoria (TAJANA G. *et al*, 2011).



Figura 8: Livido (FUNT D. *et al*, 2013).

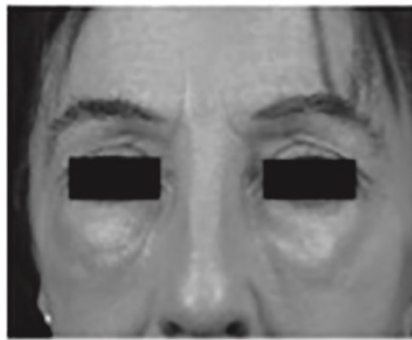


Figura 9: Edema malare (FUNT D. *et al*, 2013).

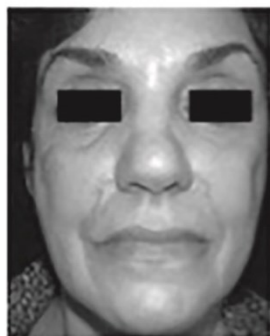


Figura 10: Eritema (FUNT D. *et al*, 2013). Figura 11: Granuloma (FUNT D. *et al*, 2013).

6. AREE DEL VISO TRATTATE CON FILLERS DI AI



1. Rughe di corrugazione
(rughe glabellari)
2. Appiattimento della guancia
(atrofia malare)
3. Solchi naso-labiali
4. Rughe del labbro
(rughe periorali)
5. Assottigliamento del labbro
(atrofia del labbro)
6. Discesa degli angoli della bocca
(depressione delle commessure)
7. Rughe della marionetta
(rughe mento-labiali)
8. Solco mentoniero
(solco labio-mentoniero)
9. Solco mentoniero esteso
(solco labio-mentoniero esteso)
10. Appiattimento del mento
(atrofia del mento)

Figura 12: Rughe, solchi e irregolarità del volto (SMALL R, 2014).

6.1 Fillers di AI per la zona superiore del viso

Le aree della parte superiore del viso che vengono maggiormente trattate con fillers di AI sono:

Glabella

La glabella è la zona tra le sopracciglia in cui si formano generalmente rughe più o meno superficiali dovute al movimento prolungato dei muscoli sopracciliari che si attivano quando si corruga la fronte. Nel trattamento di quest'area, è molto importante che il filler di AI sia iniettato con estrema precisione, evitando un'eccessiva correzione, in quanto si tratta di una zona molto delicata e sensibile all'occlusione dei vasi sanguigni. Una dose di AI eccessiva, infatti, può portare facilmente ad una necrosi cutanea. La combinazione di fillers più consigliata per quest'area risulta essere quella di BTX-A e AI (BRANDT FS. *et al*, 2008) e la tecnica più consigliata è quella lineare retrograda (SMALL R, 2014).

Fronte

Le rughe della fronte sono il risultato dell'azione dinamica dei muscoli frontali e si distinguono in rughe dinamiche e non dinamiche. Le prime sono anche dette "rughe d'espressione", proprio perché compaiono sul volto solo quando si compiono determinati movimenti facciali (ad esempio si sorride o si corruga la fronte), mentre le seconde sono visibili anche a volto rilassato (www.pintomedicalspa.it). Nel caso delle rughe dinamiche, le iniezioni di BTX-A hanno un effetto eccellente, mentre nel secondo caso i fillers di AI sono più consigliabili (BRANDT FS. *et al*, 2008). La tecnica più consigliata per la correzione di quest'area è quella lineare retrograda (SMALL R, 2014).

Area Perioculare

I muscoli sottostanti la regione periorbitale si attivano quando si sorride e si strizzano gli occhi, e questo movimento frequente porta alla formazione delle cosiddette "zampe di gallina". Questo tipo di rughe risponde molto bene alla terapia con il BTX-A, mentre i solchi più profondi della zona sottostante l'occhio rispondono meglio al trattamento con i fillers di AI tramite la tecnica a deposito (SMALL R, 2014). Trattandosi di una zona molto delicata, non è rara la formazione di grumi o lividi in seguito all'iniezione del filler. Per questo, la tecnica di applicazione migliore consiste nel far seguire all'iniezione un lieve massaggio dell'area trattata, per evitare la formazione di grumi; in caso di necessità, inoltre, si possono anche applicare degli

impacchi di ghiaccio allo scopo di ridurre il rischio di insorgenza di lividi (BRANDT FS. *et al*, 2008).

La figura 13 illustra il risultato ottenuto dalla somministrazione dello Juvéderm® Ultra da 24 mg/mL per correggere la perdita di volume nella zona dei dotti lacrimali in una donna di 30 anni. Subito dopo l'iniezione, è stato effettuato un lieve massaggio ed è stato applicato del ghiaccio nella zona trattata per ottimizzare il risultato (GOLD M, 2009).

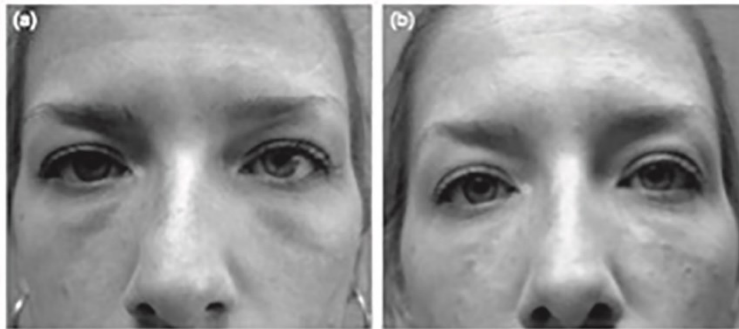


Figura 13.

6.2 Fillers di AI per la zona centrale del viso

Le aree maggiormente trattate della parte centrale del viso sono:

Area orbitale inferiore

Vi sono molti fattori che influenzano la perdita di volume e la conseguente formazione di rughe e borse nella regione periorbitale, quali la mancanza di sonno notturno, lo stress e le diete estreme. A questo proposito, i fillers di AI sono molto efficaci nel donare un'espressione più fresca e giovanile a queste aree, riducendo, così, l'apparente stanchezza. Il filler di AI deve essere iniettato in profondità attraverso la tecnica a deposito (SMALL R, 2014) facendo seguire un lieve massaggio nella zona trattata. A causa dell'elevata presenza di vasi sanguigni in quest'area, i lividi sono i principali effetti collaterali che si manifestano dopo l'iniezione (BRANDT FS. *et al*, 2008).

Guance e area malare

Negli ultimi anni, sono aumentate notevolmente le richieste di correzione della zona degli zigomi e dei solchi nasolabiali poiché si tratta delle parti del viso più

soggette alla perdita di volume con l'avanzare dell'età. I fillers più utilizzati a tale scopo sono quelli a base di AI, che danno risultati molto soddisfacenti. Grazie all'uso di questi fillers, infatti, non solo si correggono i solchi nasolabiali, ma si ridona anche un'aspetto più giovanile al viso (BRANDT FS. *et al*, 2008). Dal punto di vista reologico, i fillers di AI più efficaci per correggere queste aree devono avere un modulo elastico (G') sufficiente a sopportare le forze di taglio date dalla ripetuta contrazione dei muscoli del viso, e una coesività medio-alta per resistere alle forze di compressione che si esercitano quando i muscoli del viso si contraggono (PIERRE S. *et al*, 2015). Nella pratica, i fillers di AI più utilizzati dai medici per la correzione della zona malare sono il Restylane®, il Perlane® e lo Juvéderm® Ultra Plus XC, proprio perché meccanicamente forti al punto tale da assicurare un risultato più preciso e duraturo (BRANDT FS *et al*, 2008). La tecnica più consigliata per quest'area è quella a deposito (SMALL R, 2014).

La figura 14 illustra il risultato ottenuto in seguito all'iniezione dello Juvéderm® da 24 mg/mL per ridonare volume agli zigomi di una donna di 66 anni (GOLD M, 2009).

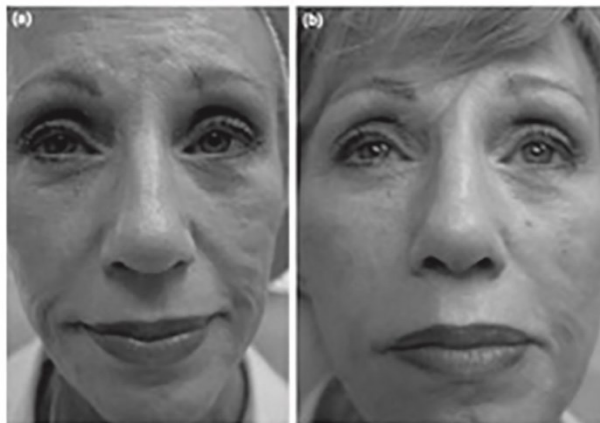


Figura 14.

6.3 Fillers di AI per la zona inferiore del viso

Le aree maggiormente trattate della parte inferiore del viso sono:

Labbra

Da sempre, le labbra simboleggiano bellezza e sensualità, soprattutto nelle donne, e sono al centro dell'attenzione per quanto riguarda la medicina estetica. Anche le

labbra, infatti, sono soggette alla perdita di volume, definizione e forma con l'avanzare dell'età, e tendono a diventare strette, pallide e piatte. In questo caso, i fillers di AI sono consigliati per ridonare loro volume e turgidità, conferendo anche un aspetto più giovanile e gradevole al viso (BRANDT FS. *et al*, 2008). Dal punto di vista reologico, nella scelta del filler ideale per questo tipo di trattamento è necessario tenere in considerazione l'estrema mobilità di quest'area. Per questo motivo, il filler ideale deve essere abbastanza morbido da essere facilmente iniettabile, deve potersi integrare bene con il viso seguendone i movimenti naturali e non deve essere palpabile al tatto. Questo si traduce in un filler con un moderato modulo elastico (G') ed una coesività da bassa a media. In caso di solchi profondi, tuttavia, è possibile utilizzare anche un filler ad alta viscosità (come lo Juvéderm® Ultra Plus) per dare una correzione più duratura (PIERRE S. *et al*, 2015). Le tecniche più utilizzate per la correzione di quest'area sono quella a ventaglio, quella a reticolo e lineare retrograda (SMALL R, 2014).

La figura 15 illustra il risultato ottenuto dalla somministrazione dello Juvéderm® Ultra Plus da 24 mg/mL per ridare volume e uniformità alle labbra in una donna di 40 anni. (GOLD M, 2009).

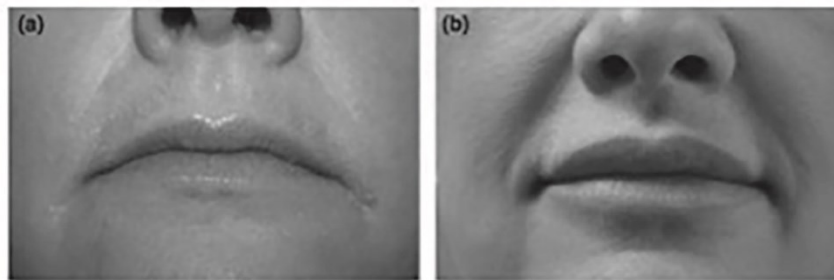


Figura 15.

Mento

La perdita di collagene e dei cuscinetti adiposi sottocutanei sono all'origine dei solchi che possono formarsi sul mento e che sono spesso oggetto di correzione attraverso i trattamenti estetici. I fillers di AI conferiscono un effetto eccellente e duraturo nella correzione di quest'area, (BRANDT FS. *et al*, 2008) e il filler ideale deve caratterizzarsi per un elevato modulo elastico (G') e per un'elevata coesività (ad esempio, Juvéderm® Ultra Plus), in modo tale che possa sopportare la tensione e la compressione dei muscoli prominenti l'osso (PIERRE SÉBASTIEN *et al*, 2015). La tecnica più consigliata per quest'area è quella lineare retrograda (SMALL R, 2014).

CONCLUSIONI

La medicina estetica è in continua espansione grazie alle crescenti esigenze del mercato che rispecchiano un pubblico sempre più orientato ai canoni di bellezza e cura del corpo.

Anche in Italia il ricorso alla medicina estetica è fortemente aumentato negli ultimi anni. Nel 2013, infatti, sono stati eseguiti circa 956.500 interventi di chirurgia e di medicina a fine estetico, di cui il 75% è costituito da soli interventi estetici (correzione dei difetti del viso, riempimento dei tessuti molli e ridefinizione dei contorni del volto). Rispetto al precedente 2012, il numero totale di interventi di medicina estetica è cresciuto del 6,8% e i DF più utilizzati sono stati AI, al primo posto dal 2011 a oggi (289.607 interventi, +14,5% rispetto al 2012), BTX-A (223.500 interventi, +10,4% rispetto al 2012) e CaHA (che ha triplicato gli interventi, arrivando a 45.000 procedure, +72,8% rispetto al 2012) (www.aicpe.org/public/Files/rif000052/896/statistica%202014.pdf). Nel 2014, il numero di trattamenti di chirurgia plastica e medicina estetica ha superato persino il milione (1.016.377 per la precisione) e, di tali interventi, il 76% è rappresentato da soli trattamenti estetici (www.aicpe.org/public/Files/rif000052/3173/statistiche_aicpe_2014.pdf). Per la prima volta, l'intervento più eseguito è stato quello con BTX-A (274.870 procedure, +22,9%), superando di poco quello con l'AI (265.324, -8,3%) (www.aicpe.org/public/Files/rif000052/3173/statistiche_aicpe_2014.pdf). I grafici sottostanti riportano i dati in discussione, emersi al congresso AICPE, tenutosi a Firenze dal 9 al 13 Marzo 2015, sulla base dell'indagine eseguita tra i chirurghi plastici estetici in merito a chirurgia e medicina estetica.

2011		638.655		
2012			673.950	
2013				719.708
2014				772.276

Tabella 2: Interventi di medicina estetica svolti in Italia dal 2011 al 2014 (www.aicpe.org/public/Files/rif000052/896/statistica%202014.pdf). Fonte: Indagine tra i chirurghi plastici italiani a cura di AICPE.

Intervento	Num. Procedure	Variazione % vs. 2013	Posizione classifica 2014	Posizione classifica 2013	Posizione classifica 2012	Posizione classifica 2011
Iniettabili						
BTX-A	274.870	+22.9	1	2	2	2
CaHA	37.473	-16.7	3	3	5	8
AI	265.324	-8.3	2	1	1	1
PLLA	8.536	-25.5	14	8	17	13
Fillers permanenti	30	-90.6	20	18	16	17
Altri tipi di fillers	21.321	+4.7	6	6	15	17
Tecniche per il ringiovanimento del viso						

Tabella 3: Interventi di medicina estetica svolti in Italia dal 2011 al 2014 (www.aicpe.org/public/Files/rif000052/896/statistica%202014.pdf). Fonte: Indagine tra i chirurghi plastici italiani a cura di AICPE.

Tossina botulinica di tipo A		274.870 (+22,9%)
Acido ialuronico		265.324 (-8,3%)
Idrossiapatite di calcio	37.473 (-16,7%)	

Tabella 4: Interventi di medicina estetica più eseguiti in Italia nel 2014 e, tra parentesi, la variazione % rispetto al 2013 (www.aicpe.org/public/Files/rif000052/896/statistica%202014.pdf). Fonte: Indagine tra i chirurghi plastici italiani a cura di AICPE.

Da queste indagini, inoltre, è emerso che anche gli uomini fanno sempre più ricorso a trattamenti estetici per contrastare l'invecchiamento del viso. Nel 2013, la percentuale totale di uomini italiani che si sono sottoposti a trattamenti estetici è stata del 24,4%, contro il 75,60% del pubblico femminile.

Fascia d'età	Totale	Donne	Uomini
19-34	30,70%	22,90%	7,80%
35-50	32,40%	25,00%	9,40%
51-64	25,60%	20,50%	5,10%
Over 65	9,30%	7,20%	2,10%
Totale	100,00%	75,60%	24,40%

Tabella 5: Pazienti che per la prima volta hanno eseguito un trattamento di medicina estetica nel 2013 (www.aicpe.org/public/Files/rif000052/896/statistica%202014.pdf). Fonte: Indagine tra i chirurghi plastici italiani a cura di AICPE.

Questi dati, quindi, confermano che i fillers di AI sono più utilizzati nei trattamenti di medicina estetica per via dei loro molteplici vantaggi, tra cui in primis l'elevata biocompatibilità dell'AI. La relativa facilità e rapidità di applicazione dei DF di AI, inoltre, li rendono estremamente versatili e adatti, quindi, ad una vasta gamma di pazienti. Nonostante i numerosi DF a base di AI già sul mercato, attualmente vi sono ancora molti prodotti innovativi (nell'ambito dei DF) in fase di sperimentazione o in attesa di approvazione da parte della FDA; questi saranno prossimamente disponibili sul mercato. Anche la Cina, paese in cui la domanda di trattamenti estetici ha subito un forte aumento negli ultimi anni, è diventata un punto di riferimento nella produzione e commercializzazione dell'AI, diventando, così, la principale concorrente americana.

I DF, quindi, e in particolare quelli a base di AI, si presentano attualmente e sono destinati a presentarsi in futuro come eccellenti alternative alla chirurgia plastica, poichè assicurano risultati notevoli e meno invasivi, comportando pochi eventuali effetti collaterali.

RIFERIMENTI BIBLIOGRAFICI

- BORREL MARCOS, B DUSTIN, TEZEL LESLIE & AHMET (2011) *Lift capabilities of hyaluronic acid fillers*. Journal of Cosmetic and Laser Therapy 13: 21-27.
- CARRUTHERS JEAN, MD, CARRUTHERS ALASTAIR, MD, TEZEL AHMET, PhD, KRAEMER JENNIFER, BSc (HONS), MSc, AND CRAIK LINDSAY, BA, BAA (2010) *Volumizing with a 20-mg/mL Smooth, Highly Cohesive, Viscous Hyaluronic Acid Filler and Its Role in Facial Rejuvenation Therapy*. Dermatol Surg 36: 1836-1892.
- CAVALLINI M, MD; GAZZOLA R, MD; METALLA M, MD; VAIENTI L, MD (2013) *The Role of Hyaluronidase in the Treatment of Complications From Hyaluronic Acid Dermal Fillers*. Aesthetic Surgery Journal 33(8): 1167-1174.
- CHONG BF, BLANK LM, McLAUGHLIN R, NIELSEN LK (2005) *Microbial hyaluronic acid production*. Appl Microbiol Biotechnol 66: 341-351.
- D. RICHARD, PRICE MG BERRY, HARSHAD A, NAVSARIA (2007) *Hyaluronic acid: the scientific and clinical evidence*. Journal of Plastic, Reconstructive et Aesthetic Surgery 60, 1110-1119
- DEREK H., JOHNS MD, (2009) *Semipermanent and Permanent Injectable Fillers*. Dermatol Clin 27: 433-444.
- FAKHARI A, BERKLAND C (2013) *Applications and emerging trends of hyaluronic acid in tissue engineering, as a dermal filler and in osteoarthritis treatment*. Acta Biomaterialia 9, 7081-7092.
- GOLD MICHAEL, MD (2009) *The science and art of hyaluronic acid dermal filler use in esthetic applications*. Journal of Cosmetic Dermatology, 8, 301-307.
- JAROSLAV DROBNIK (1991) *Hyaluronan in drug delivery*. Advanced Drug Delivery Reviews, 7; 295-308.
- KABLIK JEFFREY, MONHEIT GARY D, MD, YU LIPING, PhD, CHANG GRACE, and GERSHKOVICH JULIA (2009) *Comparative Physical Properties of Hyaluronic Acid Dermal Fillers*. Dermatol Surg; 35:302-312.
- KONTIS THEDA C, MD (2012) *Contemporary Review of Injectable Facial Fillers*. Arch Facial Plast Surg.
- LAJAVARDI LAURE, CAMELO SERGE, AGNELY FLORENCE, LUO WEI, GOLDENBERG BRIGITTE, NAUD MARIE-CHRISTINE, BEHAR-COHEN FRANCINE, DE KOZAK YVONNE, BOCHOT AMÉLIE (2009) *New formulation of vasoactive intestinal peptide using liposomes in hyaluronic acid for uveitis*. Journal of Controlled Release 139: 22-30.
- LAPČIK LUBOMR JR., LAPČIK LUBOMR, DE SMEDT STEFAAN, DEMEESTER JOSEPH AND CHABREČEK PETER (1998) *Hyaluronan: preparation, structure, properties and applications*. Chem Rev, 98(8): 2663-2684.
- LAURENT TC, LAURENT UBG, FRASER JRE (1995) *Functions of hyaluronian*. Ann Rheum Dis 54: 429-432.

- LIAO YH, JONES SA, FORBES B, MARTIN GP, BROWN MB, (2005) *Hyaluronian: Pharmaceutical characterization and drug delivery*. Drug Deliv 12: 327-342.
- LIAO YONG-HONG, JONES STUART A, FORBES BEN, MARTIN GARY P, AND BROWN MARC B. (2005) *Hyaluronan: Pharmaceutical Characterization and Drug Delivery*. Drug Deliv, 12: 327-342.
- MAYOL L, QUAGLIA F, BORZACCHIELLO A, AMBROSIO, LA ROTONDA MI (2008) *A novel poloxamer/hyaluronic acid in situ forming hydrogel for drug delivery: rheological, mucoadhesive and in vitro release properties*. Eur J Pharm Biopharm 70: 199-206.
- MENDOZA G, PRIETO J.G., REAL R, PÉREZ M, MERINO G. AND ALVAREZ A.I. (2009) *Antioxidant Profile of Hyaluronan: Physico-Chemical Features and its Role in Pathologies*. Mini- Reviews in Medicinal Chemistry 9: 1479-1488.
- MORGEN MICHAEL, TUNG DAVID, BORAS BRITTON, MILLER WARREN, MALFAIT ANNE-MARIE, AND TORTORELLA MICKY TORTORELLA (2013) *Nanoparticles for Improved Local Retention after Intra-Articular Injection into the Knee Joint*. Pharm Res 30(1): 257-68.
- O'REGAN M, MARTINI I, CRESCENZI F, DE LUCA C, LANSING M (1994) *Molecular mechanisms and genetics of hyaluronan biosynthesis*. Int J Biol Macromol 16: 283-286.
- PAVICIC T, GAUGLITZ GG, LERSCH P, SCHWACH-ABDELLAOUI K, MALLE B, KORTING HC, FARWICK M (2011) *Efficacy of cream-based novel formulations of hyaluronic acid of different molecular weights in anti-wrinkle treatment*. J. Drugs Dermatol, 10(9) 990-1000.
- PIERRE SÉBASTIEN, PHD, LIEW STEVEN, MD, AND BERNARDIN AUDE, PHD (2015) *Basics of Dermal Filler Rheology*. Dermatol Surg; 41: S120-S126.
- SANTORO STEFANO, RUSSO LUISA, ARGENZIO VINCENZO, BORZACCHIELLO ASSUNTA (2011) *Rheological properties of cross-linked hyaluronic acid dermal fillers*. Appl Biomater Biomech; Vol. 9 no. 2, 127-136.
- SCOTT JE, (1989) *The biology of hyaluronian*. Ciba Foundation Symposium 143, Wiley, Chichester, p. 6
- SCOTT JE, HEATLEY F (1999) *Hyaluronian forms specific stable tertiary structures in aqueous solution: A C NMR study*. Proc Natl Acad Sci USA 96: 4850-4855.
- SMALL R. (2014) *Filler Dermici*. Piccin Nuova Libreria S.p.A., Padova.
- SUNDARAM H, MD, VOIGTS B, MS, BEER K, MD AND MELAND M, BS (2010) *Comparison of the Rheological Properties of Viscosity and Elasticity in Two Categories of Soft Tissue Fillers: Calcium Hydroxylapatite and Hyaluronic Acid*. Dermatol Surg 36:1859-1865.
- TAJANA G, BIANCHI L, IORIO V, LISI P (2011) *Efficacia e sicurezza dell'acido ialuronico in dermocosmesi: il "caso" Viscoderma®*. Annali Italiani di Dermatologia allergologica 65:106- 112.
- TEZEL AHMET & FREDRICKSON GLENN H. (2008) *The science of hyaluronic acid dermal fillers*. Journal of Cosmetic and Laser Therapy; 10: 35-42.

L'Acido ialuronico (AI) nei trattamenti estetici, una review critica

VOLPI N, SCHILLER J, STERN R, SOLTES L (2009) *Role, metabolism, chemical modifications and applications of hyaluronan*. *Curr Med Chem* 16: 1718-1745.

www.aicpe.org/public/Files/rif000052/896/statistica%202014.pdf

www.dermatologiaLegale.it

www.fda.gov/MedicalDevices/ProductsandMedicalProcedures/CosmeticDevices/WrinkleFillers/default.htm

www.fda.gov/MedicalDevices/ProductsandMedicalProcedures/DeviceApprovalsandClearances/Recently-ApprovedDevices/ucm280839.htm

www.obvieline.fr www.pintomedicalspa.it

www.sicpre.it/Documenti/Stampa/Uomini_Britannici_Italiani_Confronto.pdf

YAMADA T, KAWASAKI T. (2005) *Microbial synthesis of hyaluronan and chitin: New approaches*. *J Biosci Bioeng* 99: 521-528.

Botanical photo-protection alternatives to synthetic UV filters

Stefano Manfredini^{b,c}, Matteo Radice^a, Paola Ziosi^c, Valeria Dissette^b, Piergiacomo Buso^b, Arianna Fallacara^b, Alessia Bino^b and Silvia Vertuani^{b,c}

a. *Universidad Estatal Amazónica (Km 2 ½ Via Napo (paso lateral), Puyo, Pastaza, Ecuador*

b. *Department of Life Sciences and Biotechnology, Master Course in Cosmetic Science and Technology, University of Ferrara, Via L. Borsari 46, 44121 Ferrara, Italy*

c. *Ambrosialab Srl, Via Mortara 171, 44121 Ferrara, Italy*

E-mail address: mv9@unife.it

Abstract. Besides the unquestionable positive effects of solar exposure for human health, UV rays have been widely investigated for toxicology aspects related to excessive UVB and UVA doses, which involve sunburns, skin aging, DNA skin damage and tumorigenesis. In the last 10 years, in the United States, the incidence of melanoma has doubled. The highest rates of incidence are found in Australia, New Zealand, and Northern Europe where it increased up to 30%. At present, synthetic and mineral sunscreens are used to protect against UV damages, but several natural molecules can provide protection, including also synergic effect (i.e. antioxidant) or enhanced photo stability to synthetic filters. Although a large number of herbal extracts and plant origin molecules can deserve potential applications, most of the study reported utilizes different method and different strategies of investigation, making thus difficult to understand the real versus claimed potential. This is possibly one of the reasons why, beside the large body of literature, there are no officially approved (FDA/EMA/PCC) natural commercial sun-filters; notwithstanding that a consistent number of solar products (sunscreens) on the market contain herbal derivatives. In this context we have developed, in recent years, a discovery strategy based on characterization of photo-protective molecules from plant extracts and their structure-activity investigation on the light of the most recent approaches. Structural modifications have also been applied in order to understand mechanistic aspects. Some interesting results will be reported and discussed.

Design, synthesis and biological evaluation of novel hydroxy-phenyl-1H-benzimidazoles as radical scavengers and UV-protective agents.

Bino A, Baldisserotto A, Scalambra E, Dissette V, Vedaldi DE, Salvador A, Durini E, Manfredini S, Vertuani S. *J Enzyme Inhib Med Chem.* 2017 Dec;32(1):527-537. doi: 10.1080/14756366.2016.1265523.

Essential Oil Extraction, Chemical Analysis and Anti-Candida Activity of Calamintha nepeta (L.) Savi subsp. glandulosa (Req.) Ball-New Approaches.

Božović M, Garzoli S, Sabatino M, Pepi F, Baldisserotto A, Andreotti E, Romagnoli C, Mai A, Manfredini S, Ragno R. *Molecules.* 2017 Jan 26;22(2). pii: E203. doi: 10.3390/molecules22020203.

A multitarget approach toward the development of a new series of 8-substituted purines for photoprotection and prevention of ultra violet (UV) related damages.

Nicaise Djuidje E, Dissette V, Bino A, Benetti S, Balzarini J, Liekens S, Manfredini S, Vertuani S, Baldisserotto A. *ChemMedChem.* 2017 Apr 18. doi: 10.1002/cmdc.201700137.

Herbal extracts, lichens and biomolecules as natural photo-protection alternatives to synthetic UV filters. A systematic review.

Radice M, Manfredini S, Ziosi P, Dissette V, Buso P, Fallacara A, Vertuani S. *Fitoterapia.* 2016 Oct;114:144-162. doi: 10.1016/j.fitote.2016.09.003. Epub 2016 Sep 15.

Factors affecting SPF in vitro measurement and correlation with in vivo results.

Dimitrovska Cvetkovska A, Manfredini S, Ziosi P, Molesini S, Dissette V, Magri I, Scapoli C, Carrieri A, Durini E, Vertuani S. *Int J Cosmet Sci.* 2016 Oct 26. doi: 10.1111/ics.12377.

Design, synthesis and biological activity of a novel Rutin analogue with improved lipid soluble properties.

Baldisserotto A, Vertuani S, Bino A, De Lucia D, Lampronti I, Milani R, Gambari R, Manfredini S. *Bioorg Med Chem.* 2015 Jan 1;23(1):264-71. doi: 10.1016/j.bmc.2014.10.023.



Review

Herbal extracts, lichens and biomolecules as natural photo-protection alternatives to synthetic UV filters. A systematic review

Matteo Radice^a, Stefano Manfredini^{b,c,*}, Paola Ziosi^c, Valeria Dissette^b, Piergiacomo Buso^b, Arianna Fallacara^b, Silvia Vertuani^{b,c}^a Universidad Estatal Amazónica, Km 2 ½ Via Napo (paso lateral), Puyo, Pastaza, Ecuador^b School of Pharmacy and Health Products, Department of Life Sciences and Biotechnology, Master Course in Cosmetic Science and Technology, University of Ferrara, Via L. Borsari 46, 44121 Ferrara, Italy^c Ambrosialab Srl, Via Mortara 171, 44121 Ferrara, Italy

ARTICLE INFO

Article history:

Received 25 July 2016

Received in revised form 12 September 2016

Accepted 14 September 2016

Available online 15 September 2016

Keywords:

Natural UV filters

Antioxidants

Sunscreen

Formulation strategies

ABSTRACT

Besides the unquestionable positive effects of solar exposure for human health, UV rays have been widely investigated for toxicology aspects related to excessive UVB and UVA doses, which involve sunburns, skin aging, DNA skin damage and tumorigenesis. At present, synthetic and mineral sunscreens are used to protect against these damages but several natural molecules can provide UV protection, including also synergic effect or enhanced photo stability. Although a large number of herbal extracts and plant origin molecules can deserve potential applications, most of the study reported utilizes different method and different strategies of investigation, making thus difficult to understand the real versus claimed potential. This is possibly one of the reasons why, beside the large body of literature there are no officially approved natural commercial sun-filter but a consistent number of commercially available solar products (sunscreens) on the market that contain herbal derivatives. In this review we have evaluated the papers appeared in the last 15 years and we have critically collected the most significant data. Several databases, namely Scifinder, Pubmed, Google Scholar, ISI-Web of Science and Scopus, were used as literature sources; excluding patents and symposium or congress papers. Only articles in the English language have been selected. New formulation, new skin delivery systems, skin penetration enhancers and boosters are most likely the next frontier of investigation in order to better understand the role of whole herbal extracts in exerting their photo protective activity.

© 2016 Published by Elsevier B.V.

Contents

1. Introduction	145
2. Materials and methods	145
3. Skin care mechanisms	145
3.1. UV toxicology	145
3.2. UV filter activity	148
3.3. UV synthetic filters	149
3.4. Natural UV filters	149
3.5. Photochemistry	150
4. Results and discussion	150
4.1. Measuring UV filtering effects	150
4.2. Antioxidants	152

Abbreviations: BCC, basal cell melanoma; CoQ₁₀, coenzyme Q₁₀; CPDs, cyclobutane pyrimidine dimers; COX-2, cyclooxygenase-2; DDE, D. Don herbal extract; GSH, endogenous reduced glutathione; EGCG, epigallocatechin gallate; GAE, gallic acid and ethyl gallate; GTP, green tea polyphenols; NHDF, human dermal fibroblast cells; iNOS, inducible nitric oxide synthase; IRA, infrared A radiation; MMPs, matrix metalloproteinases; MPF, membrane protection factor; MED, minimal erythemal dose; NLCs, nanostructured lipid carriers; NO, nitric oxide; NMSC, non-melanoma skin cancer; OMC, octylmethoxycinnamate; PPD, persistent pigment darkening; ROS, reactive oxygen species; SCC, squamous cell carcinoma; SPF, sun protection factor; TCA, trans-communic acid; TNF- α , tumor necrosis factor- α .

* Corresponding author at: School of Pharmacy and Health Sciences, Department of Life Sciences and Biotechnology, Master Course in Cosmetic Science and Technology, University of Ferrara, Via L. Borsari 46, 44121 Ferrara, Italy.

E-mail address: mv9@unife.it (S. Manfredini).

4.3. Formulation strategies	153
4.4. Synergic photoprotective effects from herbal extracts	154
4.5. UV filter and antioxidant synergic activities of lichens extracts	156
4.6. Additional studies on pure natural molecules as photoprotective additives.	157
4.7. Eco-sustainability	158
5. Future trends.	159
6. Conclusions	159
Conflict of interest	160
Acknowledgements	160
References	160

1. Introduction

The sun is life for living beings and earth; oxygen, water and food cycles are connected with UV radiation. Regarding human health, most of the positive effects of solar radiations are mediated by UVB production of vitamin D in skin. However, several other effects may be considered: tanning (increases melanin in skin as sunscreen) and improvement of psoriasis, vitiligo, atopic dermatitis and localized scleroderma by heliotherapy or phototherapy (artificial UV radiation). Furthermore, reductions of blood pressure and antimicrobial effects have been attributed to UV-induced nitric oxide (NO) production, which can also act as a neurotransmitter. Finally, UV exposure may improve mood through the release of endorphins. All these effects have been extensively reviewed in recent works. Keratinocytes produce opioid Beta-endorphin following UV exposure and this effect may be implicated in tanning 'addiction'. Sun exposure is associated with improved mood and increased energy levels. Melatonin and serotonin regulation is influenced by sunlight, and improvement in cognition is observed with increased sun exposure particularly in depressed individuals [1,2].

However, UV light is included in the Tenth Report on Carcinogens from the National Institute of Environmental Health Sciences, and UV radiation is deemed as the main etiological agent of a large number of skin cancers, sunburns and oxidative stress. In a recent study, Valachovic and Zurbenko [3] highlighted that skin cancer has been diagnosed in >2 million individuals, every year, in the United States. Chronic exposure of human skin to solar UV radiation is widely recognised as the key factor responsible for photoaging. For these reasons the role of photoprotection is critical to avoid skin cancer and others undesired effects [4].

The natural products are reasonably likely to be the future of cosmetics, and this trend necessarily involves solar products and specifically the UV filters. So if the current trend is to seek the naturalness and sustainability, you must always communicate with greater transparency the structure of supply chains, the origin of cosmetic raw materials and the ecological footprint that can leave. The efforts in research and innovation are directed to set new sustainability protocols, geared mainly to organic certification, with the aim of ensuring the final consumer about the safety, the ethic and sustainability of the product [5].

Finally, one should consider the sun protection as a complex issue, based on mixed factors, including oral and topical applications, physical blockers and chemical filters, boosters (i.e. antioxidant) clothing and glasses [4].

This review summarizes current topics in the research of natural UV filters, with special emphasis on photoprotective properties of different molecules from natural origin or their antioxidant and repairing mechanisms. List of different plants containing several organic molecules have been discussed in this review with respect to their photo-protective activity via different mechanism and represented in Tables 1 and 2. The same approach has been applied to lichens extracts, as reported in Table 3. Table 4 summarize additional studies regarding pure molecules that have been investigated for their photo protection capability.

2. Materials and methods

The present systematic review was performed adopting the following electronic databases: Scifinder, Pubmed, Google Scholar, ISI-Web of Science and Scopus. Three reviewers extracted data independently and the final papers selection were completed avoiding duplication of data. Systematic searching includes articles from the past 15 years; moreover, we also considered some key papers from 1974 to 2015, for the first three chapters (introduction, materials and methods, skin care mechanism). Selection criteria were defined including only natural herbal extracts, lichens extracts and pure molecules available from plant sources, in according with green trends of cosmetic markets. We decided to exceptionally include some enzymes, available by biotechnology process. Animal raw materials have been considerate an exclusion criterion for the data included in the present review.

The following keywords were selected: sunscreen, SPF or Sun Protection Factor, plant oils, UV filter, natural UV filter. All key words were searched individually and in combination. Only articles in the English language have been selected and were excluded data from patents, symposiums and congress abstracts; these latter because not enough complete to warrant an effective comparison with full papers. As described in Fig. 1, the above mentioned criteria allowed selecting 103 eligible articles, excluding 10 papers which did not satisfied the selection methodology. Rejected papers did not show a clearly botanical identification.

3. Skin care mechanisms

3.1. UV toxicology

In Australia it has been reported the highest incidence of non-melanoma skin cancer (NMSC), including basal cell melanoma (BCC) and squamous cell carcinoma (SCC). A recent review analysed 21 Australians studies that investigated the incidence of NMSC. The result per 100,000 person-years was estimated to be 555 in 1985; 977 in 1990; 1109 in 1995; 1170 in 2002 and 2448 in 2011, indicating probably an increasing health problem. Incidence varied across the country with the highest value in Queensland. The prevalence of NMSC was estimated to be 2% in Australia in 2002 [6].

Regarding UV protection, epithelial skin cancer and the role of UV protection in melanoma prevention, there are substantial evidence that UV protection is important in order to reduce the risk of squamous cell carcinoma, actinic keratosis and probably also the risk of melanoma [7].

A recent study about sunlight-induced melanoma can arise from cyclobutane pyrimidine dimers (CPDs) generated into the melanocytes and CPDs are generated for >3 h after exposure to UVA. This study confirms that the chemical excitation of melanin derivatives induces DNA photoproducts long after UV [8].

Furthermore, the pattern is complicated by synergic potentiation of UV rays by chemical environment and by the altitude at which the irradiation occurs, sometimes with unpredictable effects [3,9].

Table 1
List of plant extracts with photo protection properties.

Plant name	Plant part(s) used	Plant extract	Type of compound(s)	Main effect(s)	Ref.
<i>Antarctic plants (Deschampsia antarctica, Colobanthus quitensis, Polytrichum juniperinum)</i>	Aerial parts	Methanolic extract	Flavonoids, flavones, and flavonols	NF, SPE	[67]
<i>Buddleja cordata</i>	Leaves	Methanolic extract	Phenolic compounds	NF, A, SPE	[66]
<i>Calendula officinalis</i>	Flower	Hydroalcoholic extract	Polyphenol, flavonoid	SPE	[52,53]
<i>Calluna vulgaris</i>	Entire plant	Hydroethanolic extract	Flavonoids	SPE	[75]
<i>Camellia sinensis</i>	n.r.	n.r.	Polyphenols	A, SPE	[12,27,42–44,49,50,54,55]
<i>Capparis spinosa</i>	Flower buds	Lyophilized extract	Phenolic compounds	A, SPE	[12]
<i>Castanea sativa</i>	Leaf	Lyophilized extract	n.r.	A	[45]
<i>Citrus sinensis varieties: Moro, Tarocco, Sanguinello</i>	Fruits	n.r.	Cyanidin 3-glycosides	SPE, A	[13]
<i>Codium fragile</i>	n.r.	Methanolic extract	n.r.	SPE	[46]
<i>Coffea genus (10 species)</i>	Green dry coffee beans	Chloroform extract	Lipid fraction	NF	[40,41]
<i>Commiphora mukul</i>	Resin	Essential oil	n.r.	NF	[16]
<i>Crataegus pentagyna</i>	Fruits	Methanolic ultrasonic extract	Phenolic compounds, Flavonoids	NF	[33]
<i>Culcitium reflexum</i>	Leaf	Ethanolic extract	Phenolic compounds, flavonols	A, SPE	[12,70]
<i>Cyclopia intermedia</i>	n.r.	Ethanol, acetone extract	Polyphenol	SPE	[30]
<i>Disporum sessile D. Don</i>	n.r.	Methanol extract	n.r.	SPE	[68]
<i>Dracocephalum moldavica</i>	n.r.	Ethyl acetate extract	Phenolic compounds flavonoids, flavon aglycone, tannins	NF	[34]
<i>Eucheuma cottonii</i>	n.r.	Aqueous and methanol extract	K-carrageenan, flavonoids, phlorotannins	A, SPE	[47]
<i>Fragaria x ananassa</i>	Fruits	n.r.	Anthocyanins and hydrolyzable tannins.	A, SPE	[13,56]
<i>Feijoa sellowiana</i>	Fruits	Methanolic extract	Phenolic compounds, Flavonoids	NF	[33]
<i>Galinsoga parviflora</i>	n.r.	Water and ethanolic extracts	Flavonoids	A, SPE	[69]
<i>Galinsoga quadriradiata</i>	n.r.	n.r.	n.r.	A, SPE	[12]
<i>Ginkgo biloba</i>	Green leaves	n.r.	n.r.	A, SPE	[12]
<i>Glycine max</i>	Seed	Soybean cake	Soy isoflavone	A, SPE	[4,12,13,79]
<i>Garcinia brasiliensis</i>	Fruits	Ethanolic extract	Polyphenolic compounds, polyisoprenylated benzophenone	SPE	[81]
<i>Krameria triandra</i>	Root	n.r.	Phenolic compounds, neolignans, oligomeric proanthocyanidins	SPE	[12]
<i>Larrea tridentate</i>	n.r.	n.r.	Polyphenolic compounds	SPE	[12]
<i>Leontopodium alpinum</i>	n.r.	n.r.	Lutein derivatives	NF	[35]
<i>Moringa oleifera</i>	Seeds	Petroleum ether extract	Lipid fraction	NF	[57,58]
<i>Moringa concanensis, Nimmo</i>	Seeds	Petroleum ether extract	Lipid fraction	NF, SPE	[31]
<i>Neoglaziovia variegata</i>	Leaves and flowers	Various extracts	Flavonoids, phenolic compounds	SPE	[36]
<i>Nigella sativa L.</i>	Seeds	Hexane extract	n.r.	NF	[37]
<i>Ocimum basilicum</i>	Leaf	Essential oil	n.r.	NF	[32]
<i>Oryza sativa</i>	Rice bran	Water-soluble enzymatic extract	GAMMA-oryzanol, inositol, fatty acids	A, SPE	[26]
<i>Passiflora incarnata</i>	n.r.	Dry extract (Grupo Centro Flora, Brazil)	Flavonoids	SPE	[60]
<i>Peumus boldus</i>	n.r.	n.r.	n.r.	NF	[38]
<i>Pinus densiflora</i>	Pine needles	Various extract	n.r.	SPE	[71]
<i>Pinus pinaster</i>	Bark	Picnogenol	Phenolic compounds, polyphenols, procyanidin derivatives	SPE	[4,12]
<i>Pimenta pseudocaryophyllus</i>	Leaves	Ethanolic extract	Flavonoids and polyphenolic compounds	SPE	[61,62]
<i>Polygonum multiflorum thumb</i>	Root	n.r.	n.r.	SPE	[4]
<i>Polypodium leucotomos</i>	n.r.	Hydrophilic extract	n.r.	SPE	[4]
<i>Pongamia glabra</i>	Seeds	n.r.	n.r.	NF	[39,48]
<i>Pothamorphe umbellata</i>	Roots	n.r.	n.r.	NF	[34]
<i>Prunella vulgaris</i>	n.r.	n.r.	n.r.	SPE	[34]
<i>Prunus persica</i>	Flower	n.r.	Kaempferol glycoside derivatives	SPE	[12]
<i>Punica granatum</i>	Fruits, peel	n.r., methanol extract	Anthocyanidins, hydrolyzable tannins	SPE	[4,48,63,64]
<i>Sanguisorba officinalis</i>	Root	n.r.	Tannins	SPE	[12]
<i>Schinus terebinthifolius</i>	Leaves	Lyophilized crude extract	Phenolic compounds	A, NF	[72]
<i>Silybum marianum</i>	Seeds	n.r.	Flavonolignans	SPE, A	[4,12]
<i>Sedum telephium</i>	Leaf	n.r.	Polysaccharides, flavonol glycosides	SPE	[12]
<i>Trifolium pratense</i>	n.r.	n.r.	Isoflavonoid compounds	SPE	[4,13]
<i>Taraxacum officinale</i>	Leaf and flower	Water-soluble extract	n.r.	NF, SPE, A	[73]
<i>Vaccinium myrtillus L.</i>	Fruits	n.r., water-soluble extract	Polyphenols, anthocyanins	SPE	[13,80]
<i>Vaccinium uliginosum L.</i>	Fruits	n.r.	Anthocyanins	SPE	[13]
<i>Viola tricolor L.</i>	n.r.	Ethyl acetate extract.	flavonoids	NF	[34]
<i>Vitis vinifera</i>	Seed	n.r.	Polyphenols	SPE	[12,74–76]

Not reported (n.r.), natural UV filter (NF), antioxidant (A), synergic photoprotective effects (SPE)

Table 2
List of plant species with major constituents and main biological effects.

Plant name	Major constituent(s)	Main effect(s)	Reference(s)
<i>Antarctic plants (Deschampsia antarctica, Colobanthus quitensis, Polytrichum juniperinum)</i>	n.r.	UV absorber, sun protective activity, stimulate DNA-repair processes.	[67]
<i>Buddleja cordata</i>	Verbascoside, linarin.	Protect against UVB-induced skin damage, UV absorber, antioxidant	[66]
<i>Calendula officinalis</i>	Rutin, narcissin	Prevent UV irradiation-induced oxidative stress	[52,53]
<i>Calluna vulgaris</i>	n.r.	Prevention/reduction of UV-induced skin damage and skin diseases	[75]
<i>Camelia sinensis</i>	EC - (-)-epicatechin, ECG - (-)-epicatechin-3-gallate, EGC - (-)-epigallocatechin, EGCG - (-)-epigallocatechin-3-gallate	Anticarcinogenic, anti-inflammatory, photostabilizing capacity	[12,27,42–44,49,47,54,55]
<i>Capparis spinosa</i>	Kaempferol quercetin derivatives caffeic, ferulic, p-cumaric, and cinnamic acids	Antioxidant, reduces UVB-induced skin erythema	[12]
<i>Castanea sativa</i>	n.r.	Antioxidant	[45]
<i>Citrus sinensis</i> varieties: Moro, Tarocco, Sanguinello	n.r.	Protection against UV skin damage, protective effect on DNA cleavage, antioxidant	[13]
<i>Codium fragile</i>	Clerosterol	Protection against UVB-induced pro-inflammatory and oxidative stress	[46]
<i>Coffea</i> genus (10 species)	Linoleic acid, palmitic acid	UV absorber, emollient	[40,41]
<i>Commiphora mukul</i>	n.r.	UV absorber	[16]
<i>Crataegus pentagyna</i>	n.r.	UV absorber	[33]
<i>Calcitium reflexum</i>	Rutin, kaemp-ferol, quercetin and its glycosylated derivatives, cinnamic acid derivatives.	Antioxidant, reduces UVB-induced skin erythema, free radical scavenging effect.	[12,70]
<i>Cyclopia intermedia</i>	Hesperidin, mangiferin	Prevention/reduction of UV-induced skin damage and skin diseases	[30]
<i>Disporum sessile</i> D. Don	n.r.	Prevention of UVB-mediated cutaneous alterations and photoaging	[68]
<i>Dracocephalum moldavica</i>	Rosmarinic acid, caffeic acid, apigenin, luteolin	Sun protective activity, SFP >20.	[34]
<i>Eucheuma cottonii</i>	n.r.	Antioxidant activity and protective effects against UV-induced ROS degeneration in keratinocytes	[47]
<i>Fragaria x ananassa</i>	Pelargonidin	Antioxidant, reduces UVB-induced skin erythema, anti-inflammatory, diminishing DNA damage on UVA-induced skin damage	[13,56]
<i>Feijoa sellowiana</i>	n.r.	UV absorber	[33]
<i>Galinsoga parviflora</i>	Caffeic acid, caffeoyl glucarates and caffeoyl quinic acids	Antioxidant, UV-protecting activity	[69]
<i>Galinsoga quadriradiata</i>			
<i>Ginkgo biloba</i>	Flavone glycosides, quercetin, kaempferol derivatives, terpenes	Antioxydant, decrease the number of UV-induced sunburns in mice skin	[12]
<i>Glycine max</i>	Genistein	Antioxidant reduce skin photo damage and transepidermal water loss (TEWL)	[4,12,13,79]
<i>Garcinia brasiliensis</i>	7-Epiclusianone, guttiferone-A	Reduces UVB-induced skin damages	[81]
<i>Krameria triandra</i>	n.r.	Reduces UVB-induced skin erythema, free radical scavenging effect	[12]
<i>Larrea tridentate</i>	Nordhydroguaiaieteric acid	Photoprotective activity	[12]
<i>Leontopodium alpinum</i>	Luteolin, glycosylated luteolin, hydroxyethylated luteolin, 3',4',5,7-tetralipoyloxyflavones, 5-hydroxy-3',4',7-trilipoyloxyflavones	UV absorber	[35]
<i>Moringa oleifera</i>	n.r.	UV absorber	[57,58]
<i>Moringa concanensis</i> , Nimmo	n.r.	UV absorber, Sun protective activity	[31]
<i>Neoglaziovia variegata</i>	Isoquercetin, kaempferol-3-O-rhamnoside, caffeic, protocatechuic, p-coumaric and vanillic acids	Photoprotective activity	[36]
<i>Nigella sativa</i> L.	Linoleic acid, oleic acid, palmitic acid	Potential UV absorber	[37]
<i>Ocimum basilicum</i>	Linalool, methyl cinnamate, methyl linalool, methyl eugenol, citral, methyl chavicol, thymol, p-cymene, α-pinene	UV absorber	[31]
<i>Oryza sativa</i>	Gamma-oryzanol, tocopherols	Antioxydant, UVA absorber	[26]
<i>Passiflora incarnata</i>	Rutin	Improved the protective defence against UVA	[60]
<i>Peumus boldus</i>	Boldine	UV absorber	[38]
<i>Pinus densiflora</i>	Trans-communic acid and dehydroabietic acid	Suppress UVB-induced MMP-1 expression	[71]
<i>Pinus pinaster</i>	Catechin, epicatechin, taxifolin, caffeic, ferulic, p-hydroxybenzoic, vanillic, gallic, protocatechuic acid	Reduces UVB-induced skin erythema, free radical scavenging effect	[4,12]
<i>Pimenta pseudocaryophyllus</i>	n.r.	Inhibiting UV-B irradiation-induced inflammation and oxidative stress of the skin. Antioxidant, decrease oxidative damages of the skin.	[61,62]
<i>Polygonum multiflorum</i> thumb	n.r.	Improve superoxide dismutase 1 immunoreactivity, protected against UVB-induced stress, inhibits oxidative stress induced by UVB irradiation	[4]
<i>Polypodium leucotomos</i>	n.r.	Reduces UVB-induced skin erythema	[4]
<i>Pongamia glabra</i>	Pongamol, karanjin	Potential UV absorber	[39,48]
<i>Pothomorphe umbellata</i>	n.r.	Sun protective activity, SFP >20.	[34]
<i>Prunella vulgaris</i>	n.r.	Protection against UV-induced skin erythema	[34]
<i>Prunus persica</i>	Multiflorin B, trifolin, afzelin, astragalil	Inhibits UVB/UVC induced damage, antioxidant, inhibit dose dependently UVB-induced erythema	[12]
<i>Punica granatum</i>	Delphinidin, cyanidin, and pelargonidin	Decrease in the number of UVB-induced dimers in human	[4,48,63,64]

(continued on next page)

Table 2 (continued)

Plant name	Major constituent(s)	Main effect(s)	Reference(s)
		skin, synergic photoprotective activity in nanostructured lipid carrier	
<i>Sanguisorba officinalis</i>	n.r.	Inhibits UVB induced damage (wrinkle)	[12]
<i>Schinus terebinthifolius</i>	Gallic acid, ethyl gallate	Antioxidant, UV absorber	[72]
<i>Silybum marianum</i>	Silymarin, silibin, silidianin, silychristin, isosilybin	Inhibits UVB-induced damage, antioxidant	[4,12]
<i>Sedum telephium</i>	Gallic acid, quercetin, kaempferol	Reduces UVB-induced skin erythema	[12]
<i>Trifolium pratense</i>	Genistein equol, isoequol dehydroequol	Protection from UV induced inflammation and immune suppression, reduce the inflammatory edema reaction	[4,13]
<i>Taraxacum officinale</i>	n.r.	Potential UV absorber, inhibits UVB-induced damage, antioxidant	[73]
<i>Vaccinium myrtillus</i> L.	n.r.	Reduction of UV A stimulated ROS formation, attenuation of UVA caused peroxidation of membrane lipids and depletion of intracellular GSH	[13,80]
<i>Vaccinium uliginosum</i> L.	Cyanidin-3-glucoside, petunidin-3-glucoside, malvidin-3-glucoside, and delphinidin-3-glucoside	Protected against UVB-induced skin photoaging	[13]
<i>Viola tricolor</i> L.	Violanthin, rutin, violaquercitrin and salicylates	Sun protective activity, SFP >20.	[33]
<i>Vitis vinifera</i>	Flavan-3-ol derivatives, catechin, epicatechin, oligomeric proanthocyanidins	Free radical scavenging effect, prevent UVB and UVC induced lipid peroxidation, reducing the oxidative stress and apoptosis	[12,74–76]

Not reported (n.r.)

UV radiation represent only a small region of the electromagnetic radiation spectrum and it composes from three subdivisions: UVC (200–290 nm), UVB (290–320 nm), and UVA (320–400 nm). The depletion of the ozone layer can lead to a substantial increase in UV transmission to the Earth surface, increasing the skin damage on human population. Moreover, UV radiation only account for approximately 7% of the sun energy, and Infrared A radiation (IRA) (760–1440 nm) can also play an important role as a damaging factor to skin through its ability to modify the gene expression of skin cells at multiple points, causing accelerated skin aging and contributing to the development of cancer.

3.2. UV filter activity

In 1934, Friedrich Ellinger firstly reported the concept of minimal erythral dose (MED) for protected and unprotected skin, proposing a coefficient of protection that decreased in value to the extent that protection increased [10]. Only in 1974 Greiter introduced the term Sun Protection Factor (SPF) [11]. The SPF is defined as the UV energy required for producing a minimal erythema dose (MED) on

protected skin, divided by the UV energy required producing a MED on unprotected skin. MED is defined as the lowest time interval or dosage of UV light irradiation sufficient for producing a minimal, perceptible erythema on unprotected skin. SPF usually expresses the efficacy of a sunscreen molecule; a higher SPF indicates a stronger photoprotective activity.

UV radiation is absorbed by the skin which contains different chromophores as DNA, RNA, melanin, aromatic amino acids such as tryptophan and tyrosine, lipids, etc. UV radiation induces photo-chemical reactions which result in harmful effects: especially pyrimidines suffer structural modifications forming adducts, cyclobutane dimers and hydration products. Mutations can be transmitted. Moreover, the UV-induced damage acts decreasing the photoprotective mechanism which inhibits replications and apoptosis of mutant cells [4].

UVB radiations are more genotoxic than UVA and damage mainly the epidermal basal cell layers, inducing photocarcinogenesis. Others effects of UVB damages are free radical production in the skin, photoaging, skin-aging. UVA radiation is about 1000 times more effective than UVB in the darkening of epidermis, but generates burns, skin sagging and wrinkling, suppressing some immunological effects [12].

Table 3

List of lichens with photo protection properties.

Lichens name	Type of compound(s)	Major constituent(s)	Lichens part(s) used	Main effect(s)	Reference(s)
Lichens 1 (<i>Erioderma leylandii</i> , <i>Xanthoparmelia farinosa</i> , <i>Coelopogon epiphorellus</i> , <i>Pseudocyphellaria bereberina</i>)	n.r.	Epiphorelic acid I and II 1-chloropannarine, usnic acid, calicin	n.r.	UV absorber, antioxidant	[38,82]
Lichens 2 (<i>Diploicia canescens</i> , <i>Lichina pygmaea</i> , <i>Ochrolechia parella</i> , <i>Tephromela atra</i> , <i>Diploschistes scruposus</i> , <i>Flavoparmelia caperata</i> (L.) Hale and <i>Pertusaria pseudocoralina</i> (Lilj.) Arnold, <i>Teloschistes chrysophthalmus</i> (L.) Th. Fr. and <i>Usnea rubicunda</i> , <i>Umbilicaria deusta</i> (L.) Baumg, <i>Umbilicaria cylindrica</i> (L.) Delise, <i>Cetraria islandica</i> (L.) Ach.	n.r.	Diploicin, dechlorodiploicin, 4-O-methyldiploicin, 4-O-methyldechlorodiploicin, scencidin, secalonin acid B y D, buellin	n.r.	UVA absorber	[83]
Lichens 3 (<i>C. islandica</i> U. hirta, <i>L. pustulata</i>)	Depsides, depsidones	Salizinic acid, gyrophoric acid	n.r.	PF-UVA boosters candidates, UVB absorber, antioxidant	[84]
Lichens 4 <i>Erioderma leylandii</i> , <i>Xanthoparmelia farinosa</i> , <i>Pseudocyphellaria bereberina</i> , <i>Coelopogon epiphorellus</i> , <i>Teloschistes flavicans</i> .	n.r.	Calycine, 1'-chloropannarine, usnic acid, epiphorelic acid I and II, vicanicine	n.r.	Sun protective activity	[85]
Lichens 5 <i>Usnea rocellina</i> Motyka	n.r.	3-Methoxycarbonyl-2-hydroxy-6-methoxy-4-methylbenzoic acid, (+)-(-9b-R)-usnic acid and decarboxyhamnolic acid	n.r.	Antioxidant and broad spectrum absorbing properties	[86]

Table 4
List of pure molecules with photo protection properties.

Molecule(s)	Prevalent mechanism(s)	Reference(s)
Apigenin	Prevention of UV-induced skin tumourgenesis	[12]
Astaxanthin	Antioxidant, prevent from photoinduced damage	[4]
Bioflavonoids from rosemary and citrus	Oral photoprotection, antioxidant	[87]
Caffeic acid	Antioxydant, UV absorber	[12]
Carnosic acid	Antioxydant, chemoprotective effects against carcinogens	[12]
Carotenoids: β -carotene and lycopene	Antioxydant, free radical scavenger	[14]
Enzymes: Photolyase enzyme and endonuclease	Photoreactivation, UV-damage compensation	[14]
Ferulic acid	Antioxydant, UV absorber	[12]
Genistein	Antioxydant, proapoptotic agent	[88]
Hesperetin and naringenin	Topical photo-protective agents in presence of penetration enhancers	[89]
Quercetin and Quercitrin	Antioxydant, chelating agent Topical carrier formulation enhance bioactivity	[12,28,29,90–92]
Resveratrol	UVA and UVB filters enhancer Antioxydant, anti-inflammatory and antiproliferative activity, synergic photo stabilizer and safety enhancer	[4,12,95,96]
Myricetin	Antioxydant	[51]
Retinoids	Antioxydant, UV absorber	[98]

3.3. UV synthetic filters

Usually, organic molecules used as sunscreens are conjugated aromatic compounds with carbonyl groups. These molecules can absorb ultraviolet radiations and release lower energy rays, defending the skin from UV damage effects [13].

Some studies reveal controversies regarding the sunscreens effect, both in vitro and in vivo. Some reports highlight UV sunscreen products estrogenic potencies, their ability to cause disturbs of the thyroid hormone homeostasis and immunosuppressive effects. Moreover, there are some researches about photon induced reactions (photoirritation, photosensitization and contact dermatitis) possibly caused by sunscreen products application. The studies evidence a relation between the mentioned damages and the contact with synthetic photo-protective agents like cinnamates, p-amino benzoic acid and oxybenzone. UV absorption by chemical sunscreens promotes these molecules into higher energetic state suitable to cause reaction with skin biomolecules, resulting in adverse reactions, as contact dermatitis and photosensitivity effects [13].

Skotarczak and co-workers [14] reported that physical filters, as titanium dioxide, do not cause adverse reactions or allergies; however, when the cosmetic product provides an occlusive application in order

to optimize the UV refraction, it can be comedogenic. There are alarming data about titanium dioxide in nano form and synthetic chemical UV filters: has been reported that they could provoke photoallergic contact dermatitis. PABA and its derivatives have been recognised responsible for many allergic reactions. Also avobenzone, octocrylene, and benzophenone-3, even if endowed by recognised allergenic properties, are widely used in cosmetics. It has been reported, in human volunteers, the presence of benzophenone-3 in urine and plasma even after four days the initial topical application of sunscreen products. The last data, beyond to be unacceptable for the EU Regulation 1223/2009, alarm us about the diffusion of UV filters into the circulatory system, where their accumulation may cause unknown effects or adverse reactions on other organs.

Anyway, despite a review describing UV filters efficacy and safety do not indicate evidence about the unsafety of the 9 UV filters, the photoallergy and phototoxicity of aminobenzoates remain a main concern [4,15]. It has been reported that cosmetics containing chemical sunscreen ingredients can increase occurrence of allergies and contact dermatitis, contact urticaria, phototoxic and photo-allergic reactions, and even isolated cases of severe anaphylactic reactions [16]. Clearly, although these increasing reports, it is crucial to protect against UV light, by the use of photoprotective measures.

Following the definition at the art. 2, regulation (EC) 1223/2009, a UV-filter “means substances which are exclusively or mainly intended to protect the skin against certain UV radiation by absorbing, reflecting or scattering UV radiation”, but a solar finished product is much more than a dermocosmetic base plus filters. Indeed, the pattern is much more complicated, as modern solar products are composed by filters, film-forming ingredients, emollients, active ingredients, functional ingredients and boosters. All together these components work as a chord to the final effect, expressed by an imperfect index which is the SPF. Since its introduction in 1974 the SPF has been used as a number related to the filter composition, to define the hours of allowed exposition. However, taking into account the more complex pattern introduced by synergic components in the formulation, it would be more rational to express protection as an efficacy factor, that would take into account all the components and not only the filters.

3.4. Natural UV filters

In the last decades, consumers' attention on health matters has increased. At the same time, natural trend in cosmetic has gained a strong interest, confirming a relevant attention on “safe” molecules, natural products, plant origin raw materials, organic certified brands. The awareness that planet resources are not inexhaustible is bringing more consumers to change their habits of life, seeking such cosmetic products more sustainable, more environmentally friendly and safer in their skin application. Recent studies by Sánchez-Quiles and Tovar-Sánchez [17] focused the potential risk to improve the pollution of water coastal marine areas, due to an increased use of sunscreens and

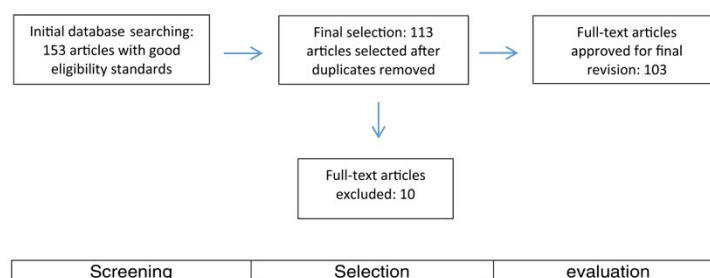


Fig. 1. Criteria used to select the 103 articles for the data presented in this review.

cosmetics with UV-filters and their capability to be bioconcentrated and/or bioaccumulated in the food web. Other authors investigated new “non-animal” photo-safety screening assays for cosmetic, in order to contribute to an animal-friendly research approach [18]. Moreover, it becomes more and more widespread awareness that the entire production is sustainable, thus favouring products with brand Fair Trade or organic certification, in the hope that this means even greater respect for the producers of raw materials and for the workers involved in production and collection of plant species. It, therefore, becomes imperative the role of innovation in the direction indicated by the principles of “green chemistry”, an inescapable path that cut across different sectors, from energy to the gourmet, through the world of fashion and of course reaching the cosmetics sector. As always, the cosmetics industry is sensitive to trends in the market, and it is characterized by a high level of competitiveness, as consumers continually seek new products; the response to this increasing demand is inevitable. However, these increasingly significant innovations are often presented to the consumer in a not sufficiently understandable manner, if not misleading at times.

3.5. Photochemistry

The main protection mechanism of organic UV filters is the absorption of UV radiation and subsequent emission of less harmful energy.

By the absorption of a UV photon, an organic molecule goes from the electronic ground state (S_0) to the first excited electronic state (S_1). This absorbed energy can be released via several pathways. From the S_1 state, it may be lost directly via fluorescence (a radiative transition) or by undergoing photoreactions. There are also radiationless transitions by which the absorbed energy is redistributed inside the molecule: intersystem crossing (ISC) leads to the first triplet state T_1 and internal conversion (IC) to the state S_0^* , which is the electronic ground state but with the excitation energy now migrated into vibrational modes of the molecule.

From the first triplet state T_1 , the energy may be dissipated by emission of a photon (phosphorescence), by energy transfer to other molecules (sensitization), or via photoreactions. The fate of the energy after IC to the vibrational-excited ground state S_0^* can be emission of infrared (IR) photons (i.e., heat), or collisional deactivation of the vibrational modes via collisions with surrounding molecules. Since the rate constant for emission of IR quanta is very small, collisional deactivation will be the main process after IC, rendering the molecule in its electronic ground state S_0 . In photoreactions, structural changes occur, which may be reversible, as with isomerization (cis/trans or keto/enol), or irreversible as decomposition.

The mechanism of UV attenuation of synthetic UV absorber can be identified in IC reactions such as cis-trans isomerization (benzylcamphore derivatives and cinnamates) or keto/enolic isomerization (benzophenones, salicylates, dibenzoylmethane) and rarely degradation, while natural compounds can undergo decomposition or internal electron-transfer reactions.

Natural molecules are generally larger molecules in respect of synthetic filters, containing chromophores and functional groups that influence the maximum wavelength of absorption (λ_{max}) and consequently the capability of act as UV absorbers.

Despite synthetic filter, natural derivatives are a mixture of a variety of substituted molecules and they present a photochemical fingerprint that cover a boarder range of wavelength in respect of chemical pure molecules, including also the visible region. For examples anthocyanes and flavonoids present broad-spectrum of absorbance in which at least two bands can be consider, the major in the visible range and the second in the UV range. The intensity of the molar absorptivity of the two bands is generally comparable, even if solvent or pH may influence them in greater extent than synthetic filters.

According to the spectrophotometric data [19] chemical synthetic filters are generally characterized by a molar extinction coefficient value higher than $10.000 \text{ M}^{-1} \text{ cm}^{-1}$ at λ_{max} in UV region. Having

premised the greater variability in function of solvent and pH, the preferred characteristic for a natural sunscreen filter, acting as UV absorber, should be a comparable value of molar absorptivity as for synthetic filters.

For example, some polyphenols that are identified as UV absorbers, ferulic acid, caffeic acid, rutin, quercetin, catechin, are characterized by molar absorptivity values higher than $10.000 \text{ M}^{-1} \text{ cm}^{-1}$ at 300 nm [20]. Anthocyanins present two distinctive bands of absorption, one in the UV-region (260 to 280 nm) and another in the visible region (490 to 550 nm), with a similar intensity. Because of a lack of data regarding the molar extinction coefficient at λ_{UV-max} , one can consider similar the molar absorptivity for both the bands with values in the range $10.000\text{--}45.000 \text{ M}^{-1} \text{ cm}^{-1}$ [21].

Generally, natural derivatives have to present a significant absorption band in UV region with a molar extinction coefficient (ϵ) value quite similar to the synthetic filters.

4. Results and discussion

4.1. Measuring UV filtering effects

As a general consideration, in critically examining the works here reported, it should be taken into account that the traditional and only officially accepted method is the in vivo method of determination of SPF (i.e. FDA, United States; former COLIPA, European Union). All of these involve 10 to 20 human volunteers of both sexes, with appropriate skin types. The in vivo method is always accompanied by in vitro measurement during explorative phases. The in-vitro broadly applied method is the well-known Diffey-Robson approach [22].

It is a spectrophotometric based measurement of transmission. Its determination was developed using the SPF as a relative index. The SPF was calculated using the following equation:

$$SPF = \frac{\sum_{290}^{400} A(\lambda)E(\lambda)d\lambda}{\sum_{290}^{400} \frac{A(\lambda)E(\lambda)}{MPF(\lambda)d\lambda}}$$

where $d(\lambda)$ is 1 nm, $A(\lambda)$ represents the erythema action spectrum, $E(\lambda)$ represents the sun's radiation power, MPF is the inverse of the transmission ($1/T$) at a given wavelength and $MPF(\lambda)$ represents how much radiation is absorbed and the ability of the skin to be damaged. This in vitro testing approach was chosen for the current study since comparative analyses of in vivo SPF and in vitro SPF results showed a high degree of correlation ($R^2 = 0.94$), as reported by Castanedo-Cázares and co-workers [23].

Other methods are used but with lesser correlation with in vivo results. Several articles about SPF evaluation used in vitro test, based on the models proposed by Gharavi group [24] or Mansur and co-workers [25]. The first one is based on the following equation:

$$SPF = \frac{\sum_{292.5}^{337.5} E(\lambda) \epsilon(\lambda)}{\sum_{292.5}^{337.5} E(\lambda) \epsilon(\lambda) T(\lambda)}$$

where: $T(\lambda)$ is the measured sunscreen transmittance at λ ; $E(\lambda)$ is the spectral irradiance of terrestrial sunlight at λ ; and $\epsilon(\lambda)$ is the erythema action spectrum at λ .

Test determination proposed by Mansur and co-workers [25] is explained on this equation:

$$SPF \text{ spectrophotometric} = CF \times \sum_{290}^{320} EE(\lambda) \times I(\lambda) \times Abs(\lambda)$$

where CF is a correction factor (equal 10), $EE(\lambda)$ indicates the erythemal effect of solar radiation at each wavelength λ , $I(\lambda)$ means sunlight intensity at wavelength λ and $Abs(\lambda)$ is the spectrophotometric reading of sample absorbance, at each wavelength. In this equation

CF was determined so that a standard sunscreen formulation containing 8% homosalate presented a SPF value of 4, determined by UV spectrophotometry.

These are useful in an early phase of selection of active ingredient and not in a phase of final assessment, especially if ethanol extracts of herbal are compared with commercial creams. The ethanol solution is much different than evaluating the extracts formulated into a standard finished product. Therefore, caution should be paid in correlating these results with SPF obtained by the Diffey-Robson method [22] or by in vivo methods.

The SPF is an imperfect measure of skin damage, because invisible damage and skin aging are also caused by UV type A (UVA, wavelengths 315–400 or 320–400 nm), which does not primarily cause reddening or pain. The UVA protection (UVA-PF) can be determined by both in vivo and in vitro models: in vivo models are several depending on different countries, as a unique protocol is not yet available. The persistent pigment darkening (PPD) is an in vivo Japanese method, similar to the SPF, of measuring sunburn protection, but instead of reddening; it measures the tanning of the skin. In the EU, there is a requirement to provide the consumer with a minimum level of UVA protection in relation to the SPF. This should be a “UVA-PF” of at least 1/3 of the SPF (certified by a specific UVA circled label). Thus, a label “broad spectrum protection” can be made only if UVA protection is demonstrated proportional to the UVB protection, using a standardized testing method. The Cosmetic Europe (former COLIPA) in vitro recently introduced method for UVA-PF (ISO 24443:2012) is claimed as equivalent to the in vivo PPD model and thus more ethically correct for the saving of volunteers.

The UK Boots “star” rating system is a proprietary in vitro method to measure UVA to UVB protection of creams and sprays. Based on original work by Brian Diffey, the Boots Company developed a standard method that has been adopted in the UK.

With the current methodology, the lowest rating is three stars, the highest being five stars. The method uses a spectrophotometer to measure absorption of UVA versus UVB; to give a better indication of UVA protection and photostability when the product is used, the samples are pre-irradiate before analysis.

The Protection Grade of UVA (PA), is based on the PPD reaction. According to the Japan Cosmetic Industry Association, PA+ corresponds to a UVA protection factor between two and four, PA++ between four and eight, and PA+++ more than eight.

About in vivo models, substitutes have been proposed: indeed, several authors suggested different methods using cells and regenerated tissues [26,27] or animals [28–30].

With these premises, and taking all this into account, we critically examined literature on the natural extracts and molecules with potential UV filtering activity. In this chapter we consider, as strengths of each research, the UVB absorption of herbal extract a basic prerequisite to suppose a promising UV protection. Anyway, these studies do not add information about synergic antioxidant or preventive UV damage effects (in vivo or in vitro), skin penetration enhancer activity, booster properties or formulation strategies. In our opinion, even if the data and methodologies are scientifically pertinent, a positive result about UV absorption represents a prerequisite for further studies but do not ensure a “natural” UV photoprotection.

Kale and co-researchers [31] studied the sunscreen activity of an emulsion containing essential oil from the resin of *Commiphora mukul* using absorption spectroscopy and transmission spectroscopy methods. Authors reported that the SPF was 2.23 ± 0.48 , in compliance with official acceptance criteria, concluding that the cream formulated can be considered as an efficient herbal sunscreen product.

Another study by Kale group [32] reports the in vitro SPF determination of an emulsion containing *Ocinum basilicum* essential oil. SPF value of a sunscreen cream was found to be 1.19 with boot-star rating 1. Considering that values higher than 2 has been classified as effective sunscreen activity, emulsions containing *O. basilicum* can be considered as good candidates for sunscreen purposes.

As reported by Ebrahimzadeh and co-workers [33], the methanolic ultrasound extract and the methanol extract of *Crataegus pentagyna* and *Feijoa sellowiana* were evaluated as potential herbal additives for sunscreen formulations in a study which involved five different species. The highest SPF value (2 mg/7 mL of methanol), determined by the Gharavi method [24], was reached by the ultrasonic extract of *C. pentagyna* (SPF = 24.47), followed by the extract of *F. sellowiana* (SPF = 1.30). Moreover, although a good correlation between SPF and phenolic contents was found, no correlations between SPF and flavonoid contents or antioxidant activity were observed.

Other authors [34] reported the UV protective effects of sixteen ethyl acetate extracts of medicinal plants, rich in flavonoids and other phenolic compounds, using diffuse transmittance method and calculating SPF in solution by Gharavi equation model [24]. Only two plants, *Dracocephalum moldavica* and *Viola tricolor*, showed high SPF values, respectively 24.79 and 25.69. The same plants also displayed the highest amounts of flavonoids and phenolic compounds, which could explain the SPF values reported.

As reported in another research about *Leontopodium alpinum*, several luteolin derivatives were synthesized and isolated in order to study the UV absorber properties of this plant. Three distinct UV-absorbers were found, respectively lutein (330 nm) as UVA absorber, 3',4',5,7-tetralipolyoxyflavones (290 nm) as UVB absorber and 5-hydroxy-3',4',7-trilipolyoxyflavones (aprox. 260 nm) as UVC absorber [35].

Oliveira-Junior and co-workers studied six different extracts from *Neoglaziovia variegata* in order to determine the photoprotective effect, the antibacterial activity and the phytochemical composition [36]. The SPF was evaluated by an in vitro method based on Mansur equation [25]. Chloroform extracts from flowers showed higher SPF at a concentration of 100 mg/L (11.45 ± 2.87), followed by the ethanol extract and ethyl-acetate extract (5.95 ± 1.65 and 5.48 ± 1.54 , respectively). A concentration-dependent efficacy has been reported. The efficacy against bacteria was found especially on *Bacillus cereus*, *Escherichia coli*, *Salmonella enterica*, *Serratia marcescens* and *Shigella flexneri*. It was possible to identify the presence of two flavonoids (isoquercetin and kaempferol-3-O-rhamnoside) and four phenolic acids (caffeic, protocatechuic, p-coumaric and vanillic acids).

Other authors studied the chemical composition and physicochemical characteristics of the lipid fraction of *Nigella sativa* and reported that the oil can be used to give protection against UV radiations. *N. sativa* seed oil may provide protection against both UV-A and UV-B radiations due to its absorption in the UV range 290–400 nm [37].

In a valuable study about boldine, an alkaloid obtained from *Peumus boldus*, it was observed an interesting SPF in vivo (UVPF = 3.4) and in vitro (MPF = 3.9), in comparison with a commercial Nivea sun Spray, which reported 5 as SPF value [38].

Authors summarized that boldine showed, in vivo as in vitro, a UV light-filtering potency comparable to that of the commercial synthetic filters.

As reported by Gore and Satyamoorthy [39] the *Pongamia glabra* fixed oil contain pongamol and karanjin, two molecules which present respectively a chemical structure similar to 4-t-butyl-4'-methoxydibendoyl methane (Parsol 1789, UVA chemical filter) and 4-chromone moiety with potential UVB sunscreen activity. Pongamol showed the maximum absorption at 350 nm and 250 nm, karanjin reported the maximum absorption at 302 nm and 260 nm. In both cases it might be hypothesized a UVB and UVA sunscreen activity for both molecules, further studies are recommended to confirm this supposition.

Wagemaker and co-workers [40] studied the photoprotective activity and lipid composition of ten species of Coffee genus (*C. arabica*, *C. canephora*, *C. congensis*, *C. eugenioides*, *C. heterocalyx*, *C. kapakata*, *C. liberica*, *C. racemosa*, *C. salvatrix* and *C. stenophylla*). The SPF values, calculated by the spectrophotometric method proposed by Mansur and co-workers [25], were found interesting for *C. eugenioides* (2.6), *C. salvatrix* (2.2–3.1) and *C. stenophylla* (0.9–4.1). *C. arabica*, the most cultivated

specie, showed a lower SPF value (1.24–1.78), but the highest unsaponifiable matter content (13.54%): both data suggest the use of lipid fraction of green coffee beans as useful ingredients for high quality sunscreen cosmetics. In a further research on *C. arabica* seed oil, several *in vivo* and *in vitro* studies have been carried out on 4 topical formulations with different oil amounts (2.5%, 5.0%, 10% and 15% respectively) [41]. Formulations with 5% and 10% of oil showed good stability properties and interesting data concerning the post-radiation protection effect. Even if *C. arabica* seed oil did not evidence a significant difference in erythema indexes when compared with the control, others *in vivo* test on adult male hair-less mice have detected a depletion of the number of sunburn cells and a reduction of the trans-epidermal water loss in the treated animal groups. Again, the highest unsaponifiable matter content and the fatty acid composition may explain these eudermic effects, and *C. arabica* seed oil seems to be a synergic ingredient for sunscreen formulation.

4.2. Antioxidants

Antioxidant effect is a key mechanism of the photo protective activity of herbal extracts. The UV skin damage mainly depends from generation of reactive oxygen species, named ROS. These species include peroxy radicals, hydroxyl radicals, superoxide anion and, mainly, their active precursors: ozone, hydrogen peroxide and singlet oxygen. The ROS presence determines the membrane cell lipo-peroxidation and enhances skin aging and tissue damage. Antioxidants from herbal sources may provide new possibilities for the treatment and prevention of UV-mediated damages. Phenolic, polyphenolic compounds and flavonoids represent an important source of natural antioxidant extracts. The modern approach to UV protection strategies includes the UV filter activities, the topical application of antioxidant substances and the inclusion of phenols, polyphenols and flavonoids into the daily human diet [12].

In this chapter, we analysed researches which strengths are related to bioactivity assays and UV damage reduction. These data, obtained from *in vitro* internationally recognised test, can provide favourable information for the development of natural sunscreen products, considering in any case the necessary to verify the efficacy of topic formulation by *in vivo* studies.

Several authors highlight in their works the usefulness to include natural antioxidants extracts in topical products [4,12,13,42–44]. Some others have reported on possible correlation between antioxidants and UV protective effects of natural compounds from plants [33].

Almeida and co-workers [45] reported a study regarding the effect of *Castanea sativa* leaf extract against UV mediated-DNA damage in a human keratinocyte cell line. The research showed that *C. sativa* extract is able to prevent, in HaCaT cells, the UV-skin damage, thanks to a dose-dependent direct antioxidant effect provided by the presence of a pool of different phenolic antioxidants. Moreover, no genotoxic or phototoxic effects have been observed in case of incubation of HaCaT cells with ECS. These data suggested a potential new ingredient for sun care application.

As mentioned by Saewan and Jimtaisong [13] a red orange complex obtained from the mixture of three red orange varieties (*Citrus sinensis* varieties: Moro, Tarocco, Sanguinello) is effective against photooxidative skin damage when topically applied. The extract also provides protective effect on DNA cleavage, free radical scavenging capacity, inhibition of xanthine oxidase activity and anti-lipoperoxidative capacity.

Several extracts from *Codium fragile* and the isolated compound clerosterol have been tested against UVB-induced pro-inflammatory and oxidative damages in HaCaT cells and BALB/c mice [46]. All fractions showed an effective protection against UVB-induced inflammatory and oxidative skin damages when applied before the UVB irradiation. *C. fragile* extracts showed the inhibition of the expression of pro-inflammatory proteins including cyclooxygenase-2 (COX-2), inducible nitric oxide synthase (iNOS), and tumor necrosis factor- α (TNF- α). It has

been also reported a suppression of oxidative damages caused by UVB-induced lipid peroxidation and/or protein carbonylation, which seemed to be mediated by up-regulation of antioxidant defence enzymes.

Lim and co-researchers [47] studied the antioxidant effect and protective activity against ROS damage, in HaCaT cells, of the aqueous and methanol extracts of *Eucheuma cottonii*. In several assays, a significant antioxidant activity (DPPH Radical Scavenging Assay), probably due to the polyphenols presence, has been showed. Both extracts were able to decrease the UV-induced ROS damages *in vitro*, even if the aqueous extract exhibited a slight cytotoxic activity. Finally, the authors conclude that *E. cottonii* extracts could be proposed as new potential ingredients for skin care formulations.

Another study reports the antioxidant effects of a water-soluble enzymatic extract from rice bran (*Oryza sativa*), which have been tested in two cell models: keratinocyte monolayers and human reconstructed epidermis [26]. Studies showed that a diluted extract (1% in water) is not cytotoxic for concentrations lower or equal to 100 mg/mL. Moreover, they demonstrated that the extract can protect against free radical produced by UVB irradiation, reducing the cellular damage. Authors have also found that *O. sativa* extract exhibited a sun protection factor of 4.8, obtained *in vitro* by the method proposed by Diffey and Robson [22]. Antioxidant and photo protective activity of rice bran extract can be explained as due to the presence of gamma-oryzanol, ferulic acid and tocopherols.

As reported above, Gore and Satyamoorthy [39] investigated UV filtering activity of *Pongamia glabra* fixed oil, and in recent years the extract has been brought to the market as an “unofficial” filter. Patil and co-workers [48] reported also the sun protection effect of some sunscreen formulations containing a mixture of *Pongamia pinnata* and *Punica granatum*, used as sun-protecting factor boosting agent. Two formulations were prepared using a mixture of methanol leaves extract of *P. pinnata* and ethanol peel extract of *P. granatum* (3:2), at 5% and 10% respectively. Using COLIPA standard method (now Cosmetic Europe), SPF values of 2.18 and 5.78, for the 5% and 10% extract respectively, were recorded. These results indicated a Boots star rating of 3, which is considered a sufficient sunscreen activity.

The protection against UVA and UVB, calculated by transmission spectroscopy, was found to be 93.1% and 88.0% for the emulsion containing the 5% of extract, and 98.7% and 97.3% for the emulsion containing the 10% of extract. For both formulations the average UVA protection factor was 8.4 and 10.2 respectively. When absorption spectroscopy using Mansur equation method [25] was applied, 5% formulated cream performed SPF values of 1.79, 2.22, and 5.4 for 50 μ g/mL, 100 μ g/mL, 200 μ g/mL respectively. In case of 10% formulated cream, SPF values were found to be 3.6, 6.06, 11.1 at 50 μ g/mL, 100 μ g/mL, 200 μ g/mL respectively. These findings need more investigations, but are in agreement with a modern concept of safe and eco-friendly sunscreen formulation.

As reported by Svobodová and co-researchers [12], *Camelia sinensis* is a rich source of polyphenols which has been widely studied for anti-carcinogenic and anti-inflammatory activities. Green Tea Polyphenols (GTP) showed chemoprotective effects in mice and mouse test and seems to be able to prevent cutaneous edema, erythema and lipid peroxidation. Moreover, it might increase antioxidant defence of skin enzyme system. *C. sinensis* extracts may also prevent oxidative DNA single strand damage caused by UV exposure and they may reduce CPDs formation in human dermis and epidermis. Active ingredients from *C. sinensis* may prevent UV photo-damage due to synergic effects, which involve apoptosis in human epidermal carcinoma, reduction of lipid peroxidation, erythema and ROS production. Other authors [42, 43,49,50] studied the photo-protective properties of *C. sinensis* compounds and showed the preventive effects of epigallocatechin gallate (EGCG) against UV-radiation-induced infiltration of activated leukocytes in mouse skin, responsible of UV-induced suppression of immune responses and oxidative stress. Furthermore, *in vivo* studies on GTP and

specifically on EGCG evidenced attenuation of UVB-induced oxidative stress and decrease of the oxidative stress-mediated by MAPK proteins, responsible of cutaneous carcinogenesis risk. GTP can act also as antioxidant showing beneficial effects in protecting human skin disorders and photo-aging. Authors demonstrated, in human skin studies, that topical application of EGCG can inhibit the erythema and H₂O₂ production after UVB exposition. Moreover, it has been reported the suppression of leukocyte infiltration, a characteristic feature of skin inflammation, and the suppression of UVB-induced enhanced generation of PG metabolite. It is worth to mention that EGCG does not absorb or block UVB radiation and that it is not considered a sunscreen compound. Thus the photo-protective properties are related to the antioxidant activity. Huang and co-workers [51] described the ECG in vitro photo-protective effects against UVB-induced damage, focusing on the inhibition of intracellular H₂O₂ generation, lipid peroxidation and MAPKs activation, in compliance with a strong antioxidant activity.

4.3. Formulation strategies

The following studies represent for us a cluster of innovative and modern approaches to the UV skin protection. Connecting synergic effects (UV protection and bioactivity) and formulation strategies looks to us as the most productive way to obtain suitable information for a next generation of "green" sunscreen products. In this case, obviously, further studies regarding stability of the formulations are necessary in order to achieve an industrial development.

Fonseca and co-researchers [52,53] studied the in vivo protective effect of the hydro-alcoholic extract of *Calendula officinalis* against UVB-induced oxidative stress and the efficacy of its different topical applications. Proliferation of L929 mouse fibroblasts was not interfered by small concentrations of extract (15 mg/mL), that became toxic only at higher concentrations (35 mg/mL). In addition, inhibition of cellular proliferation of human breast cancer cells T47D was observed at all dosage. Despite these controversial results about a dose-dependent cytotoxic effect, the oral treatment with 150 and 300 mg/kg of the hydro-alcoholic extract showed a protective effect against UVB irradiation-induced GSH (endogenous reduced glutathione) depletion. This test is considered as a sensitive probe of UVB-induced epidermal oxidative stress and it indicates in *C. officinalis* extract a promising product also due to the in vitro antioxidant results. The authors reported a higher activity in scavenging superoxide radicals produced in the xanthine/luminol/XOD system, as compared to quercetin, but a lower activity against the hydroxyl, peroxy and alkoxyl radicals produced during lipid peroxidation and by the DPPH radical. The results of the topical application of the hydroalcoholic extract in three different formulations were especially interesting: if compared with two emulsions containing two self-emulsifying additives, the gel was the most effective for the delivery of the extract in the viable epidermis. It was reported that gel formulation maintained GSH reduced levels close to those of non-irradiated animals. In addition, the application of the gel formulation in hairless mice reduced the histological skin damages induced by UVB irradiation. Rutin and narcissin were identified as the main components of the extract, probably responsible of the observed effects.

In a preliminary study on *Camellia sinensis*, it is reported a research regarding the photostabilizing capacity of two extracts, green tea and black tea respectively [54]. The study considered to completely replace the aqueous external phase of the oil in water (O/W) sunscreen emulsion by the mentioned *C. sinensis* extracts. All the formulations tested contained avobenzene and octyl methoxycinnamate as synthetic UV filter. Stability upon storage and in vitro photoprotection assays showed that both extracts were able to improve the photostabilizing ability of the formulations, if compared with a pure water external phase. As reported in these study and several other researches, these findings allow to consider *C. sinensis* extracts as potential synergic agents for safer and more efficient sunscreen formulations [12,42,43,49,50,51,55].

The photoprotective effects of cosmetics based on *Fragaria × ananassa* (strawberry) extract were performed on dermal fibroblast [56]. Due to the presence of anthocyanin (pelargonidin glycoside and cyanidin glycosides) and vitamin (vitamin C and β-carotene), *F. Ananassa* showed a strong antioxidant activity. The photoprotective activity of several formulations containing *F. ananassa* extract and coenzyme Q₁₀ (CoQ₁₀) was measured on human dermal fibroblast irradiated with UVA. Later the decrease of cell death was determined by MTT assay. All the formulations showed a significant increase of the cell viability. Particularly, the emulsion containing *F. ananassa* extract and 100 µg/mL of CoQ₁₀, even in absence of an SPF, may provide a result closer to non-irradiated samples, showing a strong recovering effect of cell viability. One more time, a formulation strategy that imply a synergic effect of chemical UV filters, natural extract and active ingredients seems to be an interesting choice for photoprotection.

Gaikwad and Kale [57] studied the in vitro sun protection factor (SPF) of *Moringa oleifera* oil in a cream formulation, using the former Colipa method. The study investigated an emulsion containing 20% (w/w) of fixed oil from *M. oleifera* seeds. The SPF has been reported to be 1.06 with Boots Star Rating 3.

In another work [58], the SPF of three formulation containing respectively lutein ester (extracted from *Tagetes erecta*), *M. oleifera* seed oil and *M. oleifera* seed oil with lutein ester were evaluated. Physical Parameters of the emulsions were performed and no irritation reaction was observed (Patch test). Cream containing lutein ester had SPF = 1.09 and showed Boots Star Rating 4, *M. oleifera* Lam seed oil cream was endowed by SPF = 1.05 with Boots Star Rating 3 and *M. oleifera* Lam seed oil containing lutein ester showed SPF = 1.063 with Boots Star Rating 3. Taking together all formulations, they can be considered as efficient validated sunscreen products due to measurable SPF values (Former Colipa method).

A similar study [59] reported the sunscreen activity of a cream formulated with *Moringa concanensis* fixed oil, by means of an in vitro SPF method. The value found was of 1.46, with ultra-boot star rating 1. Although not confirmed in volunteers, this data are indicative of sunscreen activity.

Velasco and co-authors [60] reported delivery strategies for rutin, *Passiflora incarnate* L. and *Plantago lanceolata* extracts associated or not with organic synthetic and inorganic UV filters. Using diffuse transmittance measurements coupled to an integrating sphere, the sunscreen efficacy of delivery system films was determined, whereas UVA protecting ability was measured by the Boots Star method. Authors found that a broad sunscreen spectrum was achieved by adding 1.68% (w/w) *P. incarnata* L. dry extract to a formulation containing 7.0% (w/w) ethylhexyl methoxycinnamate, 2.0% (w/w) benzophenone-3 and 2.0% (w/w) TiO₂. This formulation showed, in vitro, an estimated SPF of 20.072 ± 0.906. The emulsion with rutin also showed a synergistically effect and an appreciable SPF value (28.064 ± 2.429) when associated with 7.0% (w/w) ethylhexyl methoxycinnamate, 2.0% (w/w) benzophenone-3 and 2.0% (w/w) TiO₂. Rutin and *P. incarnata* L. dry extract have been increased UVA filtering effects as compared with control. Additionally, the work has confirmed the relevance of the sunscreen vehicle. Emulsions are largely used to deliver UV filters and it has been proved that emulsified systems may favour or inhibit anti-UV protection, due to the chemical characteristics of their excipients. In this study, emulsions developed using phosphate-base emulsifiers seemed to achieve a stronger UV filter activity. Authors recommend considering the UV filter concentration and the appropriate formulation design as key factors for a successful sun-care product.

Campanini and co-researchers [61] investigated the inhibition of UV-B irradiation-induced oxidative stress and inflammation damage using two different topical formulations containing *Pimenta pseudocaryophyllus* ethanolic extract. A non-ionic emulsifier, with high lipid content, and an anionic emulsifier, with low lipid content, emulsions were tested, containing 5% of *P. pseudocaryophyllus* ethanol extract. Both creams inhibited UV-B-induced edema formation (89% and

86%), myeloperoxidase activity (85% and 81%), IL-1 β production (62% and 82%), MMP-9 activity (71% and 74%), GSH depletion (73% and 85%), superoxide anion (83% and 66%) and TBARS (100% and 100%) levels, increased glutathione reductase (2.54 and 2.55-fold) and reduced gp91phox (67% and 100%) mRNA expression, respectively. The sample named F2 containing PPE also increased IL-10 levels. Because emulsion containing the lower lipid amount also improved IL-10 levels, this suggests that less lipid content might be a better choice to deliver the extract.

In another similar study on the same *P. pseudocaryophyllus* extract and emulsions, it has been reported that PPE extract presents 199.33 ± 3.79 and 28.32 ± 1.46 mg/g of polyphenols and flavonoids, respectively [62]. Eugenol, rutin, and tannic acid were identified as the major compounds. *P. pseudocaryophyllus* extract showed antioxidant activity, as confirmed by DPPH and ABTS assays. Moreover, *P. pseudocaryophyllus* extract also demonstrated ferric-reducing antioxidant power. Anyway, only the capacity to scavenge DPPH radical of the extract was maintained in the two emulsions. Both formulations evidenced a satisfactorily release of the extract and good stability studies data. Furthermore, the emulsions were able to maintain the capacity to scavenge radical (DPPH) showed from the methanol extract. In vivo treatment with the two emulsions on mice significantly increased the capacity to scavenge ABTS radical and the FRAP of skin if compared to vehicle-treated animals.

There are interesting studies regarding a synergic effect between several vegetable oils, chemical UV filter and nanostructured lipid carriers [63,64]. Particularly, it has been demonstrated the efficacy of *P. granatum* seed oil to act as natural boost of chemical UV filter, enhancing the photoprotective properties of the nanostructured lipid carriers (NLCs). Moreover, particularly the NLCs containing a combination of *P. granatum* seed oil with *Triticum vulgare* germ oil showed good antioxidant properties (enhanced when compared to the non-encapsulated vegetable oils), the highest UV protection activity, including good encapsulating UVA filter performance. The study highlighted the importance of a formulation strategy focused on synergic photoprotective effects and natural plant sources. Other authors also studied the prevention and treatment of basal cellular carcinoma with NLCs [65]. The nanocarriers were prepared with natural *Amaranthus tricolor* seed oil (enriched in squalene), 5-fluorouracil (a hydrophilic chemotherapeutic drug) and ethylhexyl salicylate (a lipophilic UV-B sunscreen ingredient). The NLCs structure showed a sustained release of the drug (respecting the Fick law of diffusion) and amaranth oil performed a good scavenging free radicals activity. The research represents an important starting point for in-depth studies regarding the synergic effect of natural oils, drugs, and chemical UV-filter as synergic therapeutic strategy for the treatment of basal cellular carcinoma.

4.4. Synergic photoprotective effects from herbal extracts

Avila-Acevedo and co-workers [66] studied the in vitro and in vivo photoprotective activity of the methanolic extract of *Buddleja cordata* leaves, from Pedregal de San Angel (Mexico). The main components of the extract were linarin and verbascoside. The authors reported a synergic effect of the extract in various biological activities. For example, the extracts can absorb in the UVB spectrum at 224, 290 and 324 nm, showing an absorption spectrum quite similar to the octyl methoxycinnamate. Moreover, the herbal extract exhibited excellent OH radical scavenging ability (IC₅₀ 1.85 μ g/mL) when compared with gallic acid (IC₅₀ 335.8 μ g/mL). In UVB treated mouse skin, the reduction of erythema, of sunburned cell, of the vessel congestion and of the epidermal thickening was reported; all factors are known to enhance skin aging. Finally, the extract of *B. cordata* did not exhibit genotoxicity in the micronucleus test.

In a pioneer study on the photoprotective effect of plants from the Antarctic region, it is reported that the methanolic extracts of *Deschampsia antarctica*, *Colobanthus quitensis* and *Polytrichum*

juniperinum present photoprotective properties due to their antioxidant activity [67]. UV-absorbing properties as well as the stimulation of DNA-repair processes mechanism. Moreover, as a result of ozone layer depletion in the stratosphere, it must be considered an elevated risk of UVC skin damage. These authors [67] studied the effect of UVC damage in several in vitro models. In particular, quantitative determination analysis showed that *D. antarctica* presented the higher total flavonoid content (28.36%) and the flavanone content was higher in *C. quitensis* (7.91%). The extracts from these Antarctic species noticeably decreased DNA damage and mutation by UVC explosion in the yeast *S. cerevisiae* and V79 cells. Also in wild type yeast, a pre- and co-treatment with all extracts allowed protection against UVC toxicity and decreased induced mutagenesis rate. The extracts obtained in the study markedly decreased UVC-induced lipid peroxidation.

Aziz-Mohamed and co-workers [68] investigated the effect of *Disporum sessile* D. Don herbal extract (DDE) against photoaging. Researchers reported a significant inhibition of MMP-1 mRNA and protein expression levels HaCaT cells; moreover, it has been found that DDE can increase collagen production in UVB-irradiated human dermal fibroblast cells (NHDF). Taken together, these results suggested *D. sessile* D. Don as a potential ingredient in order to prevent skin photoaging and treat UVB-induced skin damage.

As reported in another study [69], in vitro antioxidant and UV-protecting studies were performed on aqueous and ethanolic extracts from *Galinsoga parviflora* and *Galinsoga quadriradiata*. While ethanolic extracts showed cytotoxic effects and improved ROS generation after UVB irradiation, both aqueous extracts (for both plants) exhibited interesting photoprotective activities. The extracts contrasted the depletion of proliferation activity and the increased apoptosis caused by UVA and UVB irradiation, showing also the inhibition of ROS generation in a concentration-dependent manner. These effects could be due to the presence of caffeic acid and caffeic acid derivatives (mainly caffeoyl glucarates).

Svobodová and co-authors [12] summarized the researches about natural phenolics in the prevention of UV induced skin damage. The study reported several usefulness herbal extract respectively from *Capparis spinosa*, *Culcitium reflexum*, *Ginkgo biloba*, *Krameria triandra*, *Pinus pinaster*, *Prunus persica*, *Sanguisorba officinalis*, *Sedum telephium*, *Vitis vinifera*. The lyophilized extract of *C. spinosa* and the ethanolic extract of *C. reflexum* showed UVB-induced skin erythema suppression, in human volunteers, by topical application, probably due to the presence of kaempferol, rutin, quercetin derivatives, cinnamic, caffeine and ferulic acids and p-coumarin. Both extracts were reported as strong antioxidant products or free radical scavenging agents.

In case of *C. reflexum*, a study reported a significant antioxidant effect probably due to the presence of phenolic compounds [70]. Furthermore, it was observed an excellent photoprotection against UV-B induced skin damage. *G. biloba* leaves extract contains flavone glycosides, mainly quercetin and kaempferol derivatives, and terpenes. Studies on mice skin demonstrated that this extract decrease the number of cells with sunburns effects by UVB irradiation; moreover, its oral administration enhances superoxide dismutase activity in UVB-irradiated mice skin. Phenolic compounds from the dried roots of *K. triandra* have been investigated and the suppression of UVB-induced skin damage in human keratinocyte cells has been reported.

Huh and co-authors [71] summarized several results regarding photoprotection and anti-skin aging activities of *Pinus densiflora*. The research highlighted that *P. densiflora* extract, due to the presence of trans-coumaric acid (TCA), inhibits UVB-induced MMP-1 expression in a dose-dependent manner. Moreover, TCA reduces collagen degradation and attenuates MMP-1 expression in a human skin equivalent model. These findings allowed including *P. densiflora* extract in further researchers on photoprotective agents.

The standardized extract of *P. pinaster*, which trade name is Pycnogenol, showed excellent free radical scavenging activity and inhibits UV-kB-dependent gene expression in HaCaT keratinocytes. The

effect showed a concentration dependent manner. Furthermore, the prevention of UV-induced erythema in rat, by topical application, and in human studies by oral intake was demonstrated. Gonzalez et al. reported that topical application of Pycnogenol increases the protection from UV radiation induced acute inflammation, immunosuppression and carcinogenesis, in a dose dependent manner [4].

In case of *P. persica*, the extract contains kaempferol glycoside derivatives as multi florin B, trifolin, aphelion and astragalol. The extract has been shown to inhibit UVB/UV-C induced DNA damage and lipoperoxidation in skin fibroblast. *P. persica* exhibited an inhibitory effect on UVB-induced erythema in guinea pigs and ear oedema in IRC mice. In a study on UVB-induced skin carcinogenesis in SKH-1 hairless mice, the *P. persica* extract was showed to delay tumor development [12].

Topical application of the extract of *Sanguisorba officinalis* has been reported to be able to prevent wrinkle formation, loss of elasticity and decrease of elastic fiber linearity in rat hind limb skin, in a dose dependent manner. The hydrolyzable tannins from roots are the main active compounds of *S. officinalis* extract. Flavonol glycosides (quercetin and kaempferol), gallic acids and polysaccharides from *S. telephium* leaf extracts were used in topical application, using gel formulation, and they were demonstrated to prevent UV-induced skin erythema in human volunteers [12].

Bulla and co-workers [72] studied the photoprotective effects and the percutaneous penetration of the *Schinus terebinthifolius* Raddi extract. Gallic acid and ethyl gallate (GAE) were found as the main components and the total phenolics amount was 384.64 ± 2.6 mg GAE g⁻¹ of extract. The extract showed a strong antioxidant activity, higher than BHT (DPPH assay), higher than citric acid and rutin and quite similar to the quercetin value (β -carotene bleaching assay). The *S. terebinthifolius* leaves extract performed absorption in the UV region and the SPF values (at concentrations of 10% and 25%) were 2.403 ± 0.132 and 6.895 ± 0.276 , respectively. Two formulations were evaluated, a gel and an emulsion, with 10% (w/w) of the crude extract; both formulations exhibited high absorption in UV region. The ex-vivo evaluation of the formulations showed penetration through the skin, an occurrence that should be avoided for synthetic filters; however, no histopathological adverse reactions changes were observed in the treated animals. These findings indicated that although further studies are necessary to investigate photostability, *S. terebinthifolius* leaves extract could be a natural alternative for skin care products and sunscreen application.

Silybum marianum was reported as a natural source of flavonolignans, which the main component is silymarin. Topical application of silymarin showed the inhibition of sunburn, apoptotic cells and UVB-induced oedema. In mouse model, a decreased level of catalase has been reported. Treatment with silymarin prevents the formation of cyclobutane-pyrimidine dimers and the oxidative stress caused by infiltration of inflammation leukocytes [12].

Yang and Li [73] investigated the effect of *Taraxacum officinale* water extracts, from root, leaf and fruits, as photoprotective agents. The extracts allowed prevention of the oxidative stress-induced premature senescence: leaf and flower extracts showed to be more effective than root extract. Extracts were able to protect NHDF with treatment either before or immediately after UVB radiation. The extracts also worked as UV absorbers and in the decrease of oxidative stress and matrix metalloproteinases activity (MMPs). These results consent to suggest *T. officinale* extracts as effective, safer, and environmentally friendly option for sunscreen formulations.

Vitis vinifera seeds are rich in polyphenols, mainly flavan-3-ol derivatives, catechins, epicatechins and oligomeric proanthocyanidins. Svobodová and co-authors [12] reported for grape seeds extract an important free radical scavenging effect, stronger than vitamins C and E. Moreover, prevention of UVB/UV-C induced lipid peroxidation has been reported. Filip and co-researchers [74,75] studied *V. vinifera* grape seeds extract in two different studies. In the first one the topical application on mice produced inhibition of UVB induced sunburned cells, restoring

of the superoxide dismutase (MnSOD) activity, increase in CAT and GPx activities and reduction of IL-1 β level, at 2.5 mg polyphenols/cm². A higher dose treatment, 4.0 mg polyphenols/cm², showed a decreased GSH level and the reduction of the percentage of CPDs positive cells in skin. After UV-B irradiation, for both extracts concentration, an increased MnSOD and GPx activity and the reduction of the formation of sunburn cells in skin was reported. The second one was performed by in vivo test on SKH-1 mice skin. The topical application of *V. vinifera* grape seeds extract inhibited UVB-induced sunburn cells and CPDs formation twenty hours after the UV irradiation. Pre-treatment with *V. vinifera* extracts resulted in significantly reduced levels of IL-6 and TNF- α as compared to UVB alone. In the same study the extract of *C. vulgaris* was also evaluated, showing similar, but lower, efficacy if compared with *V. vinifera* grape seed extract. Other authors [76] reported that a pre-treatment with *V. vinifera* grape seeds extract increases HaCat cells viability after UVB irradiation, decreases lipid peroxides level, DNA photolesion and cells apoptosis [73].

Svobodová and co-authors [12] reported the photoprotective activity of nor-dihydroguaiaretic acid, which has been demonstrated to be able to inhibit UVB-induced c-fos and AP-1 transactivation in the HaCaT keratinocyte cell line. It was also observed the reduction of the activity of phosphatidylinositol 3-kinase, an UVB-inducible enzyme, that can act in the in the expression of AP-1 and its component proteins c-Fos.

Photoprotective effects from *Glycine* max, particularly soybean cake, were studied by Saewan and Jimtaisong [13]. Soy isoflavone extract from *G. max* exhibited an important antioxidant activity, better than genistein, daidzein, genistin, and daidzin [77]. Chiang and co-workers [78] have also reported the inhibition of UVB induced keratinocyte death, the release of hydrogen peroxide (H₂O₂) and UVB induced MAPK phosphorylation. Another article [79] reported in vitro studies in which UVB-induced HaCaT cell death decreased when isoflavone extracts were applied prior to UVB irradiation. Same effects were reported about the phosphorylation of p38, JNK, and ERK1/2. The in vivo studies demonstrated the UVB irritation reduction, the decrease of epidermal thickness and the expressions of COX-2. Furthermore, an increased PCNA and catalase concentration was detected; showing that isoflavone extracts from soybean cake can be considered as inhibitors of UVB-induced apoptosis and inflammation. *G. max* is also a rich source of genistein, a potent anti-photocarcinogenic and anti-photoaging molecule. Genistein showed to be able to prevent UVB radiation induced skin burns in human and molecular damage in hairless skin [4].

Svobodová and co-workers [12] observed that genistein decreases UVB-induced H₂O₂ production in the skin and inhibits oedema formation and skin hypersensitivity, when applied topically.

Petrova and co-researchers [30] described, using a mouse model, a plausible mechanism of photoprotection by polyphenolic extracts of green and fermented *Cyclopia intermedia*, and by the two major components, hesperidin and mangiferin. The study provided the first evidence that both honeybush extracts can modulate UVB-induced damage. Results about the purified compounds hesperidin and mangiferin were partially conflicting and they hypothesized a synergic effect of the phyto-complex. Other authors mentioned that the photoprotective activity of the *C. intermedia* extracts is multifactorial and comprises UVB absorption, decrease level of lipid peroxidation and oxidative DNA damage, protection against decreases in SOD, CAT and GSHT, inhibition of UVB-induced erythema, oedema and hyperplasia, and lower expression of COX-2 and ODC (markers of inflammation and cell proliferation respectively) [30].

Saewan and Jimtaisong [13] reported the photo-protective activity of *Fragaria x ananassa* extracts, which main components are Pelargonidin (as the major representative aglycone) and some cyanidin derivatives. An increased cellular viability and a lower DNA damage on UVA-induced skin damage have been demonstrated. The same authors and other authors have reported that the topical application of *Trifolium pratense* extracts showed a protective effect against UV induced

inflammation and immune suppression in hairless mice [4,13]. Main components of *T. pratense* are genistein, daidzein and equol. Equol could be able to inhibit UV-induced tumor promotion due to the synergic interaction with metallothionein, a cutaneous antioxidant involved in physiological UV repair mechanism. The photo protection activity seems to be related to isoflavonoid compounds.

Also anthocyanins from *Vaccinium myrtillus* L. have been evaluated as SPF effective ingredients, showing in in vitro assay the reduction of hydrogen peroxide induced radicals, the inhibition of lipid peroxidation and scavenge superoxide activity. It has been reported that pre-treatment (1 h) or post-treatment (4 h) of HaCaT keratinocytes with *V. myrtillus* extract (titred 25% anthocyanins) decreased UVA-stimulated ROS formation, UVA-induced peroxidation of membrane lipids, and the presence of intracellular GSH [13]. Additional researches by Calò and Marabini [80] investigated the photoprotective activity of a water-soluble extract of *V. myrtillus* on HaCaT cells. It was demonstrated the capability of the extract to reduce the UVB-induced cytotoxicity, genotoxicity and lipid peroxidation, even if no effect was observed against ROS UVB-produced damage. Also in case of UVA-induced damage, the extract was able to reduce genotoxicity, the unbalance of redox intracellular status and the UVA-induced apoptosis showing a desirable free radical scavenging affect and the depletion of oxidative stress and apoptotic markers.

Similar results have been showed by *Vaccinium uliginosum* L. extract, which major components are cyanidin-3-glucoside, petunidin-3-glucoside, malvidin-3-glucoside, and delphinidin-3-glucoside. The studied antocyanins were able to protect skin against UVB-induced photoaging due to the capability to stop collagen degradation and inflammatory responses. It seems that *V. uliginosum* L. extracts can block transcriptional mechanism of NF- κ B and MAPK.13

Figueiredo and co-workers [81] investigated the in vitro and in vivo photo-protective and photochemopreventive potential of *Garcinia brasiliensis* epicarp extract. A high level of polyphenols was found. Studies identified 7-Epiclusianone, a polyisoprenylated benzophenone, as major component. The study reports that 7-Epiclusianone showed a capacity to absorb UVB radiation five times smaller than benzophenone-3. In the respect of this latter, despite its lower UVB absorption activity, 7-Epiclusianone presents less penetration into the skin, and thus only a slight irritating effect. Moreover, in vitro studies on fibroblasts cell culture, showed that solutions and cream gel formulations containing *G. brasiliensis* extract (10% and 20% respectively) had photoprotective properties comparable with commercial sunscreen from two different brands with three different sun protection factors (15, 30 and 60). About in vivo photoprotective properties, on 3-month-old, sex-matched hairless mice, GSH depletion induced by UVB radiation was completely inhibited by *G. brasiliensis* formulation, probably due to the prevention of the generation of ROS and/or scavenging of radical reactive species. Irradiated mice skin was treated with *G. brasiliensis* formulation and showed similar myeloperoxidase activity if compared with non-irradiated skin, suggesting a preventing activity on the inflammatory process induced by radiation. Thus, UVB radiation absorption activity and the concomitant antioxidant properties, prevent oxidative stress and lipid peroxidation. Indeed, the extract efficiency prevents any increase in MPO activity, the inhibition of neutrophil migration toward the exposed area, and also the inhibition of the synthesis of the pro-inflammatory cytokines (as TNF- α and IL-1 β) induced by UVB radiation, indicating activity on first and second phase of the UVB driven inflammatory process. Authors concluded that the extract has a great potential to be used as a sunscreen, in addition to synthetic UV filters, contributing to the reduction of synthetic filters in the formulations. Furthermore, the extract comes from the peel of the fruit that is a by-product of *G. brasiliensis*, which represents a sustainable application.

González and co-authors [4] reviewed the photoprotective effects of topical application of several natural ingredients; among them *Polygonum multiflorum* thumb extract activity can be explained with an increased superoxide dismutase 1 immunoreactivity after UVB

irradiation. *P. multiflorum* thumb seems to be able to reduce the UVB-induced oxidative stress avoiding the photo aging effects. In the same review the authors discussed the antioxidant and anti-inflammatory activity of the *Polypodium leucotomos* hydrophilic extract, which can inhibit the erythema generated from in vivo UVB light and PUVA therapy. This effect can be probably explained by the extract capability to inhibit pro inflammatory cytokines, tumor necrosis factor- α or interleukin-6. Furthermore, *P. leucotomos* extract preserves Langerhans cells characteristics (morphology and number) when irradiated by UV light and PUVA therapy. At the same time, attention has been drawn to the reduction of chronic UVB-induced elastosis and probable prevention of photo induced skin tumor, due to the capability of hydrophilic extract to inhibit UVB light and PUVA therapy induced erythema and the inhibition of proinflammatory cytokines. The same authors described also the photo protective activity of *Punica granatum*. Probably due to the presence of hydrolyzable tannins and anthocyanidins, the specie possesses known antioxidant and anti-inflammatory properties. *P. granatum* can inhibit UVB-dependent activation of NF- κ B and mitogen-activated protein kinase pathways, protecting the skin against UVB radiation damage.

4.5. UV filter and antioxidant synergic activities of lichens extracts

Rancan and co-workers [38] studied the in vivo and in vitro UV-light filters activity of 4 molecules (1'-chloropannarin, usnic acid, epiphorelic acids I and II, calicin) obtained from 4 Chilean lichens: *Erioderma leylandii*, *Xanthoparmelia farinosa*, *Coelopogon epiphorellus*, *Pseudocyphellaria bereberina*, respectively. The in vivo test was made following the FDA protocol, and the protection factors ranged between 2.0 and 4.2. The UV protection factors determined on volunteers showed that usnic acid reached the highest value, 4.2. The benchmark commercial product, Nivea sun Spray, achieved an average of 4.2 with a label SPF of 5. The in vitro test membrane protection factor (MPF) is principally an index of membrane destruction. Values obtained from the 4 natural molecules were compared with octylmethoxycinnamate (OMC), a very common synthetic filter, as reference. Again usnic acid resulted as the best UVB filter, with an average of 4.5. The other lichen extracts gave similar values. Moreover, molecules tested in this study showed a different absorption after prolonged UV irradiation, indicating the presence of by-products. Usnic acid photo by-products have still a good absorbance in UVB region after irradiation. The authors finally asserted that usnic acid was one of the best natural UV filter, at least the better among those tested in this study.

Photoprotective effects of the same natural compounds were investigated also by Kohlhardt-Floehr and co-researchers [82], focusing the cell survival and cell metabolism of human lymphocyte cell line (Jurkat-cells) under UV-B-irradiation. Usnic acid was obtained from *Xanthoparmelia farinosa*, and the results of this study suggested that usnic acid can act either as a pro-oxidant or as an antioxidant, depending on the specific concentration and UVB doses.

Table 1 summarized some relevant information about the reviewed literature, including plant name, plant part used, type of extract, mayor constituents and finally the main biological effects. The different effects of the extracts were gathered into three groups, respectively classified for the main effect(s). Table 2 reports, for each plant species, the major constituents (if reported) and a brief description of the main biological effects.

The cells incubated with usnic acid in low concentrations (1×10^{-8} and 1×10^{-6} M) and low doses of UVB radiation (up to 0.1 J/cm²) showed a higher cell survival and a normal metabolism if compared to the control. At higher concentrations (1×10^{-4} M) and UVB doses (up to 14 J/cm²) the cell survival was the opposite.

As described by Millot and co-workers [83], extracts obtained from 12 lichens were investigated in order to isolate and characterize new photo-absorbing molecules. Secalonic acid B showed a main band at 338 nm (UVA range) and a low toxicity with respect to the other

compounds; this is the reason why the authors recommended for further studies in order to develop new sunscreens molecules.

Lohézic-Le Dévéhat and co-researchers [84] studied the photo-protective effects of the extract of three lichens, *Cetraria islandica*, *Usnea hirta*, *Lasallia pustulata*. Specifically, fumarprotocetraric acid, usnic acid and gyrophoric acid have been isolated. They are, respectively, the major secondary metabolites of *C. islandica*, *U. hirta* and *L. pustulata*. Afterwards, their photoprotective properties have been investigated. Salazinic acid and *L. pustulata* extract might be useful as UVA-PF boosters candidates (UVA-PF > 2), and gyrophoric acid resulted to be the best UVB photoprotector, in agreement with previous literature. *L. pustulata* extract and its major metabolite gyrophoric acid seem to be interesting UV-filters (SPF > 5 and PF-UVA-PF > 2), and also after 2 h of irradiation (650 W/m²) >90% efficacy was maintained. Salazinic acid and gyrophoric acid did not show any radical scavenging activity according to the DPPH assay, while *L. pustulata* extract was categorized as a weak free radical scavenger, in comparison to ascorbic acid. Despite the conflicting result of DPPH assay, salazinic acid was observed to possess good superoxide scavenging activity (3.9 ± 1 µg/mL) when compared to ascorbic acid (6.2 ± 0.2 µg/mL). No phototoxicity was observed for all tested compounds. Other studied molecules did not show significant SPF values, but they can be added to cosmetic formulations as filter boosters. Especially variolaric acid, evermic acid, vulpinic acid and above all salazinic acid resulted effective in term of UVA protection. Based on these data, authors recommended some of the molecules tested in this study as synergistic additives in sunscreen formulation.

Boehm and colleagues [85] studied the photophysical properties of six potential sunscreens molecules extracted from the following lichens: *Erioderma leylandii*, *Xanthoparmelia farinose*, *Pseudocyphellaria bereberina*, *Coelopogon epiphorellus*, *Teloschistes flavicans*. Six polyaromatic compounds, respectively Calycine, 1'-chloropannarine, usnic acid, epiphorelic acid I and II and vicanicine, were extracted from lichens and investigated in order to determine their value as sunscreen additives. The radical cations of usnic acid and calycine showed efficient scavenging activity, suggesting a possible synergic use as antioxidants additives in combination with vitamins E and C. Finally, the authors concluded that considering their previous study, calycine certainly deserves further investigation for photo protection activities.

As described in literature [86], *Usnea roccellina* Motyka was investigated as potential source of photoprotective actives. Three molecules were isolated, 3-methoxycarbonyl-2-hydroxy-6-methoxy-4-methylbenzoic acid, (+)-(9b-R)-usnic acid and decarboxythamnolic acid, respectively. All isolated compounds showed a strong UV absorption activity. Moreover, the SPF values of the three evaluated compounds were not significantly different ($p < 0.05$) from benzophenone-3 SPF. For these reason, molecules obtained from *U. roccellina* may be compared with commercial synthetic UVB filter and can be suggested as UVB photo-protective agents. Moreover, decarboxythamnolic acid was found to be a strong antioxidant agent by in vitro assays (DPPH test and Ferric reducing power test). These findings allow identifying especially decarboxythamnolic as a promising photoprotective agent, due to the antioxidant and UV-absorber activity.

4.6. Additional studies on pure natural molecules as photoprotective additives

Due to the presence of the same natural molecules in different plants, several studies and reviews investigated the photo protective effects of these purified molecules, irrespective to the natural source.

As reported by Svobodová and co-authors [12] apigenin, a flavonoid widely present in herbs, fruits and vegetables, has been recognised as effective ingredient in the prevention of UVA/B-induced skin carcinogenesis in SKH-1 mice. This molecule can also decrease the UV-mediated activation of ornithine decarboxylase, enhancing tumor free survival

and reducing tumor indigence. It has been also found to be an inhibitor of the cell cycle and cyclin-dependent kinases.

The same authors also reported in this work the antioxidant activity of caffein and ferulic acids, two very similar molecules based on a 3,4-dihydroxycinnamic structure. These molecules are able to stop the propagation of UV-induced lipoperoxidation and to inhibit UV-induced erythema. Ferulic acid is employed in cosmetic formulation as UV absorber. Also carnosic acid, the main component of *Rosmarinus officinalis* and *Salvia officinalis*, was shown to be a strong antioxidant compound, which possesses chemoprotective effect against carcinogenesis. Moreover, it displayed inhibition of metalloproteinase-1 mRNA, a negative effect related to UVA light exposure.

Other authors [87] reported a study about the in vitro and in vivo photoprotective activity of a mixture of citrus and rosemary bioflavonoids. Researchers investigated the effects of the extracts on human HaCaT keratinocytes and in human volunteers. The combinations of both extracts showed a higher survival of cells if compared with data regarding the individual extract. Moreover, it has been observed antioxidant activity expressed by the depletion of intracellular ROS, and it was also performed a reduction of prevented DNA damage in HaCaT cells, and less chromosomal aberrations in X-irradiated human lymphocytes. On human volunteers a significant improved MED has been detected by oral daily consumption of 250 mg of the mixture, showing after 8 weeks and 12 weeks an enhancement of 34% ($p < 0.05$) and 56% ($p < 0.01$) respectively. Finally, even if the mechanism of action needs additional researches, authors concluded that citrus and rosemary bioflavonoids can be considered promising oral photoprotective agents. Antioxidant properties of astaxanthin have been summarized by González and co-workers [4]. Furthermore, it has been shown that this pigment seems to be able to reduce lipoperoxidation and the concentration of UVA-induced free polyamines, thus reducing skin damages. As reported in scientific literature [88], a new pharmaceutical strategy consists of nanoemulsion formulations able to enhance the efficacy of soy isoflavone genistein against UVB-induced skin damage (in vitro assay). Nanoemulsion prototypes including genistein and tocotrienol-(T3)-rich fraction of red palm oil (Tocomin®) were able to provide a slow-release effect, showing also excellent biocompatibility and UVB protection efficacy on cultured subcutaneous L929 fibroblasts. These data suggested the potential of nanoemulsion technology in the photoprotective treatment.

Saija and co-workers [89] studied the effect of topical application of naringenin and hesperetin (flavonoids), in presence of skin penetration enhancers, for the prevention of UV-B-induced skin damage. In vitro and in vivo studies showed improved naringenin and hesperetin skin penetration, by pre-treatment with α -limonene and lecithin, two known penetration enhancers. On the contrary, α -limonene and lecithin alone were completely ineffective in inhibiting UV-B-induced erythema; at the same time, also formulations containing only hesperetin and naringenin were found to be completely ineffective in decreasing UV-B-induced erythema. Only the formulations containing both penetration enhancers and the above mentioned flavonoids were able to markedly reduce skin erythema. Both α -limonene and lecithin enhanced the photoprotective activity of naringenin and hesperetin. In conclusion, the authors demonstrated that hesperetin and naringenin can be successfully applied as topical photoprotective ingredients in presence of skin penetration enhancers, which seems to be essential to optimize the photo-protective activity.

Quercetin has been investigated in several studies for its protective skin damage capability. Svobodová and co-authors [12] reported in vivo data regarding the antioxidant effects of quercetin, due to its capability to protect several physiological antioxidant enzymes as glutathione peroxidase, catalase, superoxide dismutase, glutathione reductase. It has been shown also quercetin capability to reduce UVB-induced immunosuppression activity in SKH-1 hairless mice, by oral intake, and the inhibition of peroxidation in liposomal membranes caused by UVC radiation. In Table 3, a list of lichens is provided.

Yin and colleagues [90] studied potential effect of quercitrin, the glycosylated derivatives of quercetin, to inhibit UVB light oxidative damage both in vitro and in vivo. Results showed the activity of quercitrin to reduce ROS generation in JB6 cells after UVB irradiation. Quercitrin was able to enhance the cattle expression and GSH/GSSG ratio (reduced by UVB exposure), two relevant antioxidant enzymes. The study demonstrated that the quercitrin works as an antioxidant against UVB radiation-induced oxidative damage to skin.

Another research group [28,29] studied the effect of topical formulations containing quercetin (in vivo test in hairless mice) as protective agent against UVB-induced oxidative stress. Quercetin was applied using two different cosmetic formulations, the first one characterized by the presence of non-ionic emulsifier and with high lipid content, the second one by anionic emulsifier and low lipid content. Both formulations were able to inhibit the MPO activity (62% and 59%, respectively), GSH depletion (119% and 53%, respectively) and proteinases secretion/activity. Results also showed the enhanced protective activity by the second emulsion, formulated with anionic emulsifier and low lipid content, indicating the relevant impact of formulation on skin care treatment. A second study, by the same authors, reported the in vitro antioxidant activity of quercetin, by the inhibition of malondialdehyde formation. In this study, both the formulations previously described were used to investigate preventive effect of quercetin in UVB-induced oxidative/inflammatory skin damages. The in vitro release studies showed that the low lipid content emulsion can release the drug about two times faster than the high lipid content formulation ($14.9 \pm 0.1 \times 10^{-12} \text{ cm}^2/\text{s}$ and $7.5 \pm 0.02 \times 10^{-12} \text{ cm}^2/\text{s}$, respectively). These results confirm the influence of the formulation in the final activity. Moreover, after 12 h experiment, the maximal antioxidant activity of both formulations ($54.0\% \pm 5.5$ and $42.0\% \pm 5.9$, respectively) was reached with no difference among the two formulations.

Vicentini and co-workers [91] evaluated both in vitro, using porcine ear skin, and in vivo, on hairless-skin mice, the potential of a W/O microemulsion as a topical carrier system for delivery of quercetin. Quercetin concentration increased in stratum corneum and epidermis plus dermis at 3, 6, 9 and 12 h post-application in vitro, and 6 h post-application in vivo, without inducing skin irritation. This study suggests the usefulness of quercetin to prevent UVB irradiation-induced GSH depletion and secretion/activity of metalloproteinases.

Additionally, other authors [92] studied the effect of quercetin on the photostability of butyl methoxydibenzoylmethane (BMDMB) and octyl methoxycinnamate (OMC), very common UVA and UVB filters. They demonstrated that quercetin, even added in a relatively low concentration (0.5%, wt/wt), was able to significantly reduce the photodegradation of the synthetic UV filter, with any variation of the sunscreen activity of the formulation. The effectiveness of quercetin seems to be due to antiradical property and efficient metal ions chelation activity in the reactions which involve the formation of free radicals. In conclusion, low levels of quercetin added to sunscreen can enhance the photostability of the most widely used combination of UVA and UVB filters, BMDMB and OMC, showing a synergistic photo protective effect that include antioxidant and chelating activity.

As reported by two different works [4,12], resveratrol determines a significant reduction in UVB-induced skin oedema in SKH-1 hairless mice. Moreover, it possesses a strong antioxidant activity, due to its protective effect against UVB-induced hydrogen peroxide damage leukocytes infiltration, lipid peroxidation, cyclooxygenase and ornithine carboxylase activities. Resveratrol seems to be able to block the UVB-induced HF-kB activation in a dose and time-dependent manner. Finally, other studies [93,94] reported resveratrol capability to reduce tumor incidence or delay of tumorigenesis. Furthermore, a positive synergistic advantage has been found in the combination of trans-resveratrol and beta-carotene with common UV-filters [95,96]. The combination reduces UV-filter skin retention, causing an improved sunscreen safety. Additionally, the same combination of trans-resveratrol and beta-carotene with chemical UV filters allows an improved photostability for

sunscreen formulations, to achieve a better efficacy and safety. Resveratrol has been found to be a strong photoprotective agent in case of retinal pigment epithelial cells damage [97].

Huang and co-workers [27] studied the photoprotective activity of myricetin, a flavonoid widely present in berries, vegetables, teas, wine, and herbs. In vitro test showed that myricetin can alone enhance HaCaT cell viability, and it also can protect the same cells treated with UVB irradiation. Moreover, treatment of HaCaT cells with myricetin was shown to be able to inhibit UVB-induced lipoperoxidation, intracellular H_2O_2 production, JNK activation in keratinocytes and apoptotic DNA oligonucleosomic strand breaks in a concentration-dependent manner. In conclusion, myricetin might be useful as cosmetic ingredient in skin care and sunscreen products.

As reported in literature [98], several retinoids have been investigated as cosmetic ingredients. Despite topical retinoic acid application might induce skin irritation, this molecule is widely used for treatment of several skin diseases and to contrast the skin-aging. Experimental evidences have demonstrated that retinoids possess strong UV-light absorption with a potential UV filters activity, prevent UVB-induced apoptosis and DNA photodamage. Human study showed preventive or no effect of topical retinoids on non-melanoma skin cancers, and topical application of retinyl palmitate (2% w/w) was shown to be an efficient sunscreen product, comparable to a sunscreen emulsion with a SPF 20, regarding UVB-induced erythema and DNA photodamage. Retinoids have been also shown to exert a free radical scavenging activity in in vitro and in vivo studies.

Skotarczak and co-workers [14] summarized several potential photoprotective molecules. Probably the most innovative concern photolyase enzyme, first isolated from the cyanobacteria, *Anacystis nidulans*. Many different photoprotective activities have been related to photolyase enzyme: for example, recognition and removal of cell DNA fragments damaged by UV radiation; degradation of pyrimidine dimer caused by UV radiation; inhibition of proinflammatory cytokine, interleukin 6, responsible of skin inflammation; inhibition of UV-induced apoptosis. The inclusion of photolyase enzyme in multi-layer phospholipid envelope allows its penetration into the skin up to deeper layers, showing again the relevance of the synergic effect of active molecules and pharmaceutical or cosmetic formulation. The same authors mentioned also another enzyme able to repair UV-induced damaged cells, the cells endonuclease (obtained from *Micrococcus luteus*). The enzyme, also applied into multi-layer phospholipid envelope, improves efficiency and speed of DNA repair mechanism, improves skin regeneration and inhibits inflammatory response. Regarding β -carotene and lycopene, the skin burn prevention activity seems to be due to their ability to scavenge ROS. The same authors, mentioned also EGCG, ferulic acid, Pycnogenol® and *Polypodium leucotomos* extracts for their antioxidant and photoprotective activities.

In this field, our recent studies were focalized in the investigation of structure/activity relationships between the structures of natural polyphenols, antioxidants and UV protecting activity by modification of their structures [99–105].

To this end, slight modification of the structure by lipidization. The modification of the partition coefficient was obtained by esterification with fatty acid chains, in order to consent to the hydrosoluble glycosylated polyphenols to diffuse to the lipid part of the formulation and, then, from the formulation to the skin. Results were in strong agreement with the above described studies, pointing to a consistent influence on the efficacy (i.e. antioxidant and UV protectant) in relation to the kind of formulative approach. These evidences should be taken into account in order to compare results from literature, obtained on isolated molecules in solution or in formulation.

4.7. Eco-sustainability

Although the effects of synthetic sunscreen have been thoroughly reviewed and discussed by several authors out to date no natural

sunscreen has been so far investigated. The problem has been studied by some authors but not in relation to UV filters, which, on the contrary, express a specific toxicity beside the general one of synthetic organic insoluble molecules [106].

Recently Downs et al. [107] demonstrated toxicopathological effects of the sunscreen UV Filter, Oxybenzone (Benzophenone-3), on coral planulae and cultured primary cells and its environmental contamination in Hawaii and the U.S. Virgin Islands.

As reported by Downs et al. an oily, iridescent sheen on the surface of the water is often recognizable, supposedly caused by sunscreen washing off the swimmers.

Besides washing off swimmers' skin into the water, sunscreen can get into the sea by other means. Some synthetic sunscreen UV filters are absorbed through the skin. Oxybenzone, that is considered a synthetic UV-filter (although naturally detected in some flowers [108]) is detected in urine within 30 min from application [109] and thus can be recovered in the waste that goes in the sea. This pollution, for big towns close to the sea, is rather unavoidable.

Downs et al. demonstrated that oxybenzone induces coral bleaching by lowering the temperature at which corals will bleach when exposed to prolonged heat stress. They also showed that oxybenzone is genotoxic, meaning that it damages coral DNA as well as induces severe and lethal deformities. Oxybenzone also acts as an endocrine disruptor, causing the coral larvae to inappropriately encase itself in its own stony skeleton [110].

These pathologies can occur at concentrations as low as 62 parts per trillion (ppt), this compared to famous Hawaiian beaches which reaches 700 ppt. They also found oxybenzone is toxic to algae, sea urchins, fish and mammals. As well as the most known and widely used oxybenzone, there are other chemicals in sunscreen that are potentially toxic to coral reefs, some of which, including methoxycinnamate and camphors, and more are under investigation (i.e. nanosized physical filters).

5. Future trends

As reported above, several studies showed interesting in vitro and in vivo studies regarding synergic anti-inflammatory, anti-photoage and antioxidant activities, forecasting an optimistic sun care application for herbal extracts. A rational approach based on this cluster of information, if supported by statistically validated data, should be considered a necessary second step to develop effective formulations. Taking this into account, in our opinion, future investigation should focus on the applied studies necessary to demonstrate if herbal extract really act in vivo when delivered by suitable finished formulations. Following the above-mentioned concepts, the development of natural and effective herbal sun care products should follow three different steps, typical also of herbal drug development:

- 1) extraction and characterization of the properties of the extracts (i.e. UV absorption, mutagenicity, cytotoxicity);
- 2) In vitro evaluation of synergic physiological activity (i.e. lenitive, anti-radical, antioxidant, etc...);
- 3) Formulative strategies, new vehicles, stabilization, SPF evaluation in vitro and on volunteers.

In any event, a critical assessment of the data is essential for an appraisal of the state of the art. First of all, a debate about the validity of data has to be proposed. As described in the present work, a large number of articles showed the in vitro UV absorption activity of several herbal extracts, mainly based on the Diffey-Robson approach [22] or the models proposed by Gharavi and co-workers [24] or Mansur and colleagues [25]. To demonstrate or to predict a UVB photoprotective effects, on the base of the UV absorption activity, must be considered a prerequisite. This is normally addressed with a preliminary in vitro study, useful to address further research on a species or an extract, but not adequate to warrant an in vivo UV-damage protection. Chemical stability and photostability of the extract in a sunscreen formulation,

its absorption through stratum corneum layer and others synergic effects with the excipients, should be a second step of investigation. Finally, step 3, is very important to assess the "real" sunscreen properties and should be always part of any discovery strategy. But, on the contrary, it often lacks from the literature so far examined and we believe that in the future studies should be aimed to the reinvestigation of the extracts not completely exploited and in performing complete studies in any newly investigated extract. Taking into account that the trend for the future points to the development of "green" and/or "certified eco-bio" sunscreens, it is very important to adopt, since now, the above stated strategies in any study aimed to investigate sunscreen properties of UV absorbing natural molecules.

However, as discussed in the previous section, green and eco-bio sunscreens does not mean necessarily totally safe for the marine environment, especially for the issue related to corals and algae. Governments can play a strategic role by supporting the development of standardized methodologies and stimulating, by significant extent, collaboration in this sense between company and academy. Are there practical solutions to be adopted right now? One short-term policy should be to encourage people to use medium and high protection instead of very high. If correctly applied a medium protection (SPF 30) filter 97% of the UV-B radiation rather than 98% of an high protection (SPF 50) with significantly less filters to be used to gain only 1% more protection. On the long term the use of sunscreen filters of natural origin would be much more appealing. However, in this regards there are very scarce information yet in the scientific literature.

6. Conclusions

Several studies focused on the role of natural products in photoprotection. Besides the positive effects of solar exposure for human health, UV rays have been widely investigated and proven to be unsafe in case of excessive UVB and UVA doses, which involve sunburns, skin aging, DNA skin damage and tumourgenesis.

At present, synthetic and mineral sunscreens are considered very efficient to prevent UV-induced skin injuries but there are controversial data about adverse effects, such as photo-irritation, photosensitization and contact dermatitis. In our opinion, nowadays, the rational evolution of sunscreen formulations has to involve proven UVB absorption capability, antioxidant effects, other synergic protective mechanisms and, finally, good toxicological profiles. Several natural molecules can provide these biological activities, including also synergic effect or enhancers of photo stability. A large number of herbal extracts and plant origin molecules showed UV absorption, anti-inflammatory, anti-photoage and antioxidant activities, demonstrated by several in vivo and in vitro studies. They also demonstrate the protection against DNA and other cellular structures damages, often accompanied with low toxicity or even cell viability enhance activity, in the respects of synthetic filters.

In our opinion, despite all the evidences reported in the present review, only a few herbal extracts match the above-mentioned set of assays, i.e. green tea extracts, some lichens extracts and photolyase enzyme. A large body of studies reports only UV absorption activity (step 1), a necessary but not sufficient condition to support a proven sun care activity. The same concept can be expressed for the in vitro bio-activity studies (step 2), which represent the object of several researches; but that cannot warrant effects in the final formulations. Studies should now focus on step 3 in order to understand the whole role of herbal extract in exerting their photoprotective activity. With these premises, and taking into account best formulation practices about sunscreen products, the optimal UV absorption feature should be identified with a wide range UVA and UVB photoprotection. Natural UV filters, should be then able to absorb solar radiations between 290 and 400 nm. To fulfill these criteria, the studies about *N. sativa* [34], *P. glabra* [36] and *B. cordata* extracts, as well as for secalonin acid B [83] obtained from lichens, shows the most promising preliminary result.

We believe that, despite the large body of studies on discovery of herbal UV filters and sun care actives, the lack of evidence about finished formulation (step 3) explains why there are still no officially approved natural sun-filter (i.e. Annex VI to the EU regulation) although they were proposed in the past, as already described [111]. On the other hand, the finished solar products (sunscreens) that contain herbal derivatives are, instead, well represented on the market, and used as ancillary or ingredients with different claims. SPF factor and photo-protection activity, within these products, are mainly based on accepted synthetic or mineral UV filters. As stated above, this occurrence is mainly related to the scarce attention given to their formulation strategies, considering that, at least *in vitro*, herbal extracts can work as filters as efficiently as the synthetic ones. As for the case of natural preservatives, we believe that this field of investigation holds much promise in the development of natural and safe solar products that are currently most wanted by consumers. Moreover, in this review we have reported interesting data about the influence of different cosmetic excipients and different formulations on photo-protective effects [31,60,61,62]. Finally, researches should consider as a primary approach new formulation strategies, based on bioactive natural UV filter which are successfully tested *in vivo*.

Conflict of interest

The authors declare no conflict of interest.

Acknowledgements

S.M. and S.V. thank Ministry of Education, University and Research (MIUR Italy-PRIN, grant 20105YY2HL_006) and Ambrosialab Srl (Ferrara) for the financial support. M.R. gratefully acknowledge the financial support of the Amazonian State University of the Republic of Ecuador. The technical assistance of Elisa Durini is gratefully acknowledged.

References

- [1] A. Juzeniene, J. Moan, Beneficial effects of UV radiation other than via vitamin D production, *Dermato. Endocrinol.* 4 (2012) 109–117.
- [2] F. Wright, R.B. Weller, Risks and benefits of UV radiation in older people: more of a friend than a foe? *Maturitas* 81 (2015) 425–431.
- [3] E. Valachovic, I. Zurbenko, Skin cancer, irradiation, and sunspots: the solar cycle effect, *BioMed. Res. Int.* 11 (2014) 734–748.
- [4] S. González, M. Fernández-Lorente, Y. Gilaberte-Calzada, The latest on skin photoprotection, *Clin. Dermatol.* 26 (2008) 614–626.
- [5] P. Menguzzato, P. Ziosi, S. Vertuani, S. Manfredini, Naturale e innovazione sostenibile: il futuro della cosmesi? *Natural* 3 (2015) 44–52.
- [6] E. Perera, N. Ganeswaran, C. Staines, A.K. Win, R. Sinclair, Incidence and prevalence of non-melanoma skin cancer in Australia: a systematic review, *Australas. J. Dermatol.* (2015) <http://dx.doi.org/10.1111/aid.12282> (Feb 25).
- [7] R. Dummer, T. Maier, UV protection and skin cancer, *Recent Results Cancer Res.* 160 (2002) 7–12.
- [8] S. Premi, S. Wallisch, M.C. Mano, A.B. Weiner, A. Bacchiocchi, K. Wakamatsu, E.J.H. Bechara, R. Halaban, T. Douki, D.E. Brash, Chemiexcitation of melanin derivatives induces DNA photoproducts long after UV exposure, *Science* 347 (2015) 842–847.
- [9] D. Haluza, S. Simic, H. Moshammer, Temporal and spatial melanoma trends in Austria: an ecological study, *Int. J. Environ. Res. Public Health* 11 (2014) 734–748.
- [10] W. Henne, *In vivo* determination of the sunscreen factor of cosmetic preparations, history and the present state of art, *Parf. Kosm.* 64 (1983) 415–423.
- [11] F. Greiter, Sun protection factor-development methods, *Parf. Kosm.* 55 (1974) 70–75.
- [12] A. Svobodová, J. Pšotová, D. Walterová, Natural phenolics in the prevention of UV-induced skin damage. A review, *Biomed. Papers.* 147 (2003) 137–145.
- [13] N. Saewan, A. Jitpaisong, Photoprotection of natural flavonoids, *J. App. Pharm. Sci.* 3 (2013) 129–141.
- [14] K. Skotarczak, A. Osmał-Mankowska, M. Lodyga, A. Polanska, M. Mazur, Z. Adamski, Photoprotection: facts and controversies, *Eur. Rev. Med. Pharmacol. Sci.* 19 (2015) 98–112.
- [15] R. Rai, S.C. Shanmuga, C.R. Srinivas, Update on photoprotection, *Indian J. Dermatol.* 57 (2012) 335–342.
- [16] S. Kale, K. Kulkarni, G. Gajare, Formulation and *in vitro* evaluation for sun protection factor for oil from resin of *Commiphora mukul* sunscreen cream, *Int J Pharm. Bio. Sci* 4 (2014) 182–188.
- [17] D. Sánchez-Quiles, A. Tovar-Sánchez, Are sunscreens a new environmental risk associated with coastal tourism? *Environ. Int.* 83 (2015) 158–170.
- [18] H. Nishida, M. Hirota, Y. Seto, G. Suzuki, M. Kato, M. Kitagaki, M. Sugiyama, H. Kouzuki, S. Onoue, Non-animal photosafety screening for complex cosmetic ingredients with photochemical and photobiochemical assessment tools, *Regul. Toxicol. Pharmacol.* 22 (2015) 578–585.
- [19] B. Herzog, Prediction of sun protection factors by calculation of transmissions with a calibrated step film model, *Cosmet. Sci.* 53 (2002) 11–26.
- [20] X. Chen, D.U. Ahn, Antioxidant activities of six natural phenolics against lipid oxidation induced by Fe²⁺ or ultraviolet light, *J. Am. Oil Chem. Soc.* 75 (1998) 1717–1721.
- [21] M.M. Giusti, R.E. Wrolstad, Characterization and measurement of Anthocyanins by UV-visible spectroscopy, *Curr. Protoc. Food Anal. Chem.* F1 (2) (2001) 1–F1.2.13.
- [22] B.L. Diffey, J.A. Robson, A new substrate to measure sunscreen protection factors throughout the ultraviolet spectrum, *J. Soc. Cosmet. Chem.* 40 (1989) 127–133.
- [23] J.P. Castanedo-Cázares, K. Martínez-Rosales, D. Hernández-Blanco, G. Valdés-Rodríguez, B. Torres-Alvarez, *In vitro* assessment of commercial sunscreens available in Latin America, *Investig. Clin.* 55 (2014) 142–154.
- [24] S.M. Gharavi, N. Tavakoli, A. Pardakhti, N. Baghaei-Zadeh, Determination of sun protection factor of sunscreens by two different *in vitro* methods, *J. Res. Med. Sci.* 2 (1999) 53–54.
- [25] J.S. Mansur, M.N.R. Breder, M.C.A. Mansur, R.D. Azulay, Determinação do fator de proteção solar por espectrofotometria, *An. Bras. Dermatol.* 61 (1986) 121–124.
- [26] C. Santa-Maria, E. Revilla, E. Miramontes, J. Bautista, A. García-Martínez, E. Romero, M. Carballo, J. Parrado, Protection against free radicals (UVB irradiation) of a water-soluble enzymatic extract from rice bran. Study using human keratinocyte monolayer and reconstructed human epidermis, *Food Chem. Toxicol.* 48 (2010) 83–88.
- [27] C.C. Huang, W.B. Wu, J.Y. Fang, H.S. Chiang, S.K. Chen, B.H. Chen, Y.T. Chen, C.F. Hung, Epicatechin-3-gallate, a green tea polyphenol is a potent agent against UVB-induced damage in HaCaT keratinocytes, *Molecules* 12 (2007) 1845–1858.
- [28] R. Casagrande, S.R. Georgetti, J.W.A. Verri, D.J. Dorta, A.C. Dos Santos, M.J.V. Fonseca, Protective effect of topical formulations containing quercetin against UVB-induced oxidative stress in hairless mice, *J. Photochem. Photobiol. B* 84 (2006) 21–27.
- [29] R. Casagrande, S.R. Georgetti, J.W.A. Verri, M.F. Borin, R.F.V. Lopez, M.J.V. Fonseca, *In vitro* evaluation of quercetin cutaneous absorption from topical formulations and its functional stability by antioxidant activity, *Intern. J. Pharm.* 328 (2007) 183–190.
- [30] A. Petrova, L.M. Davids, F. Rautenbach, J.L. Marnewick, Photoprotection by honeybush extracts, hesperidin and mangiferin against UVB-induced skin damage in SKH-1 mice, *J. Photochem. Photobiol. B* 103 (2011) 126–139.
- [31] S. Kale, G. Gajbiye, N. Chaudhari, Formulation and *in-vitro* evaluation of *Moringa concanensis*, *Nimmo*, Seed oils sunscreen cream, *Int. J. Pharm. Tech. Res.* 2 (2010) 2060–2062.
- [32] S. Kale, A. Sonawane, A. Ansari, P. Ghoghe, A. Waje, Formulation and *in vitro* determination of sun protection factor of *Ocinum basilicum* Linn. leaf oils sunscreen cream, *Int. J. Pharm. Pharm. Sci.* 2 (2010) 147–149.
- [33] M.A. Ebrahimzadeh, R. Enayatifard, M. Khalili, M. Ghaffarloo, M. Saedi, Y.J. Charati, Correlation between sun protection factor and antioxidant activity, phenol and flavonoid contents of some medicinal plants, *Iran J. Pharm. Res.* 13 (2014) 1041–1047.
- [34] P. Khazaeli, M. Mehrabani, Screening of sun protective activity of the ethyl acetate extracts of some medicinal plants, *Iran J. Pharm. Res.* 7 (2008) 5–9.
- [35] F. Fischer, E. Zufferey, J.M. Bourgeois, J. Héritier, F. Micaux, UV-ABC screens of luteolin derivatives compared to edelweiss extract, *J. Photochem. Photobiol. B* 103 (2011) 8–15.
- [36] R.G. Oliveira-Junior, G. Rocha-Souza, A. Leite-Guimaraes, A.P. Oliveira, C. Souza-Araújo, J. Cabral-Silva, A.G. Marques-Pacheco, S.R.G. Lima-Saraiva, L. Araújo-Rolim, P.J. Rolim-Neto, N. Castro-Rosane, J.R.G. Silva-Almeida, Photoprotective, antibacterial activity and determination of phenolic compounds of *Neoglaziovia variegata* (Bromeliaceae) by high performance liquid chromatography-diode array detector (HPLC-DAD) analysis, *Afr. J. Pharm. Pharm.* 22 (2015) 576–584.
- [37] S. Cheikh-Rouhou, S. Besbes, B. Hentati, C. Blecker, C. Deroanne, H. Attia, *Nigella sativa* L.: chemical composition and physicochemical characteristics of lipid fraction, *Food Chem.* 101 (2007) 673–681.
- [38] F. Rancan, S. Rosan, K. Boehm, E. Fernández, M.E. Hidalgo, W. Quibot, C. Rubio, F. Boehm, H. Piazena, U. Oltmanns, Protection against UVB irradiation by natural filters extracted from lichens, *J. Photochem. Photobiol. B* 68 (2002) 133–139.
- [39] V.K. Gore, P. Satyamoorthy, Determination of pongamol and karanjin in karanja oil by reverse phase HPLC, *Anal. Lett.* 33 (2000) 337–346.
- [40] T.A.L. Wagemaker, C.R. Limonta-Carvalho, N. Borlina-Maia, S. Regina-Baggio, O. Guerreiro-Filho, Sun protection factor, content and composition of lipid fraction of green coffee beans, *Ind. Crop. Prod.* 33 (2011) 469–473.
- [41] T.A.L. Wagemaker, S.A.M. Silva, G.R. Leonardi, P.M.G.B. Maia-Campos, *Coffea arabica* L. seed oil influences the stability and protective effects of topical formulations, *Ind. Crops Prod.* 63 (2015) 34–40.
- [42] S.K. Katiyar, F. Afaq, A. Perez, H. Mukhtar, Green tea polyphenol (1)-epigallocatechin-3-gallate treatment of human skin inhibits ultraviolet radiation-induced oxidative stress, *Carcinogen* 22 (2001) 287–294.
- [43] S.K. Katiyar, H. Mukhtar, Green tea polyphenol (1)-epigallocatechin-3-gallate treatment to mouse skin prevents UVB-induced infiltration of leukocytes, depletion of antigen-presenting cells, and oxidative stress, *J. Leukoc. Biol.* 69 (2001) 719–726.
- [44] P.K. Vayalil, C.A. Elmetts, S.K. Katiyar, Treatment of green tea polyphenols in hydrophilic cream prevents UVB-induced oxidation of lipids and proteins, depletion of antioxidant enzymes and phosphorylation of MAPK proteins in SKH-1 hairless mouse skin, *Carcinogen* 24 (2003) 927–936.
- [45] I.F. Almeida, A.S. Pinto, C. Monteiro, H. Monteiro, L. Belo, J. Fernandes, A.R. Bento, T.L. Duarte, J. Garrido, M.F. Bahia, J.M. Sousa-Lobo, P.C. Costa, Protective effect of *C. sativa* leaf extract against UV mediated-DNA damage in a human keratinocyte cell line, *J. Photochem. Photobiol. B* 144 (2015) 28–34.

- [46] C. Lee, G.H. Park, E.M. Ahn, B.A. Kim, C.I. Park, J.H. Jang, Protective effect of *Codium fragile* against UVB-induced pro-inflammatory and oxidative damages in HaCaT cells and BALB/c mice, *Fitoterapia* 86 (2013) 54–63.
- [47] C.L. Lim, R.Y. Koh, T.Y. Haw, L.A. Boudville, Antioxidant activity of the sea bird nest (*Eucheuma cottonii*) and its radical scavenging effect on human keratinocytes, *J. Med. Bioeng.* 4 (2015) 461–465.
- [48] S. Patil, B. Fegade, U. Zamindar, V.H. Bhaskar, Determination of sun protection effect of herbal sunscreen cream, *World J. Pharm. Pharm. Sci.* 4 (2015) 1554–1565.
- [49] S.K. Katiyar, T.S. Mc Cormick, K.D. Cooper, H. Mukhtar, Prevention of UVB-induced immunosuppression in mice by the green tea polyphenol (–)-epigallocatechin-3-gallate may be associated with alterations in IL-10 and IL-12 production, *Carcinogen.* 20 (1999) 2117–2124.
- [50] S.K. Katiyar, M.S. Matsui, C.A. Elmets, H. Mukhtar, Polyphenolic antioxidant (–)-epigallocatechin-3-gallate from green tea reduces UVB-induced inflammatory responses and infiltration of leukocytes in human skin, *Photochem. Photobiol.* 69 (1999) 148–153.
- [51] J.H. Huang, C.C. Huang, Y.J. Fang, C. Yang, C.M. Chan, N.L. Wu, S.W. Kang, C.F. Hung, Protective effects of myricetin against ultraviolet-B-induced damage in human keratinocytes, *Toxicol. Vitro* 24 (2010) 21–28.
- [52] Y.M. Fonseca, C. Dias Catini, F.T.M.C. Vicentini, J. Coedeiro Cardoso, J.R.L.C. de Albuquerque, M.J.V. Fonseca, Efficacy of marigold extract loaded formulation against UV-induced oxidative stress, *J. Pharm. Sci.* 100 (2011) 2182–2193.
- [53] Y.M. Fonseca, C.D. Catini, F.T.M.C. Vicentini, A. Nomizo, R.F. Gerlach, M.J. Vieira Fonseca, Protective effect of *Calendula officinalis* extract against UVB-induced oxidative stress in skin: evaluation of reduced glutathione levels and matrix metalloproteinase secretion, *J. Ethnopharm.* 127 (2010) 596–601.
- [54] M. Pereira, N. Pereira, C. Rosado, C. Areias de Oliveira, D. D'Almeida-Peres, M.E. Araujo, M.V. Robles-Velasco, A. Rolim-Baby, J. Portugal-Mota, T. Santos-Almeida, Photostabilization of sunscreen by incorporation of tea as the external phase, *Biomed. Biopharm. Res.* 12 (2015) 107–116.
- [55] E. Roh, J.E. Kim, J.Y. Kwon, J.S. Park, A.M. Bode, Z. Dong, K.W. Lee, Molecular mechanisms of green tea polyphenols with protective effects against skin photoaging, *Crit. Rev. Food Sci. Nutr.* (2015) <http://dx.doi.org/10.1080/10408398.2014.1003365>.
- [56] M. Gasparrini, T.Y. Forbes-Hernandez, S. Afrin, J.M. Alvarez-Suarez, A.M. González-Paramás, C. Santos-Buelga, S. Bompadre, J.L. Quiles, B. Mezzetti, F. Giampieri, A pilot study of the photoprotective effects of strawberry-based cosmetic formulations on human dermal fibroblast, *Int. J. Mol. Sci.* 16 (2015) 17870–17884.
- [57] M. Gaikwad, S. Kale, Formulation and in vitro evaluation for sun protection factor of *Moringa oleifera* Lam (Family-moringaceae) oil sunscreen cream, *Int J Pharm Pharm Sci* 3 (2011) 371–375.
- [58] S. Kale, M. Gaikwad, S. Bhandare, Determination and comparison of in vitro SPF of topical formulation containing lutein ester from *Tagetes erecta* L. flowers, *Moringa oleifera* Lam, *Int. J. Res. Pharm. Biomed. Sci.* 2 (2011) 1220–1224.
- [59] S. Kale, G. Gajbhaye, N. Chaudhari, Formulation and in-vitro evaluation of *Moringa concanensis*, Nimmo. Seed oils sunscreen cream, *Int. J. Pharm. Tech. Res.* 2 (2010) 2060–2062.
- [60] M.V.R. Velasco, F.D. Sarraf, I.M.N. Salgado-Santos, C.A. Haroutunian-Filho, T.M. Kaneko, A. Rolim Baby, Broad spectrum bioactive sunscreens, *Int. J. Pharm.* 363 (2008) 50–57.
- [61] M.Z. Campanini, F.A. Pinho-Ribeiro, A.L.M. Ivan, V.S. Ferreira, F.M.P. Vilela, F.T.M.C. Vicentini, R.M. Martinez, A.C. Zarpelon, M.J.V. Fonseca, T.J. Faria, M.M. Baracat, W.A. Jr Verri, S.R. Georgetti, R. Casagrande, Efficacy of topical formulations containing *Pimenta pseudocaryophyllus* extract against UVB-induced oxidative stress and inflammation in hairless mice, *J. Photochem. Photobiol. B* 127 (2013) 153–160.
- [62] M.Z. Campanini, D.L. Custódio, A.L. Ivan, S.M. Martins, M.J. Paranzini, R.M. Martinez, W.A. Jr Verri, F.T. Vicentini, N.S. Arakawa, T. de J. Faria, M.M. Baracat, R. Casagrande, S.R. Georgetti, Topical formulations containing *Pimenta pseudocaryophyllus* extract: in vitro antioxidant activity and in vivo efficacy against UV-B-induced oxidative stress, *AAPS Pharm. Sci. Tech.* 15 (2014) 86–95.
- [63] G. Badea, I. Lacatusu, N. Badea, C. Ott, A. Meghea, Use of various vegetable oils in designing photoprotective nanostructured formulations for UV protection and antioxidant activity, *Ind. Crop. Prod.* 67 (2015) 18–24.
- [64] G. Niculae, I. Lacatusu, N. Badea, A. Meghea, R. Stan, Influence of vegetable oil on the synthesis of bioactive nanocarriers with broad spectrum photoprotection, *Cent. Eur. J. Chem.* 12 (2014) 837–850.
- [65] G. Badea, I. Lacatusu, C. Ott, N. Badea, I. Grafu, A. Meghea, Integrative approach in prevention and therapy of basal cellular carcinoma by association of three actives loaded into lipid carrier, *J. Photochem. Photobiol. B* 147 (2015) 1–8.
- [66] J.G. Avila-Acevedo, A.M. Espinosa-González, D.M. De Maria y Campos, J.C. Benitez-Flores, T.H. Delgado, S. Flores-Maya, J. Campos-Contreras, J.L. Muñoz-Lopez, A.M. García-Bores, Photoprotection of *Buddleia cordata* extract against UVB-induced skin damage in SKH-1 hairless mice, *BMC Complement. Altern. Med.* 281 (2014) 2–9.
- [67] B.K. Pereira, R.M. Rosa, J. Da Silva, T.N. Guecheva, I. Marques de Oliveira, M. Janistcki, V.C. Benvegnú, G.V. Furtado, A. Ferraz, M.F. Richter, N. Schroder, A.B. Pereira, J.A. Pêgas Henriques, Protective effects of three extracts from Antarctic plants against ultraviolet radiation in several biological models, *J. Photochem. Photobiol. B* 96 (2009) 117–129.
- [68] M.A. Aziz-Mohamed, M. Jung, S.M. Lee, T.H. Lee, J. Kim, Protective effect of *Disporum sessile* D. Don extract against UVB induced photoaging via suppressing MMP-1 expression and collagen degradation in human skin cells, *J. Photochem. Photobiol. B* 133 (2014) 73–79.
- [69] A. Bazytko, J. Borzym, A. Parzonko, Determination of in vitro antioxidant and UV-protecting activity of aqueous and ethanolic extracts from *Galinosa parviflora* and *Galinosa quadriradiata* herb, *J. Photochem. Photobiol. B* 149 (2015) 189–195.
- [70] R. Aquino, S. Morelli, A. Tomaino, M. Pellegrino, A. Saija, L. Grumetto, C. Puglia, D. Ventura, F. Bonina, Antioxidant and photoprotective activity of a crude extract of *Culcitium reflexum* H.B.K. leaves and their major flavonoids, *J. Ethnopharmacol.* 79 (2002) 183–191.
- [71] W.B. Huh, J.E. Kim, Y.G. Kang, G. Park, T. Lim, J.Y. Kwon, Brown pine leaf extract and its active component trans-communic acid inhibit UVB-induced MMP-1 expression by targeting PI3K, *PLoS One* 10 (2015), [e0128365](http://dx.doi.org/10.1371/journal.pone.0128365)<http://dx.doi.org/10.1371/journal.pone.0128365>.
- [72] M.K. Bulla, L. Hernandes, M.L. Baesso, A.C. Nogueira, A.C. Bento, B.B. Bortoluzzi, L.Z. Serra, A.G.D. Cortez, Evaluation of photoprotective potential and percutaneous penetration by photoacoustic spectroscopy of the *Scjinus terebinthifolius* Raddi extract, *Photochem. Photobiol.* 91 (2015) 558–566.
- [73] Y. Yang, S. Li, Dandelion extracts protect human skin fibroblast from UVB damage and cellular senescence, *Oxid. Med. Cell. Longev.* (2015), 619560.
- [74] A. Filip, D. Daicovicu, S. Clichici, P. Bolfa, C. Catoi, I. Baldea, L. Bolojan, D. Olteanu, A. Muresan, I.D. Postescu, The effects of grape seeds polyphenols on SKH-1 mice skin irradiated with multiple doses of UV-B, *J. Photochem. Photobiol. B* 105 (2011) 133–142.
- [75] A. Filip, S. Clichici, D. Daicovicu, C. Catoi, P. Bolfa, I.D. Postescu, A. Gal, A. Baldea, C. Gherman, A. Muresan, Chemopreventive effects of *Calluna Vulgaris* and *Vitis Vinifera* extracts on UVB-induced skin damage in SKH-1 hairless mice, *J. Physiol. Pharm.* 62 (2011) 385–392.
- [76] M. Perde-Schrepler, G. Chereches, I. Brie, C. Tatomir, I.D. Postescu, L. Soran, A. Filip, Grape seed extract as photochemopreventive agent against UVB-induced skin cancer, *J. Photochem. Photobiol. B* 118 (2013) 16–21.
- [77] T.H. Kao, Y.F. Lu, B.H. Chen, Preparative column chromatography of four groups of isoflavones from soybean cake, *Eur. Food Res. Technol.* 221 (2005) 459–465.
- [78] H.S. Chiang, W.B. Wu, J.Y. Fang, B.H. Chen, T.H. Kao, Y.T. Chen, C.C. Huang, C.F. Hung, UVB-protective effects of isoflavone extracts from soybean cake in human keratinocytes, *Int. J. Mol. Sci.* 8 (2007) 651–661.
- [79] T.M. Chiu, C.C. Huang, T.J. Lin, J.Y. Fang, N.L. Wu, C.F. Hung, In vitro and in vivo anti-photoaging effects of an isoflavone extract from soybean cake, *J. Ethnopharmacol.* 126 (2009) 108–113.
- [80] R. Calò, L. Marabini, Protective effect of *Vaccinium myrtillus* extract against UVA- and UVB-induced damage in a human keratinocyte cell line (HaCaT cells), *J. Photochem. Photobiol. B* 132 (2015) 27–35.
- [81] S.A. Figueiredo, F.M. Pinto-Vilela, C. Alves da Silva, T. Mattar-Cunha, M. Henrique dos Santos, M.J. Viera-Fonseca, In vitro and in vivo photoprotective potential of *Garcinia brasiliensis* epicarp extract, *J. Photochem. Photobiol. B* 131 (2014) 65–73.
- [82] C. Kohlhardt-Floehr, F. Bohem, S. Troppens, J. Lademann, T.G. Truscott, Prooxidant and antioxidant behaviour of usnic acid from lichens under UVB-light irradiation – studies in human cells, *J. Photochem. Photobiol. B* 101 (2010) 97–102.
- [83] M. Millot, F. Di Meo, S. Tomasi, J. Boustie, P. Trouillas, Photoprotective capacities of lichen metabolites: a joint theoretical and experimental study, *J. Photochem. Photobiol. B* 111 (2012) 17–26.
- [84] F. Lohézic-Lé Dévéhat, B. Legouin, C. Couteau, J. Boustie, L. Coiffard, Lichenic extracts and metabolites as UV filters, *J. Photochem. Photobiol. B* 120 (2013) 17–28.
- [85] F. Boehm, K. Clarke, R. Edge, E. Fernandez, S. Navaratnam, W. Quilhot, F. Rancan, T.G. Truscott, Lichens – photophysical studies of potential new sunscreens, *J. Photochem. Photobiol. B* 95 (2009) 40–45.
- [86] J.L. Rojas, M. Dias-Santos, N.A. Valencia-Islas, Metabolites with antioxidant and photo-protective properties from *Usnea roccellina* Motyka, a lichen from Colombian Andes, *UK J. Pharm. Biosci.* 3 (2015) 18–26.
- [87] A. Pérez-Sánchez, E. Barrajón-Catalán, N. Caturja, J. Castillo, O. Benavente-García, M. Alcaraz, V. Micol, Protective effects of citrus and Rosemary extract n UV-induced damage in skin cell model and human volunteers, *J. Photochem. Photobiol. B* 136 (2014) 12–18.
- [88] B. Brownlow, V.J. Nagaraj, A. Nayel, M. Joshi, T. Elbayoumi, Development and In Vitro Evaluation of Vitamin E-Enriched Nanoemulsion Vehicles Loaded with Genistein for Chemoprevention Against UVB-Induced Skin Damage, *Pharm. Nanotechnol.* (2015) <http://dx.doi.org/10.1002/jps.24547> Published online in Wiley Online Library (wileyonlinelibrary.com).
- [89] A. Saija, A. Tomaino, D. Trombetta, M. Giacchi, A. De Pasquale, F. Bonina, Influence of different penetration enhancers on in vitro skin permeation and in vivo photoprotective effect of flavonoids, *Int. J. Pharm.* 175 (1998) 85–94.
- [90] Y. Yin, W. Li, Y. Son, L. Sun, J. Lu, D. Kim, X. Wang, H. Yao, L. Wang, P. Pratheeshkumar, A.J. Hitron, J. Luo, N. Gao, X. Shi, Z. Zhang, Quercetin protects skin from UVB-induced oxidative damage, *Toxicol. Appl. Pharmacol.* 269 (2013) 89–99.
- [91] F.T.M.C. Vicentini, T.R.M. Simi, J.O. Del Ciampo, N.O. Wolga, D.L. Pitol, M.M. Iyomasa, M.V.L.B. Bentley, M.J.V. Fonseca, Quercetin in w/o microemulsion: in vitro and in vivo skin penetration and efficacy against UVB-induced skin damages evaluated in vivo, *Eur. J. Pharm. Biopharm.* 69 (2008) 948–957.
- [92] S. Scalia, M. Mezzena, Photostabilization effect of quercetin on the UV filter combination, butyl methoxydibenzoylmethane-octyl methoxycinnamate, *Photochem. Photobiol.* 86 (2010) 273–278.
- [93] G. Heiduschka, C. Lill, R. Seemann, M. Brunner, R. Schmid, R. Houben, J. Bigenzahn, D. Thumher, The effect of resveratrol in combination with irradiation and chemotherapy: study using Merkel cell carcinoma cell lines, *Strahlenther. Onkol.* 190 (2014) 75–80.
- [94] S. Shrotriya, R. Agarwal, R.A. Sclafani, A perspective on chemoprevention by resveratrol in head and neck squamous cell carcinoma, *Adv. Exp. Med. Biol.* 815 (2015) 333–348.
- [95] J.V. Freitas, N. Pepporine-Lopes, L.R. Gaspar, Photostability evaluation of five UV-filters, trans-resveratrol and beta-carotene in sunscreens, *Eur. J. Pharm. Sci.* 78 (2015) 79–89.

- [96] J.V. Freitas, F.S.G. Praca, M.V.L.B. Bentley, L.R. Gaspar, Trans-resveratrol and beta carotene from sunscreens penetrate viable skin layers and reduce cutaneous penetration of UV-filters, *Int. J. Pharm.* 484 (2015) 131–137.
- [97] C.M. Chan, C.H. Huang, H.J. Li, C.Y. Hsiao, C.C. Su, P.L. Lee, C.F. Hung, Protective effects of resveratrol against UVA-induced damage in ARPE19 cells, *Int. J. Mol. Sci.* 16 (2015) 5789–5802.
- [98] O. Sorg, C. Antille, G. Kaya, J.H. Saurat, Retinoids in cosmeceuticals, *Dermatol. Ther.* 19 (2006) 289–296.
- [99] D. De Lucia, O.M. Lucio, B. Musio, A. Bender, M. Listing, S. Dennhardt, A. Koeberle, U. Garscha, R. Rizzo, S. Manfredini, O. Wertz, S.V. Ley, Design, synthesis and evaluation of semi-synthetic triazole-containing caffeic acid analogues as 5-lipoxygenase inhibitors, *Eur. J. Med. Chem.* 28 (2015) 573–583.
- [100] C. Romagnoli, A. Baldisserotto, G. Malisardi, C.B. Vicentini, D. Mares, E. Andreotti, S. Vertuani, S. Manfredini, A multi-target approach toward the development of novel candidates for antidermatophytic activity: ultrastructural evidence on α -bisabolol-treated *Microsporum gypseum*, *Molecules* 20 (2015) 11765–11776.
- [101] A. Baldisserotto, G. Malisardi, E. Scalambra, E. Andreotti, C. Romagnoli, C.B. Vicentini, S. Manfredini, S. Vertuani, Synthesis, antioxidant and antimicrobial activity of a new phloridzin derivative for dermo-cosmetic applications, *Molecules* 17 (2012) 13275–13289.
- [102] A. Baldisserotto, S. Vertuani, A. Bino, D. De Lucia, I. Lampronti, R. Milani, R. Gambari, S. Manfredini, Design, synthesis and biological activity of a novel Rutin analogue with improved lipid soluble properties, *Bioorg. Med. Chem.* 23 (2015) 264–271.
- [103] I. Lampronti, M. Borgatti, S. Vertuani, S. Manfredini, R. Gambari, Modulation of the expression of the proinflammatory IL-8 gene in cystic fibrosis cells by extracts deriving from olive mill waste water, *Evid. Based Complement. Alternat. Med.* 2013 (2013) 960603, <http://dx.doi.org/10.1155/2013/960603> Epub 2013 Jul 7.
- [104] G. Malik, A. Natangelo, J. Charris, L. Pouységu, S. Manfredini, D. Cavagnat, T. Buffeteau, D. Deffieux, S. Quideau, Synthetic studies toward C-glucosidic ellagitannins: a biomimetic total synthesis of 5-O-desgalloylepunicacortein A, *Chemistry* 18 (2012) 9063–9074.
- [105] S. Vertuani, A. Baldisserotto, E. Scalambra, G. Malisardi, E. Durini, S. Manfredini, Novel molecular combination deriving from natural aminoacids and polyphenols: design, synthesis and free-radical scavenging activities, *Eur. J. Med. Chem.* 50 (2012) 383–392.
- [106] J.M. King, K.S. Coley, Toxicity of aqueous extracts of natural and synthetic oils to three species of *Lemna*, aquatic toxicology and hazard assessment, Eighth Symp. (1985) 302–309.
- [107] C.A. Downs, E. Kramarsky-Winter, R. Segal, et al., Toxicopathological effects of the sunscreen UV filter, oxybenzone (benzophenone-3), on coral planulae and cultured primary cells and its environmental contamination in Hawaii and the U.S. Virgin Islands, *Arch. Environ. Contam. Toxicol.* 70 (2016) 265, <http://dx.doi.org/10.1007/s00244-015-0227-7>.
- [108] J.E. French, NTP technical report on toxicity studies of 2-hydroxy-4-methoxybenzophenone administered topically and in dosed feed to F344/N Rats and B6C3F1 Mice, *Natl. Toxicol. Rep.* (No. 21 NIH Publication No. 92-3344).
- [109] N.R. Janjua, B. Kongsjoj, A.M. Andersson, H. Wulf, Sunscreens in human plasma and urine after repeated whole-body topical application, *J. Eur. Acad. Dermatol. Venereol.* 22 (2008) 456–461, <http://dx.doi.org/10.1111/j.1468-3083.2007.02492.x>.
- [110] S. Kim, D. Jung, Y. Kho, K. Choi, Effects of benzophenone-3 exposure on endocrine disruption and reproduction of Japanese medaka (*Oryzias latipes*)—a two generation exposure study, *Aquat. Toxicol.* 155 (2014) 244–252.
- [111] D. Coppini, P. Paganizzi, P. Santi, A. Ghirardini, Capacità protettiva nei confronti delle radiazioni solari di derivati di origine vegetale, *Cosmet. News* 136 (2001) 15–20.

A.1.3. Copyrights permissions

Rightslink® by Copyright Clearance Center

27/01/19, 22:57



RightsLink®

Home

Account Info

Help



Title: In vitro characterization of physico-chemical properties, cytotoxicity, bioactivity of urea-crosslinked hyaluronic acid and sodium ascorbyl phosphate nasal powder formulation

Author: Arianna Fallacara, Laura Busato, Michele Pozzoli, Maliheh Ghadiri, Hui Xin Ong, Paul M. Young, Stefano Manfredini, Daniela Traini

Publication: International Journal of Pharmaceutics

Publisher: Elsevier

Date: 10 March 2019

Crown Copyright © 2019 Published by Elsevier B.V. All rights reserved.

Logged in as:
Arianna Fallacara
University of Ferrara
Account #:
3001252928

LOGOUT

Please note that, as the author of this Elsevier article, you retain the right to include it in a thesis or dissertation, provided it is not published commercially. Permission is not required, but please ensure that you reference the journal as the original source. For more information on this and on your other retained rights, please visit: <https://www.elsevier.com/about/our-business/policies/copyright#Author-rights>

BACK

CLOSE WINDOW

Copyright © 2019 Copyright Clearance Center, Inc. All Rights Reserved. [Privacy statement](#). [Terms and Conditions](#).
Comments? We would like to hear from you. E-mail us at customercare@copyright.com

MDPI Open Access Information and Policy

All articles published by MDPI are made immediately available worldwide under an open access license. This means:

- everyone has free and unlimited access to the full-text of *all* articles published in MDPI journals;
- everyone is free to re-use the published material if proper accreditation/citation of the original publication is given;
- open access publication is supported by the authors' institutes or research funding agencies by payment of a comparatively low Article Processing Charge (APC) ([/about/apc](#)) for accepted articles.

<https://www.mdpi.com/about/openaccess>

The screenshot shows the MDPI article page for the paper: "Formulation and Characterization of Native and Crosslinked Hyaluronic Acid Microspheres for Dermal Delivery of Sodium Ascorbyl Phosphate: A Comparative Study". The page includes a search bar, navigation tabs (MDPI, Journals A-Z, Information & Guidelines, Initiatives, About), and a navigation menu (Login, Register, Submit). The article title is prominently displayed, along with the authors: Arianna Fallacara, Filippo Marchetti, Michele Pozzoli, Ugo Raffaello Citeresi, Stefano Manfredini, and Silvia Vertuani. The article is identified as an Open Access Article. A red circle highlights the text: "This is an open access article distributed under the Creative Commons Attribution License which permits unrestricted use, distribution, and reproduction in any medium, provided the original work is properly cited (CC BY 4.0)". Below this, there is a scifeed advertisement, a "Share & Cite This Article" section with social media icons, and the MDPI and ACS style citation information. The page also features a sidebar with article statistics (Views: 207, Downloads: 42), article versions, related info, more by authors, and export article options. A vertical banner on the right promotes publishing data sets in MDPI's open access journals.

MDPI Open Access Information and Policy

All articles published by MDPI are made immediately available worldwide under an open access license. This means:

- everyone has free and unlimited access to the full-text of *all* articles published in MDPI journals;
- everyone is free to re-use the published material if proper accreditation/citation of the original publication is given;
- open access publication is supported by the authors' institutes or research funding agencies by payment of a comparatively low Article Processing Charge (APC) ([/about/apc](#)) for accepted articles.

<https://www.mdpi.com/about/openaccess>

The screenshot shows the MDPI journal website interface. At the top, there is a navigation bar with 'MDPI Journals A-Z', 'Information & Guidelines', 'Initiatives', and 'About'. On the right, there are links for 'Login', 'Register', and 'Submit'. Below this is a search bar with fields for 'Title / Keyword', 'Author / Affiliation', 'Journal' (set to 'Polymers'), and 'Article Type' (set to 'all'). There are also 'Advanced' and 'Search' buttons. A yellow badge on the right indicates an 'IMPACT FACTOR 2.935'. The main content area features a cover image for 'Volume 10, Issue 7' of 'polymers' with the title 'Micelle Formation of Amphiphilic Block Copolymers Containing Chiral Polythiophene Chains'. Below the cover, there are statistics for 'Views: 957' and 'Downloads: 1085'. The article title is 'Hyaluronic Acid in the Third Millennium' by Arianna Fallacara, Erika Baldini, Stefano Manfredini, and Silvia Vertuani. The abstract discusses the history and applications of hyaluronic acid (HA). A 'Graphical abstract' diagram shows the chemical structures of Native HA, Conjugated HA, and Crosslinked HA, along with various applications like drug delivery, tissue engineering, and cosmetics. A red oval highlights a text box at the bottom of the article page stating: 'This is an open access article distributed under the Creative Commons Attribution License which permits unrestricted use, distribution, and reproduction in any medium, provided the original work is properly cited (CC BY 4.0)'. At the bottom of the page, there is a 'sofeed' banner and a 'Back to Top' button.



Title: Combination of urea-crosslinked hyaluronic acid and sodium ascorbyl phosphate for the treatment of inflammatory lung diseases: An in vitro study

Author: Arianna Fallacara, Laura Busato, Michele Pozzoli, Maliheh Ghadiri, Hui Xin Ong, Paul M. Young, Stefano Manfredini, Daniela Traini

Publication: European Journal of Pharmaceutical Sciences

Publisher: Elsevier

Date: 30 July 2018

© 2018 Elsevier B.V. All rights reserved.

Logged in as:

Arianna Fallacara
University of Ferrara

Account # :
3001252928

LOGOUT

Please note that, as the author of this Elsevier article, you retain the right to include it in a thesis or dissertation, provided it is not published commercially. Permission is not required, but please ensure that you reference the journal as the original source. For more information on this and on your other retained rights, please visit: <https://www.elsevier.com/about/our-business/policies/copyright#Author-rights>

BACK

CLOSE WINDOW

Copyright © 2018 [Copyright Clearance Center, Inc.](#) All Rights Reserved. [Privacy statement.](#) [Terms and Conditions.](#)
Comments? We would like to hear from you. E-mail us at customercare@copyright.com

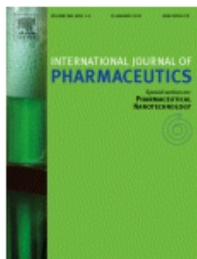
MDPI Open Access Information and Policy

All articles published by MDPI are made immediately available worldwide under an open access license. This means:

- everyone has free and unlimited access to the full-text of *all* articles published in MDPI journals;
- everyone is free to re-use the published material if proper accreditation/citation of the original publication is given;
- open access publication is supported by the authors' institutes or research funding agencies by payment of a comparatively low Article Processing Charge (APC) ([/about/apc](#)) for accepted articles.

<https://www.mdpi.com/about/openaccess>

The screenshot displays the MDPI journal website interface. At the top, there is a navigation bar with 'MDPI Journals A-Z', 'Information & Guidelines', 'Initiatives', and 'About'. On the right, there are links for 'Login', 'Register', and 'Submit'. A yellow badge indicates an 'IMPACT FACTOR 3.098'. The main content area features the journal logo 'molecules' and a search bar. The article title is 'Novel Artificial Tears Containing Cross-Linked Hyaluronic Acid: An In Vitro Re-Epithelialization Study'. The authors listed are Arianna Fallacara, Silvia Vertuani, Giacomo Panozzo, Alessandra Pecorelli, Giuseppe Valacchi, and Stefano Manfredini. The abstract describes the study on re-epithelialization of human corneal epithelium using cross-linked hyaluronic acid. The graphical abstract shows a diagram of the experimental setup and chemical structures of HA and HA-CL. A red oval highlights the Creative Commons Attribution License notice at the bottom of the page, which states: 'This is an open access article distributed under the Creative Commons Attribution License which permits unrestricted use, distribution, and reproduction in any medium, provided the original work is properly cited (CC BY 4.0)'. The sidebar on the left contains various navigation options such as 'Article Versions', 'Related Info', 'More by Authors', and 'Export Article'. The bottom of the page features a 'scifed' logo and a 'Back to Top' button.



Title: Mixtures of hyaluronic acid and liposomes for drug delivery: Phase behavior, microstructure and mobility of liposomes

Author: Naila El Kechai, Sandrine Geiger, Arianna Fallacara, Ingrid Cañero Infante, Valérie Nicolas, Evelyne Ferrary, Nicolas Huang, Amélie Bochot, Florence Agnely

Publication: International Journal of Pharmaceutics

Publisher: Elsevier

Date: 15 May 2017

© 2017 Elsevier B.V. All rights reserved.

Logged in as:
Arianna Fallacara
University of Ferrara
Account # :
3001252928

LOGOUT

Please note that, as the author of this Elsevier article, you retain the right to include it in a thesis or dissertation, provided it is not published commercially. Permission is not required, but please ensure that you reference the journal as the original source. For more information on this and on your other retained rights, please visit: <https://www.elsevier.com/about/our-business/policies/copyright#Author-rights>

BACK

CLOSE WINDOW

Copyright © 2018 Copyright Clearance Center, Inc. All Rights Reserved. [Privacy statement](#). [Terms and Conditions](#). Comments? We would like to hear from you. E-mail us at customercare@copyright.com



ACCADEMIA DELLE SCIENZE DI FERRARA

(Fondata nel 1823, eretta in Ente morale con R.D. 19 sett. 1935 n. 1785)

IL PRESIDENTE

Ferrara, 23 ottobre 2018

Gent.ma dott.ssa
ARIANNA FALLACARA
PhD Candidate

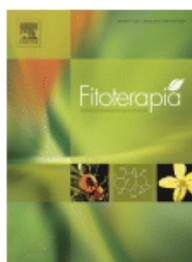
Oggetto: Nulla osta *copyrights permissions*.

Gentilissima dottoressa Fallacara,
le concediamo il nulla osta per la pubblicazione
dell'articolo *L'acido ialuronico (AI) nei trattamenti estetici, una review critica*, in Atti dell'Accademia delle
Scienze di Ferrara, vol. 93, a.a. 193, 2015-2016.

Cordiali saluti



Prof. Adolfo Sebastiani
Presidente
Accademia delle Scienze di Ferrara



Title: Herbal extracts, lichens and biomolecules as natural photo-protection alternatives to synthetic UV filters. A systematic review

Author: Matteo Radice, Stefano Manfredini, Paola Ziosi, Valeria Dissette, Piergiacomo Buso, Arianna Fallacara, Silvia Vertuani

Publication: Fitoterapia

Publisher: Elsevier

Date: October 2016

© 2016 Elsevier B.V. All rights reserved.

Logged in as:

Arianna Fallacara
University of Ferrara

Account # :
3001252928

LOGOUT

Please note that, as the author of this Elsevier article, you retain the right to include it in a thesis or dissertation, provided it is not published commercially. Permission is not required, but please ensure that you reference the journal as the original source. For more information on this and on your other retained rights, please visit: <https://www.elsevier.com/about/our-business/policies/copyright#Author-rights>

BACK

CLOSE WINDOW

Copyright © 2018 Copyright Clearance Center, Inc. All Rights Reserved. [Privacy statement](#). [Terms and Conditions](#).
Comments? We would like to hear from you. E-mail us at customercare@copyright.com

"Non gli tornava 'sta storia che un fiume, dovendo arrivare al mare, ci metta tutto quel tempo, cioè scelga, deliberatamente, di fare un sacco di curve, invece di puntare dritto allo scopo. [...] C'è qualcosa di assurdo in tutte quelle curve. [...] Qualsiasi fiume, prima di arrivare al mare, fa esattamente una strada tre volte più lunga di quella che farebbe se andasse dritto, sbalorditivo se ci pensi. [...] E' la loro natura di fiumi che li obbliga a quel girovagare continuo, e perfino esatto, tanto che tutti, e dico tutti, alla fine, navigano per una strada tre volte più lunga del necessario, anzi per essere esatti, tre volte virgola quattordici, giuro, il famoso pi greco, non ci volevo credere, in effetti, ma pare che sia proprio così, devi prendere la loro distanza dal mare, moltiplicarla per pi greco e hai la lunghezza della strada che effettivamente fanno, il che, ho pensato, è una gran figata, perché, ho pensato, c'è una regola per loro vuoi che non ci sia per noi? Voglio dire, il meno che ti puoi aspettare è che anche per noi sia più o meno lo stesso, e che tutto questo sbandare da una parte e dall'altra, come se fossimo matti, o peggio smarriti, in realtà è il nostro modo di andare dritti, modo scientificamente esatto, benché indubbiamente simile a una sequenza disordinata di errori, o ripensamenti... ma solo in apparenza, perché in realtà è semplicemente il nostro modo di andare dove dobbiamo andare, il modo che è specificatamente nostro, la nostra natura."

City, Alessandro Baricco



Bemerside, Queensland, Australia

“Per quello che vale, non è mai troppo tardi, o nel mio caso troppo presto, per essere quello che vuoi essere. Non c'è limite di tempo, comincia quando vuoi, puoi cambiare o rimanere come sei, non esiste una regola in questo. Possiamo vivere ogni cosa al meglio o al peggio. Spero che tu viva tutto al meglio, spero che tu possa vedere cose sorprendenti, spero che tu possa avere emozioni sempre nuove, spero che tu possa incontrare gente con punti di vista diversi, spero che tu possa essere orgogliosa della tua vita, e se ti accorgi di non esserlo, spero che tu trovi la forza di ricominciare da zero.”

Il curioso caso di Benjamin Button, David Fincher